Functional characterization of immune cells present in the adipose tissue of mice infected with *Neospora caninum*

João Pedro Silva Moreira
Mestrado em Bioquímica
Departamento de Anatomia
2014

Orientador
Doutora Luzia Teixeira, Investigador Auxiliar, ICBAS-UP

Coorientador
Professor Doutor Manuel Vilanova, Professor Associado, ICBAS-UP
Professora Doutora Paula Ferreira, Professor Associado, ICBAS-UP

U.PORTO

FACULDADE DE CIÊNCIAS
UNIVERSIDADE DO PORTO

INSTITUTO DE CIÊNCIAS BIOMÉDICAS ABEL SALAZAR
UNIVERSIDADE DO PORTO

Todas as correções determinadas pelo júri, e só essas, foram efetuadas.

O Presidente do Júri,

Porto, _____/_____/_____

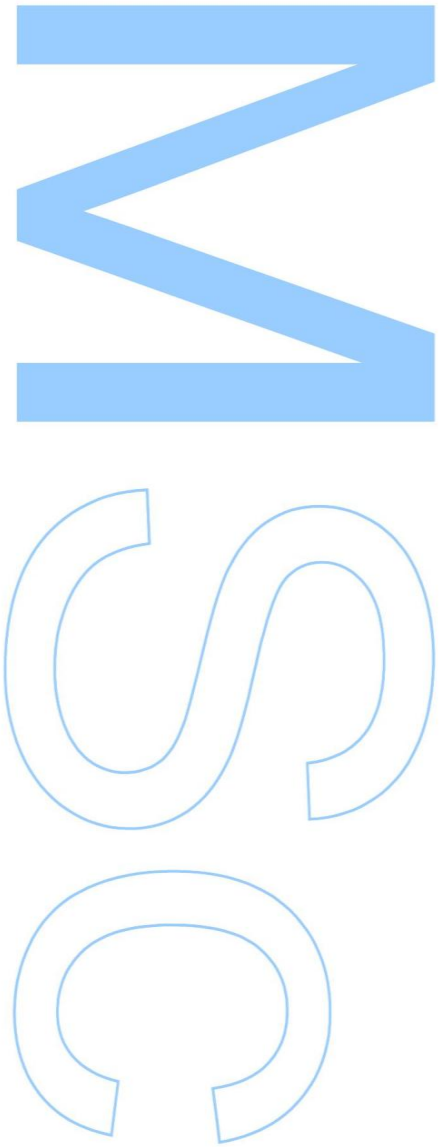

Acknowledgements

First of all, I would like to thank my supervisor Luzia Teixeira for the opportunity to work with her. Her knowledge, all the things that she taught me, all the support and encouragement was fundamental for my work and development as a professional. I could not have asked a better supervisor.

I am also thankful to my co-supervisors Professor Manuel Vilanova and Professor Paula Ferreira, for all the advices, for enlightens my doubts and for all the help and encouragement.

I am grateful to the whole Departamento de Anatomia do Instituto de Ciências Biomédicas Abel Salazar, for having welcomed me so well. To Professor Artur Águas, for allowing me the opportunity to develop my thesis in his laboratory. To Madalena, Ana, Ângela, Sofia, Tiago, Raquel, Gil and Sr. Duarte for all the help, laughs and funny stories. To Sr. Costa and D. Manuela for all the help and sympathy.

To Alexandra and Pedro Ferreirinha for enlightens my doubts and for all the help.

I am grateful to all my friends for all the help, for all the talks, all the support and funny moments, no matter how often we saw each other.

I want to thank to Filipa for all the help, all the team work, all the laughs and support. But mostly, I am so pleased to see that our friendship became very strong during this year and very delighted to realize that you became very special to me.

Finally, but not less important, I would like to thanks to my parents and my family all the support and all confidence that they put in me. Without all of you, I would not be the person that I am today. A very special thanks to all of you.

This work is supported by FEDER through COMPETE and by national funds through FCT-FCOMP-01-0124-FEDER-020158 (FCT reference: PTDC/CTV/122777/ 2010).

Abstract

Neospora caninum is an apicomplexan protozoan first described as the causative agent of neurologic disease in dogs. This parasite was identified as a pathogen responsible for abortions in cattle occurring worldwide, thus causing a negative economical impact in both dairy and beef industries. The study of protective immune mechanisms operating in *N. caninum*-infected hosts is therefore of great importance towards the development of an effective strategy that could prevent infections caused by this parasite.

The traditional view of adipose tissue as a passive reservoir for energy storage is no longer valid. This organ is now known to express and secrete a variety of bioactive peptides, known as adipokines, which may act locally and systemically. It has been described that adipose tissue is a reservoir for some microorganisms, including protozoan parasites and it may also contribute to host immunity. Previous studies suggested that the intracellular protozoan *N. caninum* might affect adipose tissue physiology. Therefore in this work we investigated the immune response in the adipose tissue of mice infected with this parasite.

For that purpose C57BL/6 mice were intraperitoneally inoculated with *N. caninum* tachyzoites and twenty-four hours, seven and twenty-one days and two months after challenge, adipose tissue from different anatomical locations was collected for characterization of the immune cellular infiltrates by using immunohistochemistry and flow cytometry analysis. Parasitic DNA could be detected in adipose tissue at least seven days after challenge and no parasitic DNA was detected by 2 months of infection indicating that adipose tissue is not a reservoir for *N. caninum* as could be assessed in the murine host.

Nevertheless, in specific adipose tissue depots an increased ratio between T helper1-type effector cells over regulatory T cells was still observed two months after infection suggesting that the inflammatory response in these tissues is maintained in the long-term.

An increase in frequency of NK cells and of $\gamma\delta^+$, $CD4^+$ and $CD8^+$ T cells producing interferon-γ was also observed in the adipose tissue depots of the infected mice. Altogether, the findings reported here show that the adipose tissue contributes for the host immune response, in mice challenged with *N. caninum* tachyzoites.
Keywords: *Neospora caninum*, adipose tissue, macrophages, Treg cells, $CD4^+$ T cell, IFN-γ

Resumo

Neospora caninum é um protozoário da família apicomplexa, primeiramente descrito como um agente causador de doença neurológica em cães. Este parasita está identificado como um agente patogénico responsável por abortos em gado bovino, causando um impacto económico negativo nas indústrias leiteira e de produção de carne. O estudo dos mecanismos imunológicos protetores desencadeados no hospedeiro na infeção por *N. caninum* é, deste modo, de grande importância para o desenvolvimento de uma estratégia para prevenir infeções causadas por este parasita.

A visão tradicional de que o tecido adiposo funciona apenas como um reservatório de energia já não é mais válida. Este órgão expressa uma série de péptidos bioativos, conhecidos como adipocinas que podem atuar de modo local bem como sistémico. Está já descrito que o tecido adiposo funciona como um reservatório para alguns microrganismos, incluindo parasitas como também está envolvido na resposta imune do hospedeiro. Estudos anteriores sugerem que o protozoário intracelular *N. caninum* pode afetar a fisiologia do tecido adiposo. Assim, neste trabalho, estudámos a resposta imune no tecido adiposo de ratinhos infetados com este parasita.

Para este propósito, ratinhos C57BL/6 foram inoculados intraperitonealmente com taquizoítos de *N. caninum* e após vinte e quatro horas, sete e vinte e um dias e dois meses após a infeção, o tecido adiposo de diferentes localizações anatómicas foi recolhido para caraterização dos infiltrados de células imunes por imunohistoquímica e citometria de fluxo. DNA do parasita foi detetado no tecido adiposo sete dias após a infeção enquanto que dois meses após a infeção DNA parasitário já não é detetado, indicando que este tecido não funciona como reservatório para *N. caninum*.

Contudo, nas amostras de tecido adiposo analisadas observou-se um aumento da razão entre células T auxiliares do tipo Th1 e células T reguladoras, dois meses após a infeção, indicando que a resposta inflamatória neste tecido se mantém a longo prazo.

Foi também observado um aumento na frequência de células NK, e de células T $\gamma\delta^+$, $CD4^+$ e $CD8^+$, produtoras de IFN-γ no tecido adiposo de ratinhos infetados. Globalmente, estes resultados demonstram que o tecido adiposo contribui para a resposta imune do hospedeiro em ratinhos infetados com taquizoítos de *N. caninum*.
Palavras-chave: *Neospora caninum*, tecido adiposo, macrófagos, células T reguladoras, células T $CD4^+$, IFN-γ

Table of contents

Acknowledgements I
Abstract II
Resumo III
List of figures VI
Abbreviations XIII
1.Introduction 1
1.1.*Neospora caninum* 1
1.1.1. Life cycle 1
1.1.2. Transmission of *N. caninum* in dogs 3
1.1.3. Transmission of *N.caninum* in cattle 3
1.2.Neosporosis 4
1.2.1. Clinical signs of affected animals 4
1.2.2. Diagnosis 5
1.2.3. Economical impact of neosporosis 5
1.2.4. Control Methods 5
1.2.5. Murine Models 6
1.3. Immunity to *Neospora Caninum* 7
1.3.1. Host immune response in cattle 7
1.3.2. Host immune response in mice 7
1.3.3. Changes in the host-parasite relationship during pregnancy 9
1.3.4. Vaccination strategies against *Neospora caninum* 9
1.4. Adipose Tissue 10
1.4.1. Classification, structure and physiology 10
1.4.2. Functions 11
1.4.3. Innate immune system in adipose tissue 11
1.4.4. Adaptive immune system in adipose tissue 12
1.4.5. Adipokines produced by adipose tissue 13
1.4.6. Adipose tissue infection by other microorganisms 14
2.Material and Methods 16
2.1. Mice 16
2.2. Parasites 16
2.3. Challenge infection 16
2.4. Collection of biological samples 16
2.5. Histopathological examination and immunohistochemistry 17

2.6. Isolation of Stromal Vascular Fraction 18
2.7. Cell sorting 18
2.8. Cytospin preparation 19
2.9. Hemacolor Staining 19
2.10. Flow cytometry analysis 19
2.11. RNA isolation and quantitative Real-Time Polymerase Chain Reaction (RT-PCR) analysis 20
2.12. DNA extraction 21
2.13. PCR for the detection of NcT 22
2.14. Cytokine serum measurements 22
2.15. Statistical analysis 22
3.Results 23
3.1.Detection of *N. caninum* tachyzoites in C57BL/6 mice infected by the intraperitoneal route 23
3.2.Characterization of $F4/80^+$ cells in adipose tissue after *N. caninum* infection 24
3.3.Characterization of T helper 1 cells in adipose tissue after *N. caninum* infection 34
3.4.Characterization of regulatory T cells in adipose tissue after infection with *N. caninum* 37
3.5.Serum levels of adipokines 48
4.Cytokine production by adipose tissue immune cell population 49
4.1. IFN-γ production by NK^+ cells in adipose tissue after challenge with *N. caninum* 49
4.2. IFN-γ, IL-10 and IL-4 production by TCRαβ+CD4+ cells in adipose tissue after challenge with *N. caninum* 51
4.3. IFN-γ and IL-10 production by $TCR\alpha\beta^+CD8^+$ cells in adipose tissue after challenge with *N. caninum* 55
4.4. IFN-γ production by $TCR\gamma\delta^+$ cells in adipose tissue of mice infected with *N. caninum* 58
5.Discussion 61
6.References 66

List of figures

Fig.1-Life Cycle of *Neospora caninum*……..3

Fig.2-Representative images of *N. caninum* immunohistochemistry staining in (A) omental adipose tissue and (B) gonadal adipose tissue of C57BL/6 mice infected with 1x10^7 *N. caninum* tachyzoites and sacrificed seven days after i.p. challenge. Specific staining (brown) corresponds to *N. caninum* tachyzoites……...23

Fig.3-Representative images of *N. caninum* immunohistochemistry staining in (A) lung and (B) brain of C57BL/6 mice infected with 1x10^7 *N. caninum* tachyzoites and sacrificed seven days after i.p. challenge. Specific staining (brown) corresponds to *N. caninum* tachyzoites……24

Fig.4-Detection of parasitic DNA by RT-PCR in lung, brain, gonadal adipose tissue (GAT), mesenteric adipose tissue (MAT) and omental adipose tissue (OAT) samples of C57BL/6 mice seven days after i.p. inoculation with *N. caninum*……..24

Fig.5-Representative images of immunohistochemistry analysis of F4/80 staining. Intramuscular adipose tissue (IMAT), subcutaneous adipose tissue (SAT), gonadal adipose tissue (GAT), mesenteric adipose tissue (MAT) and omental adipose tissue (OAT) of C57BL/6 mice sacrificed seven days after i.p. challenge with *N. caninum* (NcT) or administration of PBS (PBS) were specific stained with a monoclonal antibody anti-F4/80. Brown color corresponds to F4/80$^+$ cells……..26

Fig.6-Frequency of F4/80$^+$ stained area of analysed subcutaneous adipose tissue (SAT), mesenteric adipose tissue (MAT), omental adipose tissue (OAT), intramuscular adipose tissue (IMAT) and gonadal adipose tissue (GAT), seven days after challenge with *N. caninum* (NcT) or administration of PBS (PBS). Statistical significant differences between groups is indicated (Mann-Whitney U,**P*<0,05; ***P*<0,01; ****P*<0,005)……27

Fig.7-Representative images of immunohistochemistry analysis of F4/80 staining. Intramuscular adipose tissue (IMAT), subcutaneous adipose tissue (SAT), gonadal adipose tissue (GAT), mesenteric adipose tissue (MAT) and omental adipose tissue (OAT) of C57BL/6 mice sacrificed two months after i.p. challenge with *N. caninum* (NcT) or administration of PBS (PBS) were specific stained with a monoclonal antibody anti-F4/80. Brown color corresponds to F4/80$^+$ cells……..28

Fig.8-Frequency of F4/80$^+$ stained area of analysed subcutaneous adipose tissue (SAT), mesenteric adipose tissue (MAT), omental adipose tissue (OAT), intramuscular

adipose tissue (IMAT) and gonadal adipose tissue (GAT), two months after challenge with *N. caninum* (NcT) or administration of PBS (PBS). Bars represent the mean values of the respective group (± SD).....29

Fig.9-Immunohistochemistry analysis of F4/80 in stromal vascular fraction cells isolated from gonadal adipose tissue of infected C57BL/6 mice, sacrificed seven days after the parasitic challenge. Cells were specific stained (brown coloration) with anti-mouse F4/80 antibody and counterstained with haematoxilyn. Cells with morphology compatible with macrophages (A) and polymorphonuclear cells (B) are observed.....30

Fig.10-(A) Representative dot plots of stromal vascular fraction cells from gonadal adipose tissue of mice seven days after i.p. administration of 1×10^7 *N. caninum* tachyzoites. Hemacolor staining of sorted F4/80^{high} AF ^{high} (B) and F4/80^{int} (C) stromal vascular fraction cells from gonadal adipose tissue of mice seven days after *N. caninum*.....31

Fig.11-Flow cytometry gating strategy used to define macrophages in the stromal vascular fraction of the different depots of adipose tissue analysed. Dead cells were excluded with Fixable Viability Dye (FVD) and singlets were then selected from FSC-A versus FSC-H dot plot. Macrophages were defined as F4/80^{high}. Representative dot plots of F4/80$^+$CD206$^+$ SVF cells gated in F4/80^{high} are shown as well as respective isotype control.....32

Fig.12-Frequencies and numbers of F4/80$^+$ CD206$^+$ or F4/80$^+$ CD206$^-$ cells per gram of gonadal adipose tissue (GAT), mesenteric adipose tissue (MAT), omental adipose tissue (OAT) and subcutaneous adipose tissue (SAT) at two months after i.p. challenge with 1×10^7 *N. caninum* (NcT) or administration of PBS (PBS). Bars represent mean values of the respective group (± SD). Statistical significant differences between groups is indicated (Mann-Whitney U,**P*<0,05; ***P*<0,01; ****P*<0,005).....33

Fig.13-Relative levels of inducible nitric oxide synthase (*Nos-2*) and arginase 1 (*Arg-1*) normalized to Non-POU-domain containing octamer binding protein mRNA, detected by Real Time PCR in the SFV of gonadal adipose tissue of mice seven days after i.p. administration of 1×10^7 *N. caninum* (NcT) tachyzoites or PBS (PBS). Each symbol represents an individual mouse. Horizontal lines represent the mean values of the respective group (± SD). Statistical significant differences between groups is indicated (Mann-Whitney U, **P* < 0.05; ** *P* ≤ 0.01; *** *P* ≤ 0.001).....34

Fig.14-Relative levels of inducible nitric oxide synthase (*Nos-2*) and arginase 1 (*Arg-1*) normalized to Non-POU-domain containing octamer binding protein mRNA, detected by Real Time PCR in the SFV of gonadal adipose tissue of mice two months after i.p. administration of 1×10^7 *N. caninum* (NcT) tachyzoites or PBS (PBS). Each symbol

represents an individual mouse. Horizontal lines represent the mean values of the respective group (± SD)……...34

Fig.15-Flow cytometry representative example of gate strategy used to define Th1 cells in stromal vascular fraction isolated from adipose tissue. Dead cells were excluded with Fixable Viability Dye (FVD) and singlets were then selected from FSC-A versus FSC-H dot plot. T helper cells were defined as $CD3^+$ $CD4^+$. NK cells were excluded and Th1 cells were defined as T-bet^+ $Foxp3^-$ cells. Respective isotype control is shown.....35

Fig.16-Frequency (A) and number (B) of T-$bet^+Foxp3^-CD4^+$ cells *per gram* of gonadal adipose tissue (GAT), mesenteric adipose tissue (MAT), omental adipose tissue (OAT) and subcutaneous adipose tissue (SAT), two months after i.p. challenge with 1×10^7 *N. caninum* or PBS, as indicated. For mesenteric lymph nodes (MLN) only the frequency of cells was determined. Bars represent mean values of the respective group (± SD). Statistical significant differences between groups is indicated (Mann-Whitney U,**P*<0,05; ***P*<0,01; ****P*<0,005)……...36

Fig.17-Relative levels of *IFN-γ* mRNA, normalized to Non-POU-domain containing octamer binding protein mRNA, detected by Real Time PCR in the SFV of gonadal adipose tissue of mice seven days after i.p. administration of 1×10^7 *N. caninum* tachyzoites (NcT) or PBS (PBS). Horizontal lines represent the mean values of the respective group (± SD). Statistical significant differences between groups is indicated (Mann-Whitney U, **P* < 0.05; ** *P* ≤ 0.01; *** *P* ≤ 0.001).....37

Fig.18-Representative images of immunohistochemistry analysis of Foxp3 staining. Intramuscular adipose tissue (IMAT), subcutaneous adipose tissue (SAT), gonadal adipose tissue (GAT), mesenteric adipose tissue (MAT) and omental adipose tissue (OAT) of C57BL/6 mice sacrificed seven days after i.p. challenge with *N. caninum* (NcT) or administration of PBS (PBS) were specific stained with a monoclonal anti-mouse Foxp3. Brown color corresponds to $Foxp3^+$ cells……38

Fig.19-Frequency of $Foxp3^+$ stained area of analysed subcutaneous adipose tissue (SAT), mesenteric adipose tissue (MAT), intramuscular adipose tissue (IMAT), omental adipose tissue (OAT) and gonadal adipose tissue (GAT), seven days after challenge with *N. caninum* (NcT) or administration of PBS (PBS). Bars represent the mean values of the respective group (± SD). Statistical significant differences between groups is indicated (Mann-Whitney U,**P*<0,05; ***P*<0,01; ****P*<0,005)……39

Fig.20-Representative images of immunohistochemistry analysis of Foxp3 staining. Intramuscular adipose tissue (IMAT), subcutaneous adipose tissue (SAT), gonadal adipose tissue (GAT), mesenteric adipose tissue (MAT) and omental adipose tissue (OAT) of C57BL/6 mice sacrificed two months after i.p. challenge with *N. caninum*

(NcT) or administration of PBS (PBS) were specific stained with a monoclonal anti-mouse Foxp3. Brown color corresponds to $Foxp3^+$ cells……41

Fig.21-Frequency of $Foxp3^+$ stained area of analysed subcutaneous adipose tissue (SAT), mesenteric adipose tissue (MAT), omental adipose tissue (OAT), intramuscular adipose tissue (IMAT) and gonadal adipose tissue (GAT), two months after challenge with *N. caninum* (NcT) or administration of PBS (PBS). Bars represent the mean values of the respective group (± SD).....42

Fig.22-Flow cytometry representative example of gate strategy used to define regulatory T cells in stromal vascular fraction isolated from adipose tissue. Dead cells were excluded with Fixable Viability Dye (FVD) and singlets were then selected from FSC-A versus FSC-H dot plot. T helper cells were defined as $CD3^+$ $CD4^+$. NK cells were excluded and regulatory T cells were defined as CD25 Foxp3 double positive cells. Respective isotype control is shown.....43

Fig.23-Total number of cells (A) and percentages (B) of $Foxp3^+CD25^+$ cells, $Foxp3^+CD25^-$ cells on total $CD4^+CD3^+NK^-$cells in gonadal adipose tissue (GAT), mesenteric adipose tissue (MAT), omental adipose tissue (OAT) and subcutaneous adipose tissue (SAT) from C57BL/6 mice sacrificed two months after i.p. challenge with 1×10^7 *N. caninum* (NcT) or PBS (PBS). For mesenteric lymph nodes (MLN) only the frequency of cells was determined. Bars represent means plus one SD. Statistical significant differences between groups is indicated (Mann-Whitney U, **P* < 0.05; ** *P* ≤ 0.01; *** *P* ≤ 0.001).....44

Fig.24-Total number of cells (A) and frequencies (B) of $CD25^+$ $Foxp3^-$ cells on total $CD4^+CD3^+NK^-$cells in gonadal adipose tissue (GAT), mesenteric adipose tissue (MAT), omental adipose tissue (OAT) and subcutaneous adipose tissue (SAT) from C57BL/6 mice sacrificed two months after i.p. challenge with 1×10^7 *N. caninum* (NcT) or PBS (PBS). For mesenteric lymph nodes (MLN) only the frequency of cells was determined. Statistical significant differences between groups is indicated (Mann-Whitney U, **P* < 0.05; ** *P* ≤ 0.01; *** *P* ≤ 0.001).....45

Fig.25-Total number of cells (A) and frequencies (B) of T-bet^+ $Foxp3^+CD4^+$ cells in gonadal adipose tissue (GAT), mesenteric adipose tissue (MAT), omental adipose tissue (OAT) and subcutaneous adipose tissue (SAT) from C57BL/6 mice sacrificed two months after i.p. challenge with 1×10^7 *N. caninum* (NcT) or PBS (PBS). For mesenteric lymph nodes (MLN) only the frequency of cells was determined. Statistical significant differences between groups is indicated (Mann-Whitney U, **P* < 0.05; ** *P* ≤ 0.01; *** *P* ≤ 0.001).....46

Fig.26-The ratio of Th1 cells (T-bet$^+$Foxp3$^-$CD4$^+$) and total Treg cells (Foxp3$^+$T-bet$^-$ CD4$^+$) of gonadal adipose tissue (GAT), mesenteric adipose tissue (MAT), omental adipose tissue (OAT) and subcutaneous adipose tissue (SAT) from C57BL/6 mice sacrificed two months after i.p. challenge with 1×10^7 *N. caninum* (NcT) or PBS (PBS). Statistical significant differences between groups is indicated (Mann-Whitney U, *P < 0.05; ** $P \leq 0.01$; *** $P \leq 0.001$).....47

Fig.27-Relative levels of *IL-10* mRNA, normalized to Non-POU-domain containing octamer binding protein mRNA, detected by Real Time PCR in the SFV of gonadal adipose tissue of mice seven days (A) and two months (B) after i.p. administration of 1×10^7 *N. caninum* tachyzoites (NcT) or PBS (PBS). Horizontal lines represent the mean values of the respective group (± SD). Statistical significant differences between groups is indicated (Mann-Whitney U, *P < 0.05; ** $P \leq 0.01$; *** $P \leq 0.001$).....47

Fig.28-Serum levels of (A) leptin and (B) adiponectin, of C57BL/6 mice seven days (7d) and two months (2m) after i.p. administration of 1×10^7 *N. caninum* tachyzoites (NcT) or PBS (PBS). Horizontal lines represent the mean values of the respective group (± SD). Statistical significant differences between groups is indicated (Mann-Whitney U, *P < 0.05; ** $P \leq 0.01$; *** $P \leq 0.001$; ****$P \leq 0.0001$).....49

Fig. 29-Flow cytometry representative example of gate strategy used to define NK cells in stromal vascular fraction isolated from adipose tissue. Inside leukocyte population, TCRγδ and TCRαβ population were excluded. NK1.1$^+$ cells were selected and the production of IFN-γ was assessed. Respective isotype control is shown.....50

Fig.30-Frequency of NK1.1$^+$IFN-γ$^+$ cells in total NK1.1$^+$ TCRγδ$^-$ TCRαβ$^-$ cells in gonadal adipose tissue (GAT), mesenteric adipose tissue (MAT), omental adipose tissue (OAT) and subcutaneous adipose tissue (SAT), detected in PBS (PBS) i.p.-treated or *N. caninum* (NcT) i.p.-infected mice, twenty-four hours after challenge. Each symbol represents an individual mouse. Horizontal lines represent the mean values of the respective group (± SD). Statistical significant differences between groups is indicated (Mann-Whitney U, *P < 0.05; ** $P \leq 0.01$; *** $P \leq 0.001$; ****$P \leq 0.0001$).....51

Fig.31-Frequency of NK1.1$^+$IFN-γ$^+$ cells in total NK1.1$^+$ TCRγδ$^-$ TCRαβ$^-$ cells in gonadal adipose tissue (GAT), mesenteric adipose tissue (MAT), omental adipose tissue (OAT) and subcutaneous adipose tissue (SAT), detected in PBS (PBS) i.p.-treated or *N. caninum* (NcT) i.p.-infected mice, twenty-one days after challenge. Each symbol represents an individual mouse. Horizontal lines represent the mean values of the respective group (± SD). Statistical significant differences between groups is indicated

(Mann-Whitney U, *P < 0.05; ** $P \leq 0.01$; *** $P \leq 0.001$; ****$P \leq 0.0001$).....51

Fig.32-Flow cytometry representative example of gate strategy used to define TCRαβ$^+$CD4$^+$ cells in stromal vascular fraction isolated from adipose tissue. Inside leukocyte population, TCRαβ population was selected and NK1.1$^+$ cells excluded. Cells expressing CD4 were then selected and the expression of IL-10 and IFN-γ assessed. Respective isotype control is shown.....52

Fig.33-Frequency of (A) TCRαβ$^+$CD4$^+$IFN-γ$^+$IL-10$^-$, (B) TCRαβ$^+$CD4$^+$IFN-γ$^-$IL-10$^+$ and (C) TCRαβ$^+$CD4$^+$IFN-γ$^+$IL-10$^+$ T cells in total TCRαβ$^+$NK1.1$^-$ cells from gonadal adipose tissue (GAT), mesenteric adipose tissue (MAT), omental adipose tissue (OAT) and subcutaneous adipose tissue (SAT), twenty-four hours after i.p. challenge with PBS (PBS) or 1×10^7 *N. caninum* tachyzoites (NcT). Each symbol represents an individual mouse. Horizontal lines represent the mean values of the respective group (± SD). Statistical significant differences between groups is indicated (Mann-Whitney U, *P < 0.05; ** $P \leq 0.01$; *** $P \leq 0.001$).....53

Fig.34-Frequency of (A) TCRαβ$^+$CD4$^+$IFN-γ$^+$IL-10$^-$, (B) TCRαβ$^+$CD4$^+$IFN-γ$^-$IL-10$^+$ and (C) TCRαβ$^+$CD4$^+$IFN-γ$^+$IL-10$^+$ T cells in total TCRαβ$^+$NK1.1$^-$ cells from gonadal adipose tissue (GAT), mesenteric adipose tissue (MAT), omental adipose tissue (OAT) and subcutaneous adipose tissue (SAT), twenty-one days after i.p. challenge with PBS (PBS) or 1×10^7 *N. caninum* tachyzoites (NcT). Each symbol represents an individual mouse. Horizontal lines represent the mean values of the respective group (± SD). Statistical significant differences between groups is indicated (Mann-Whitney U, *P < 0.05; ** $P \leq 0.01$; *** $P \leq 0.001$).....55

Fig.35-Flow cytometry representative example of gate strategy used to define TCRαβ$^+$CD8$^+$ cells in stromal vascular fraction isolated from adipose tissue. Inside leukocyte population, TCRαβ population was selected and NK1.1$^+$ cells were excluded. Cells expressing CD8 were then selected and the expression of IL-10 and IFN-γ assessed. Respective isotype control is shown.....56

Fig.36-Frequency of (A) TCRαβ$^+$CD8$^+$IFN-γ$^+$IL-10$^-$, (B) TCRαβ$^+$CD8$^+$IFN-γ$^-$IL-10$^+$ and (C) TCRαβ$^+$CD8$^+$IFN-γ$^+$IL-10$^+$ T cells in total TCRαβ$^+$NK1.1$^-$ cells from gonadal adipose tissue (GAT), mesenteric adipose tissue (MAT), omental adipose tissue (OAT) and subcutaneous adipose tissue (SAT), twenty-four hours after i.p. challenge with PBS (PBS) or 1×10^7 *N. caninum* tachyzoites (NcT). Each symbol represents an individual mouse. Horizontal lines represent the mean values of the respective group (± SD).

Statistical significant differences between groups is indicated (Mann-Whitney U, *P < 0.05; ** $P \leq 0.01$; *** $P \leq 0.001$).....57

Fig.37-Frequency of (A) TCRαβ$^+$CD8$^+$IFN-γ$^+$IL-10$^-$, (B) TCRαβ$^+$CD8$^+$IFN-γ$^-$IL-10$^+$ and (C) TCRαβ$^+$CD8$^+$IFN-γ$^+$IL-10$^+$ T cells in total TCRαβ$^+$NK1.1$^-$ cells from gonadal adipose tissue (GAT), mesenteric adipose tissue (MAT), omental adipose tissue (OAT) and subcutaneous adipose tissue (SAT), twenty-one days after i.p. challenge with PBS (PBS) or 1×10^7 *N. caninum* tachyzoites (NcT). Each symbol represents an individual mouse. Horizontal lines represent the mean values of the respective group (± SD). Statistical significant differences between groups is indicated (Mann-Whitney U, *P < 0.05; ** $P \leq 0.01$; *** $P \leq 0.001$).....58

Fig.38-Flow cytometry representative example of gate strategy used to define TCRγδ$^+$IFN-γ$^+$ cells in stromal vascular fraction isolated from adipose tissue. Inside leukocyte population, TCRγδ population were selected and the expression of IFN-γ evaluated. Respective isotype control is shown.....59

Fig.39-Frequency of TCRγδ$^+$IFN-γ$^+$ T cells in total TCRγδ$^+$ in gonadal adipose tissue (GAT), mesenteric adipose tissue (MAT), omental adipose tissue (OAT) and subcutaneous adipose tissue (SAT), detected in PBS (PBS) i.p.-treated or *N. caninum* (NcT) i.p.-infected mice with 1×107 tachyzoites, (A) twenty four hours or (B) twenty one days after challenge. Each symbol represents an individual mouse. Horizontal lines represent the mean values of the respective group (± SD).Statistical significant differences between groups is indicated (Mann-Whitney U, *P < 0.05; ** $P \leq 0.01$; *** $P \leq 0.001$; ****P ≤ 0.0001).....60

Abbreviations

ABC - Avidin/Biotin complex
Arg-1 - Arginase 1
AT - Adipose tissue
BAT - Brown adipose tissue
BSA - Bovine serum albumin
CNS - Central nervous system
DAB - 3,3'diaminobenzidine
ELISA - Enzyme-Linked Immunosorbent Assay
FALC - Fat-associated lymphoid clusters
FBS - Fetal bovine serum
FVD - Fixable viability dye
GAT - Gonadal adipose tissue
HBSS - Hanks Balanced Salt Solution
HE - Haematoxylin-eosin
HPRT - Hypoxanthine phosphoribosyl-transferase I
IFAT - Indirect Fluorescent Antibody Test
IFN-γ - Interferon gamma
IL - Interleukin
IHC - Immunohistochemistry
IMAT- Intramuscular adipose tissue
i.p. – Intraperitoneal
KO - Knock out
LPS - Lipopolysaccharide
MAT - Mesenteric adipose tissue
MEM - Minimal Essential Medium
MHC - Major histocompatibility complex
MLN - Mesenteric lymph node
NAT - *Neospora* Agglutination Test
NcT - *Neospora caninum* tachyzoites
NK - Natural killer
NO - Nitric oxide
NoNo - Non-POU-domain containing octamer binding protein
Nos2 – Inducible nitric oxide synthase 2
OAT - Omental adipose tissue

PBS - Phosphate-buffered saline

RT-PCR - Real-time polymerase chain reaction

SAT - Subcutaneous adipose tissue

SDS - Sodium dodecyl sulphate

SVF - Stromal vascular fraction

TBS - Tris-buffered saline

TCR - T cell receptor

TGF-β - Transforming growth factor beta

TLR - Toll-like receptor

TNF-α - Tumor necrosis factor alpha

Treg - T regulatory

WAT - White adipose tissue

WT - Wild-type

1. Introduction

1.1. *Neospora caninum*

Neospora caninum is an obligate intracellular parasite, first identified as the causative agent of encephalomyelitis in dogs by Björkås *et al.* in 1984 [1]. The isolation and purification of this parasite was made in 1988 by Dubey *et al.* [2] which described the new genus *Neospora* belonging to the Phylum Apicomplexa, family Sarcocystidae. Neosporosis, the disease caused by *N. caninum* was first described in cattle on a dairy farm in America in 1989 by Dubey *el al.* 1989, [3]. Subsequently, clinical neosporosis has also been reported in sheep, goats, deer, rhinocerus, and horses. Moreover, antibodies to *N. caninum* have been found in the sera of water buffaloes, red and gray foxes, coyotes, camels, and felids [4-5].

Because two rhesus monkeys (*Macaca mulata*) have been successfully infected with *N. caninum* by Barr *et al*. in 1994 [6], there is a concern about the zoonotic potential of *N. caninum*. However, at present, there is no evidence that *N. caninum* successfully infects humans [6]. Some studies that assessed serological evidence of the parasite in humans were made and recently McCann *et al.* sought immunologic evidence of human exposure to the parasite in 3700 serum samples from the general population and from a high-risk group of farm workers. From these studies, no evidence of human exposure to *N. caninum* was obtained [7].

1.1.1. Life cycle

N. caninum life cycle is typified by the three known infectious stages: tachyzoites, tissue cysts and oocysts [8]. Tachyzoites and tissue cysts are the stages found in the intermediate hosts and they occur intracellularly [9]. Tachyzoites are approximately 6 × 2 µm. Tissue cysts are often round or oval in shape, up to 107 µm long and are found primarily in the central nervous system. The tissue cyst wall is up to 4 µm thick and the enclosed bradyzoites are 7-8 × 2 µm. *N. caninum* unsporulated oocysts were 11.7 × 11.3 µm in size [10].

As a definitive host, the dog sheds unsporulated oocysts in the environment for 5 to 17 days after the ingestion of tissue cysts of infected animals [8-10]. After 3 days in the environment, the oocysts sporulate. It is unclear how long oocysts will survive in the environment. Intermediate hosts, such as cattle, ingest oocysts that are found in

contaminated food and water [11]. Sporozoites are released in the intestinal tract where they penetrate cells and become tachyzoites. Tachyzoites divide and quickly spread to other host cells, which they invade and often destroy. Tachyzoites have been found in neural cells, macrophages, fibroblasts, vascular endothelial cells, hepatocytes, muscular cells [12], and the placenta in pregnant cows [13]. In neural cells, tachyzoites can transform into bradyzoites when a strong immune response is mounted against the protozoan elsewhere in the body. The bradyzoites form tissue cysts for protection [14]. Tachyzoites in placental tissue and likely bradyzoites in tissue cysts could be consumed by a dog and implanted in their gastrointestinal tract. There the parasitic forms will mature, begin to shed oocysts, and complete the horizontal transmission cycle [15].

The principal route of infection in cattle is transplacental (vertical) transmission [16-17] and the same cow can pass the infection to multiple offspring [18]. Transplacental infection can occur when tachyzoites are transmitted from an infected dam to her fetus during pregnancy. Recently, the terms “exogenous transplacental transmission” and “endogenous transplacental transmission” have been proposed to describe more precisely the origin of the transplacental infection of the fetus [2]. Exogenous transplacental transmission occurs after a primary, oocyst-derived, infection of a pregnant dam, while endogenous transplacental transmission occurs in a persistently infected dam after reactivation of the infection during pregnancy. A depressed cellular immune response to *N. caninum* antigens was reported to occur during gestation [19].

Serological evidence of *N. caninum* infection by using immunohistochemistry or polymerase chain reaction has been found in many mammals other than cattle and dogs. These include goats [20], sheep [21], horses [22], deer [23], foxes [24-25], dingoes [26], raccoons [27], and coyotes [28]. Gondim *et al*. in 2004, has confirmed that coyotes are a definitive host as well [29]. The canids listed above may also be definitive hosts, while the herbivores listed above may also be intermediate hosts.

The relative proportion of vertical versus horizontal transmission in a farm or region is likely dependent on the current seroprevalence of infection in the cattle population, as well as the distribution of infected dogs and, maybe, other canids in the region and their access to cattle and their feeds.

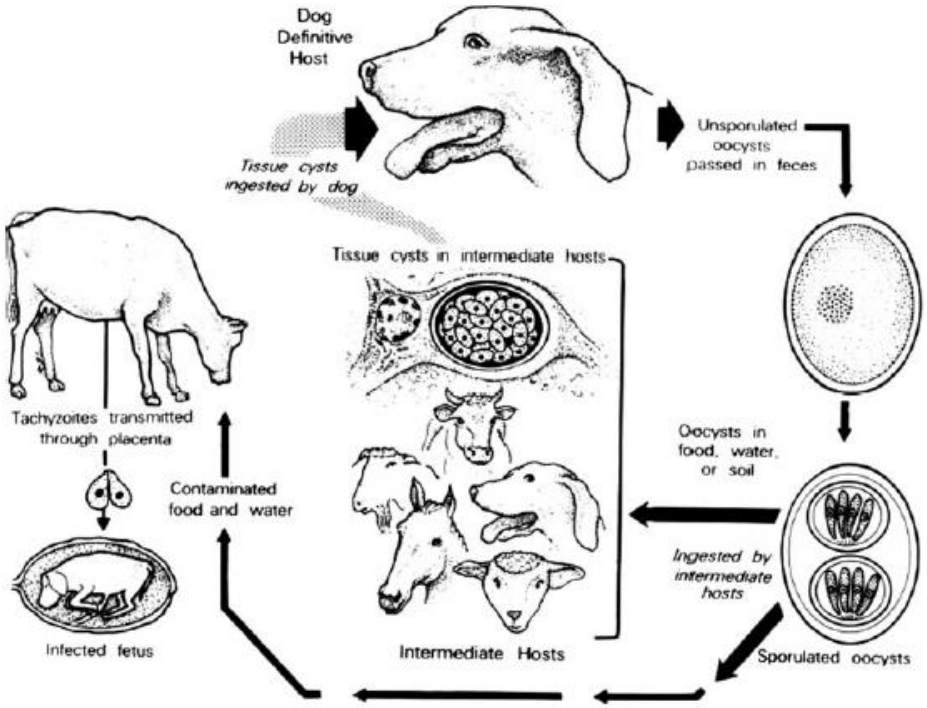

Fig.1 - Life Cycle of *Neospora caninum* [15].

1.1.2. Transmission of *N. caninum* in dogs

Historically, vertical transmission of neosporosis was first recognized in dogs when three successive litters from a bitch in Norway were found to have neosporosis [30-31]. Transplacental transmission in experimentally infected dogs was afterwards demonstrated [32]. In most cases of neonatal neosporosis, clinical signs are not apparent until 5 to 7 weeks after birth [12]. These data suggest that *N. caninum* is transmitted from the dam to the neonates on the terminal stages of gestation or postnatally via milk. According to Barber and Trees [33], vertical transmission of *N. caninum* in dogs is considered highly variable and not likely to persist in the absence of horizontal infection. However, the main route by which dogs become infected is by ingesting infected tissues [34]. Age-related prevalence data indicate that the majority of dogs become infected after birth. Higher prevalences have been documented in older than in younger dogs [35-36].

1.1.3. Transmission of *N.caninum* in cattle

N. caninum is one of the most efficiently transplacentally transmitted parasites among all known microbes in cattle. The ingestion of sporulated *N. caninum* oocysts

from the environment is the only demonstrated natural mode of infection in cattle after birth [14, 37]. To date, cow-to-cow transmission of this parasite has not been observed [37]. The primary clinical manifestation of infection in cattle is abortion. This is most common at 5–7 months of gestation, but can happen anywhere from 3 months of gestation to term. Although there are no clinical signs in the infected dam, the outcome depends on fetal age. If the fetus dies in early gestation it may be resorbed or mummified. However, the most commonly observed manifestation is expulsion of a fetus showing no gross lesions or only moderate autolysis. If the calf is carried to term there are several potential outcomes. Most commonly it will be born clinically normal but congenitally infected [38]. Such calves will maintain the infection in the herd, although they have an increased risk of abortion. Finally, an infected dam can also give birth to a non-infected calf, thus breaking the *N. caninum* life cycle [5, 39-40].

1.2. Neosporosis

1.2.1. Clinical signs of affected animals

Young dogs congenitally infected develop the most severe cases of neosporosis. They develop hind limb paresis that develops into a progressive paralysis. The hind limbs are more severely affected than the front limbs and often in rigid hyperextention. Other dysfunctions which occur include difficulty in swallowing, paralysis of the jaw, muscle flaccidity, muscle atrophy and even heart failure [41].

N. caninum causes abortion in both dairy and beef cattle. Most neosporosis-induced abortions occur at 5-6 month gestation. A fetus that acquires the infection prior to sufficient development of an immune response may become overwhelmed with a disseminated infection leading to death. This may occur through the sixth month of gestation, but later in gestation, the number of *N. caninum*-induced fetal deaths is greatly reduced [42]. In fetal death and abortion due to neosporosis, there are characteristic disseminated inflammatory lesions in the brain, lungs, heart, liver, kidney, muscles, and other organs. *N. caninum* infected calves may have neurologic signs, be underweight, or be born without clinical signs of disease. Neurologic examination may reveal ataxia, decreased patellar reflexes. Calves may have exophthalmia or asymmetrical appearance in the eyes. *N. caninum* occasionally causes birth defects including hydrocephalus [43].

1.2.2. Diagnosis

Examination of the serum from an aborting cow is only indicative of exposure to *N. caninum* and histological examination of the fetus is necessary for a definitive diagnosis of neosporosis [4]. The brain, heart, liver, placenta, and body fluids or blood serum are the best specimens for diagnosis. Although lesions of neosporosis may be found in several organs, fetal brain is the most consistently affected organ [2]. Immunohistochemical staining (IHC) is a method that can be used to identify the parasite. However, IHC staining can underestimate the true prevalence of infection due to low sensitivity. This test is still used to confirm *N. caninum* parasites in tissues where characteristic inflammatory lesions are observed on histological examination [5].

Serological diagnosis of *N. caninum* infection was reviewed recently [44]. At present, the major types of serologic tests most commonly employed for the diagnosis of this parasite infection are the enzyme-linked immunosorbent assay (ELISA), the indirect fluorescent antibody test (IFAT), and the *N. caninum* agglutination test (NAT). Some modifications to improve the specificity of *N. caninum* ELISA tests include the use of monoclonal antibodies to specific immunoglobulins [45]. Serodiagnosis is best employed for evaluation of herd exposure and risk of parasite infection. [45].

Detection of parasitic DNA by PCR is a more sensible method for the diagnosis of neosporosis. It allows not only detection of the parasite but also quantification of parasitic DNA [45].

1.2.3. Economical impact of neosporosis

The possible effects of neosporosis on productivity in cattle include reproductive losses, reduction in milk production, premature culling, and reduced weight gain [46]. Since the discovery of *N. caninum* as a cause of cattle abortions in the late 1980s, this parasite has become the most commonly diagnosed cause of abortions worldwide. Cattle industries estimated the annual global loss due to *N. caninum* abortions as at least US $2,380 million (US $1,739 million in the dairy industries and US $641 million in the beef industries, respectively) [46].

1.2.4. Control Methods

As stated earlier, *N. caninum* is efficiently transmitted vertically in cattle, perhaps for several generations. Therefore, *N. caninum* infected cows must be considered a reservoir that may allow the parasite to spread to other cattle in the herd slowly by endogenous transplacental transmission. As a consequence, farmers may

decide to remove infected cows or their progeny from the herd. The culling of infected cows is a control option that is effective [2].

Prevention of dogs and other potential definitive hosts from contaminating pastures and feedstuff with feces is recommended. In dairy farms, the presence of dogs should be avoided, or at least dog-proof fencing should be provided and the access of dogs to the housing zone and the barn and feed storage areas should be avoided. Consumption of aborted bovine fetuses does not appear to be an important source of *N. caninum* infection in dogs [6]. The consumption of placental membranes may be a source of *N. caninum* infection in dogs because the parasite has been found in naturally-infected placentas and dogs fed placentas shed *N. caninum* oocysts [2].

Other options to control neosporosis are vaccination and chemotherapy. There is no proven vaccine to prevent *N. caninum* abortion in cattle [47]. However, encouraging results have been obtained in mice [47]. Another therapeutic approach, till now only tried in research environment, is chemotherapy [2]. An effect of toltrazuril and its derivative ponazuril on tachyzoites of *N. caninum* has been shown *in vitro* and *in vivo* in calves. The major problem with this approach is about the final use of these animals which is for food purposes either as milk or meat and the possibility of affect the quality of them. Another drawback is the high cost of the treatment [2, 6].

1.2.5. Murine Models

N. caninum infection can be performed experimentally in a number of animal models. The use of murine models brings many advantages in the study of neosporosis, in spite of dogs and cattle being the main hosts affected by *N. caninum* infections. Mice small size and quick reproduction allow studies with a high number of animals. Moreover, a vast range of reagents for immunological studies are also available to study this species [48]. The validation of mice as a model to study neosporosis came from numerous studies that demonstrate mice were considered as valuable model for vaccination against *N. caninum* cerebral infection and vertical transmission and were extensively used for this purpose [47]. Moreover, immune-deficient mice were considered for the study of specific immune responses to infection or formation of tissue cysts containing bradyzoites [1].

Studies were shown that however BALB/c mice mount an immune response able to contain this parasitic infection, the presence of parasite DNA detected in the brain of the infected mice, without apparent associated pathology, indicates that a chronic asymptomatic infection may have been established, similarly to what was previously described in calves infected with this parasite [49-50]. In another study it

was shown that C57Bl/6 mice are susceptible to encephalitis associated with *N.caninum* infection [48]. As it holds true for cattle, an immunomodulation toward a Th2 type response associated with high interleukin 4 (IL-4) production is usually observed during pregnancy of BALB/c mice, thus favoring the proliferation of the parasite and the vertical transmission [51].

Tachyzoites tend to be used since they are easier to recover than are *N. caninum* oocysts, which are shed in low amounts [52-53].

1.3. Immunity to *Neospora Caninum*

1.3.1. Host immune response in cattle

A first line of defense against invading pathogens is mediated by natural killer (NK) cells [54]. *In vitro* studies have demonstrated the capacity of bovine NK cells to produce interferon gamma (IFN-γ) after the exposure to *N. caninum*-infected fibroblasts, a response independent of interleukin IL-12, but potentiated in the presence of this cytokine. Bovine NK cells were shown to have the ability to lyse *N. caninum* infected fibroblasts [55]. This may provide the cytokine environment necessary for the activation of the adaptive immune system towards a Thelper1 (Th1)-type response. Indeed, it has been shown that infected cattle elicit a Th1-type response associated with $CD4^+$ T-cell activation and IFN-γ expression [56].

Pro-inflammatory cytokines may be regulated by interleukin 10 (IL-10), IL-4 and transforming growth factor beta (TGF-β), cytokines that are highly expressed at the materno-fetal interface to avoid fetal rejection, but at the same time they allow parasite proliferation and vertical transmission [55]. The immune response of the fetus also plays a crucial role for the outcome of the infection. A specific antibody response of the fetus against *N. caninum* was found at least from day 100 of gestation onwards [58].

1.3.2. Host immune response in mice

It appears that both cellular and humoral immune responses are important to control the infection in mice [59]. Nevertheless, differences are observed between different strains of mice. The immune response in inbred strains may differ between the strains, due to their specific relative haplotype. It seems however that the principal mechanism of protection against *N. caninum* infection involves mainly IFN-γ and IL-12 [47]. The importance of this specific cytokines and their central role in resistance to acute neosporosis was observed *in vivo*. Abe *et al.* had described that

murine macrophages showed greater activation and increased IL-12, and IFN-γ production during *N. caninum* infection [60]. In fact, BALB/c mice are resistant to acute *N. caninum* infection while BALB/c background IFN-γ-deficient mice and BALB/c mice treated with an antibody neutralizing IFN-γ have increased morbidity and mortality after parasite infection [61]. Moreover, C57BL/10ScCr mice which lack a functional interleukin-12 receptor are highly susceptible to an i.p. challenge with *N. caninum*, developing lethal acute neosporosis [1].

Macrophages activation with IFN-γ exhibits a killing activity against *N. caninum*, which is associated with increased production of nitric oxide [62]. In addition to that, activation of peritoneal macrophages with IFN-γ also exhibits a killing activity against *N. caninum*, associated with increased production of nitric oxide [63]. Furthermore, macrophages activate specific T lymphocytes by presenting pathogen-derived antigens in association with major histocompatibility complex (MHC) molecules [62]. Macrophages and mostly dendritic cells appear to be the antigen presenting cell greatly responsible for generating primary T cell responses [63]. Dendritic cells were shown, with macrophages, to be the major producers of IL-12 during the initial stages of murine infection with the closely related apicomplexan parasite *Toxoplasma gondii* [64]. Teixeira *et al.* showed in a murine model that both conventional and plasmacytoid dendritic cells are early sources of IL-12 during infection with *N. caninum* [65].

Th1-type responses have a key role in immunoprotection against this parasitic infection [66]. Indeed, BALB/c mice treated with a monoclonal antibody specific for CD4 showed an increase in morbidity and mortality after *N. caninum* infection [61]. Interestingly, Tanaka *et al.* have proved a major role of $CD4^+$ T cells in response to *N. caninum* infection as compared with $CD8^+$ T cells by showing that BALB/c mice depleted of $CD4^+$ T cells succumbed to infection earlier than mice depleted of $CD8^+$ T cells [67].

The importance of the humoral immune response was also demonstrated. Intraperitoneal inoculation of *N. caninum* tachyzoites into BALB/c mice induces an acute response characterized by a rapid increase in the numbers of CD69-expressing peritoneal and splenic B cells [68]. This early B-cell stimulatory effect preceded an increase in the numbers of total and immunoglobulin-secreting splenic B cells and a rise in serum levels of *N. caninum*-specific immunoglobulins, predominantly of the immunoglobulin G2a isotype [68].

1.3.3. Changes in the host-parasite relationship during pregnancy

Neosporosis is a disease that manifests during pregnancy where the developing fetus is particularly vulnerable. Various changes occur in the maternal immune response to enable the dam to support the pregnancy and prevent immunological rejection. These natural changes in the immune system may favor the parasite and help to explain disease pathogenesis in pregnancy [55]. The pro-inflammatory cytokines such as IFN-γ and IL-12 are involved in the generation of Th1-type immune responses that may be damaging to the pregnancy. The cytokine environment of the placenta favors more regulatory Th2-type cytokines such as IL-10, IL-4 and TGF-β whose role is to counteract the inflammatory responses induced by the Th1-type cytokines [55, 69]. Thus the natural immuno-modulation occurring in the pregnant dam resulting in a bias towards Th2-type immune responses may compromise her ability to control *N. caninum* multiplication and the Th1-type immune responses, known to protect against *N. caninum*, may themselves be detrimental to the pregnancy [55].

1.3.4. Vaccination strategies against *Neospora caninum*

Beside the use of live-attenuated parasites or killed parasite lysates for vaccination of cattle, many studies focused on the use of recombinant antigens, either delivered as purified proteins or as DNA vaccines [70]. A majority of these investigations were conducted on target proteins that were involved in the adhesion/invasion process of the host cell by the parasite [47]. The basic mechanisms on how host cell invasion is achieved are clearly conserved among the phylum Apicomplexa, and *Toxoplasma gondii* has been the prime model apicomplexan to investigate this process at the molecular level [71].

An efficient vaccine against *N. caninum* infection should fulfill the following requirements: prevention of tachyzoite proliferation and dissemination in pregnant cattle to avoid transplacental transmission to the fetus; prevention or reduction of oocyst shedding in dogs; prevention of tissue cyst formation in animals that have been infected with oocysts or tissue cysts [47]. Different types of vaccines have been investigated, either in bovines or in the mouse model. These include live vaccines such as naturally less virulent isolates of *N. caninum*, attenuated strains generated by irradiation or chemical means, or genetically modified transgenic strains [70]. In experimental models, live *N. caninum* vaccines were shown to be very effective in cattle and in mice [47]. However, there are serious disadvantages in terms of safety, costs of production, and stability of the final product. Killed parasites vaccines offer a

safer alternative, but failed to confer significant protection against vertical transmission in cattle [72].

For several years a commercial vaccine against bovine neosporosis based on killed tachyzoite lysate (Bovilis Neoguard™) had been available in few selected countries. This vaccine exhibited moderate protection in field trials, with a reduction in abortion rates up to 50% [73]. However, more recent trials revealed big differences in efficacy at the farm level, and suggested that vaccination itself may increase the risk of early embryonic death [74]. The vaccine has now been withdrawn from the market. To date, the current evidence suggests that the most promising approach for prevention of *N. caninum* infection is through a live-vaccine such as the low virulence strain Nc-Nowra [47]. A recent study confirmed the efficacy of the vaccine in reducing the vertical transmission after challenge with a virulent isolate [75]. Moreover, the vaccination appeared very safe, although a reduction of pregnancy rate after artificial insemination was observed in some vaccinated groups compared to non-vaccinated controls.

1.4. Adipose Tissue

1.4.1. Classification, structure and physiology

Two types of adipose tissue can be distinguished, which have essentially antagonistic functions: white adipose tissue (WAT) stores excess energy as triglycerides and brown adipose tissue (BAT) is specialized in the dissipation of energy through the production of heat. BAT is abundant in small mammals and in newborns and helps them to survive cold temperatures [76].

White adipocytes are spherical cells whose variable size mainly depends on the size of the single lipid droplet stored in them. This lipid droplet consists of triglycerides and accounts for more than 90% of the cell volume. Mitochondria in white adipocytes are thin, elongated, and variable in amount. Brown adipocytes in contrast contain triglycerides as multiple small vacuoles; they are typically polygonal with a variable diameter. The most characteristic organelles of BAT cells are the mitochondria. They are large, spherical, and usually numerous. Because of its greater oxygen demand brown fat also contains more capillaries than white fat. Also, nerve supply is denser in BAT than in WAT [76]. The brown color of BAT is attributable to its high mitochondrial density and high vascularization. Whereas WAT stores excess energy as triglycerides, the function of BAT is to dissipate energy through the production of heat. In adult humans, brown fat has been found to be distributed throughout the cervical, supraclavicular, axillary, paravertebral, and upper abdominal regions [76].

As described by Usui *et al.*, white adipose tissue can be divided in abdominal subcutaneous fat and intraabdominal fat. Intraabdominal adipose tissue is composed of visceral fat, mainly composed of omental, mesenteric and gonadal fat [77]. The omentum is a structure within the peritoneal cavity comprised largely of adipose tissue and mesothelial cells. Distinct aggregates of lymphoid cells, termed ‘‘milky spots’’ due to their dense clustering and appearance, were first observed in the omenta of rabbits [78]. Subsequent work has demonstrated that this tissue is a rich source of lymphocytes and monocytes, and possesses tremendous antimicrobial and angiogenic properties [78]. On the other hand, visceral mesenteric and gonadal adipose tissue presents structures named *fat-associated lymphoid clusters* (FALC´s). The immune cells in the FALC´s consisted of mainly T-cells and some B-cells. The majority of T-cells were $CD4^+$ helper T (Th) cells, rather than $CD8^+$ cytotoxic T-cells [79].

1.4.2. Functions

The traditional view of adipose tissue as a passive reservoir for energy storage is no longer valid. Adipose tissue is now known to express and secrete a variety of bioactive peptides, known as adipokines, which act at both the local (autocrine/paracrine) and systemic (endocrine) level. In addition to these efferent signals, adipose tissue expresses numerous receptors that allow it to respond to afferent signals from traditional hormone systems as well as the central nervous system (CNS) [80]. Thus, besides the biological repertoire necessary for storing and releasing energy, adipose tissue contains the metabolic machinery to permit communication with distant organs including the CNS. Through this interactive network, adipose tissue is integrally involved in coordinating a variety of biological processes including energy metabolism, neuroendocrine function, and immune function [80].

Besides adipocytes, adipose tissue contains connective tissue matrix, nerve tissue, stromovascular cells, and immune cells, which constitute the stromal vascular fraction (SVF) of adipose tissue. Although adipocytes express and secrete several endocrine hormones such as leptin and adiponectin, many secreted proteins are derived from the non-adipocyte fraction of adipose tissue [81].

1.4.3. Innate immune system in adipose tissue

Innate immune-cell responses are evoked by general danger signals associated with invading pathogens, for instance via pattern-recognition receptors such as TLRs.

Innate immune cells including neutrophils, dendritic cells, macrophages, mast cells, and eosinophils have all been identified in adipose tissue [82].

Upon infection, neutrophils are generally among the first immune cells to arrive at the site of inflammation. However, only a few studies in obese mice were performed to understand the role of neutrophils in infection which suggest systemic neutrophil activation [83].

Macrophages and monocytes represent a large proportion of the SVF in adipose tissue. Based on their cytokine profile secretion and cell surfer markers, adipose tissue macrophages are classified in two main types: macrophages M1 and M2. M1 macrophages are the first line of defense against intracellular pathogens, characterized by expression of CD11c and are stimulated by IFN-γ or by LPS. M1 are producers of reaction oxygen species and nitric oxide through the expression of inducible NO synthase. M2 macrophages, characterized by expression of CD206, resulting from induction by IL-4 and IL-13 is associated with tissue repair and humoral immunity producing immunosuppressive factors, such as IL-10 or arginase [84]. In obesity, M2 macrophages polarize towards a pro-inflammatory phenotype having an enhanced pro-inflammatory cytokine production, such as TNF-α and IL-12. They express CD11c and their differentiation is promoted by agents such as IFN-γ and lipopolysaccharide (LPS) [85].

For modulation of local immune responses, tissue-resident macrophages are often assisted by other innate immune cells, such as TLR-proficient mast cells [86].

Although eosinophils are associated with allergic diseases and helmintic infections, the biologic role of these cells in adipose tissue remains incompletely defined. It has been shown that eosinophils are the main source of IL-4 and IL-13 in white adipose tissues of mice, and, in their absence, M2 macrophages are greatly attenuated [86].

1.4.4. Adaptive immune system in adipose tissue

While innate immune-cell responses are evoked by danger signals and play a key role in the initiation of infection, lymphocytes exert adaptive immune functions crucial for a specific and decisive immune response, and for the development of immunological memory [87].

$CD4^+$ T cells are crucial in achieving a regulated effective immune response to pathogens. In adipose tissue, $CD4^+$ T cells are mainly classified into the classical Th1 and T-helper2 (Th2) although new subsets have been identified including T-helper17 (Th17) [88]. The roles for $CD4^+$ T lymphocytes in adipose tissue are related to the

regulation of body weight, adipocyte hypertrophy and glucose tolerance. Thus, $CD4^+$ cells play a key role in the control of disease progression in diet-induced obesity [89]. Th1 cells show a pro-inflammatory profile, secreting IFN-γ, which elicits the production of macrophage mediators, induces leukocyte adhesion molecules, as well as increases antigen presenting capacity by macrophages [79]. On the other hand, Th2 may be considered anti-inflammatory cells and are a source of IL-4 and IL-13 [79]. The infiltration of $CD8^+$ T cells in adipose tissue seems to contribute to macrophage influx and M1 polarization initiates adipose tissue inflammation [85].

Regulatory T cells (Tregs) are critical in the preventing inappropriate immune responses such as inflammation because they control the behavior of other T cell populations and influence the activities of the innate immune system cells [90].

B1 B cells respond to pathogen-associated molecules more rapidly than B2 B cells and with a less diverse antibody repertoire. B1 B cells confer resistance to some bacterial and viral infections, probably through antibody production, which tends to be of the IgM isotype [79]. B2 cells comprise the majority of B lymphocytes in immune organs, such as spleen and lymph nodes, but also in adipose tissue. B2 cell derived high-affinity IgG2c antibodies influence macrophage polarization because the influx of adipose tissue resident B cell numbers precedes M1 polarization [86].

1.4.5. Adipokines produced by adipose tissue

1.4.5.1 Leptin

Adipocytes are the most important source of leptin, and circulating leptin levels directly correlate with adipose tissue mass. Control of appetite is the primary role of leptin. Inflammatory cytokines, including TNF, interleukin-1 (IL-1) induce leptin production [80]. Leptin regulates pancreatic islet cells, growth hormone levels, immunology homeostasis, hematopoiesis, angiogenesis, wound healing, osteogenesis, and gastrointestinal function [91]. Decreased leptin signaling or receptor function increased energy intake and lowers energy expenditure, with leptin deficiency itself being a known cause of severe early-onset obesity, hypogonadism, hyperinsulinemia, hyperphagia, and impaired T cell mediated immunity [91].

1.4.5.2. Adiponectin

Adiponectin is highly and specifically expressed in differentiated adipocytes and circulates at high levels in the bloodstream. Although adipocytes are the most

important source of adiponectin, serum adiponectin levels do not increase with obesity as leptin levels do. On the contrary, there is a tendency for reduced adiponectin levels in obese subjects [91].

The anti-inflammatory activities of adiponectin extend to inhibition of IL-6 production accompanied by induction of the anti-inflammatory cytokines IL-10 and IL-1 receptor antagonist. Inhibition of nuclear factor kB (NF-kB) by adiponectin might explain at least part of these effects. Adiponectin induces endothelial VCAM-1, ICAM-1, and pentraxin-3 expression. The hormone, by decreasing reactive oxygen, is an antioxidant. Adiponectin augments endothelial nitrous oxide production, acting to protect the vasculature by reduced platelet aggregation and vasodilation [80].

1.4.6. Adipose tissue infection by other microorganisms

Recent studies indicate that adipose tissue and adipocytes are targets for a few parasites infection. Some parasites can even use adipose tissue as a reservoir where they can remain dormant. Nagajyouthi *et al.* demonstrated that in infection with *Trypanosoma cruzi*, there was a significant influx of macrophages into adipose tissue [92]. Combs *et al.* demonstrated that adipose tissue and adipocytes are invaded by *T. cruzi* and that parasites persist in adipose tissue long after the acute phase has subsided [93].

Another example is the bacteria *Rickettsiae prowazekii* which can remain dormant for years or even decades in patients who recover from the primary infection. In certain individuals, stress or waning immunity are likely to reactivate this persistent infection [94]. Bechah *et al.* demonstrate that adipose tissue serves as a reservoir for recrudescent disease caused by dormant infection with *R. prowazekii*, and suggest that adipocytes are the specific cell type in which dormant rickettsiae reside [95].

The adipose tissue has also been identified as a tissue supporting early viral infections such as gammaherpesvirus infection. This virus is characterized by their ability to establish lifelong latent infection and there are some evidences that the omentum is a local of chronic infection that may contribute to the maintenance of that infection [96]. Gray *et al.* demonstrate a marked immunological response to this virus infection in the omentum, including growth and expansion of immune aggregates. Furthermore, the omentum harbored a stable frequency of viral genome-positive cells through early and into long-term latency, while removal of the omentum prior to infection resulted in a slight decrease in the establishment of splenic latency following intraperitoneal infection [96].

In summary, the importance of adipose tissue in participating in immune responses and its function as a reservoir for several pathogens has been documented. Therefore, in this study we will investigate the role of adipose tissue in the host immune response to *N. caninum* infection. For that, immune cell populations such as macrophages and regulatory T cells will be characterized. Since the importance of IFN-γ in *N. caninum* infection was already demonstrated, we will determine the cellular sources of this protective cytokine in the adipose tissue of mice infected with this protozoan.

2. Material and Methods

2.1. Mice

Female C57BL/6 mice (7-11 week-old) were purchased from Charles River Laboratories and housed at the animal facilities of the Instituto de Ciências Biomédicas (Porto, Portugal) during the experimental procedures. Hiding and nesting materials were provided as enrichment. All the animal procedures were performed according to the European Convention for the Protection of Vertebrate Animals used for Experimental and Other Scientific Purposes (ETS 123) and directive 2010/63/EU of the European parliament and of the council of 22 September 2010 on the protection of the animals used for scientific purposes and Portuguese rules (DL 113/2013).

2.2. Parasites

Neospora caninum tachyzoites (NcT) (Nc-1, ATCC®(50843)) were serially cultured in VERO cells and maintained at 37º C in Minimum Essential Medium (MEM), containing Earle's salts (Sigma, St Louis, USA) supplemented with 10% fetal bovine serum (FBS), 2 mM L-Glutamine, penicillin (200 IU/ml) and streptomycin (200 µg/ml) (all from Sigma, St Louis, USA) in an humidified atmosphere of 5% CO_2 in air. Free parasitic forms of NcT were obtained following a few steps. First, infected VERO cells were cultured until the host cell monolayer was 90% destroyed. Culture supernatants and adherent cells, harvested using a cell scrapper, were centrifuged at 1500 *g* for 20 minutes. The pellet was then passed through a 25G needle and washed three times in Phosphate Buffered Saline (PBS) by centrifugation at 1500 *g* for 20 minutes. The final pellet was ressuspended in 3 ml of PBS and passed through a Sephadex ™ G-25M-filled PD-10 column (Amersham Biosciences Europe GmbH, Freiburg, Germany). Parasite density was determined with a hemocytometer. The parasites used in the experiments had 4-7 *in vitro* passages from the original ATCC vial.

2.3. Challenge infection

Neospora caninum infection was performed by intraperitoneal (i.p.) route with 1×10^7 NcT in PBS. Control animals were simultaneously injected with 0.5 ml of PBS.

2.4. Collection of biological samples

Mice were isoflurane anesthetized for retro-orbital blood collection and euthanized by cervical dislocation at twenty four hours, seven days, twenty one days or two months post-infection. For flow cytometry analysis, samples from gonadal adipose tissue (GAT), mesenteric adipose tissue (MAT) and omental adipose tissue (OAT),

were collected, as well as inguinal subcutaneous adipose tissue (SAT) and mesenteric lymph nodes (MLN). Samples were removed and placed in Hanks Balanced Salt Solution (HBSS) supplemented with 4% bovine serum albumin (BSA), 10 mM HEPES Buffer (Sigma-Aldrich, St Louis, USA) for further analysis. For other experiments, in addition to adipose tissue (AT) specimens and MLN, liver, muscle, kidneys, lungs, heart, pancreas, brain, stomach, sections of small and large intestine, spleen, thymus and uterine horns were also removed. All samples were sliced in two similar pieces, and either formalin-fixed for histological analysis or stored at –80ºC for DNA extraction. Blood collected was allowed to clot overnight. Mouse serum was then obtained through centrifugation (381 g, 15 minutes) and stored at –80ºC.

2.5. Histopathological examination and immunohistochemistry

Four sagital sections (3 mm gap) of each formalin-fixed sample were sliced. Both AT samples and organs were dehydrated, embedded in paraffin, and then sliced in four serial sections. One section was stained with haematoxylin-eosin (HE), while immunohistochemistry for F4/80 and Foxp3 molecules or NcT was performed in the other three slices of adipose tissue samples, according to the modified avidin-biotin-peroxidase complex (ABC) method. Paraffin-embedded mice organs were only stained for NcT. Briefly, deparaffinized and rehydrated sections, for both Foxp3 and NcT staining, were exposed to adequate heat-induced antigen retrieval with 1M citrate buffer (pH=6.0), for 2-3 minutes and, specifically for Foxp3 staining, the subsequent inactivation of endogenous biotin was performed using Avidin/Biotin Blocking Kit (Vector Laboratories). Likewise sections for Foxp3 and NcT, slices for F4/80 staining were incubated with 0.3% hydrogen peroxide in methanol (Merck, Darmstadt, Germany) for 20 minutes, to block endogenous peroxidase activity. Sections were then incubated into a moist chamber for 20 minutes with normal rabbit serum (Dako, Glostrup, Denmark), diluted 1:5 in 10% BSA (Sigma-Aldrich, St Louis, USA), to prevent non-specific staining. Excess serum was discarded and sections were incubated with the following primary antibodies: rat/mouse anti-F4/80 (1:100, eBioscience), rat/mouse anti-Foxp3 (1:150, eBioscience) or goat anti-*N. caninum* polyclonal serum (1:1500, VMRD, Pullman, WA). Incubation periods were the following: 90 minutes, at 37 ºC for Foxp3; 75 minutes, at room temperature for F4/80 and 90 minutes, at room temperature for NcT staining. Subsequently, F4/80- and Foxp3-stained sections were incubated for 30 minutes with biotin-labelled anti-rat secondary antibody (1:200, Dako, Glostrup, Denmark) and then with the avidin-biotin-peroxidase complex (Dako, Glostrup, Denmark), for further 30 minutes. In opposition, NcT-stained slices were incubated with HRP-labelled anti-goat secondary antibody (Millipore, Billerica, MA,

USA) dilutes 1:1000 for 30 minutes. Immunohistochemical reactions were developed with 3, 3'-diamino-benzidine (DAB + Substrate System; Dako, Glostrup, Denmark). All sections were counterstained with hematoxylin and permanently mounted with Entellan ® (Merck). Liver samples from infected animals were used as positive controls, for both F4/80, NcT staining, while mesenteric lymph nodes were used to validate Foxp3-positive staining.

For F4/80 and Foxp3 analysis 20 images of a section of GAT, MAT, OAT and SAT and intramuscular adipose tissue (IMAT) from each individual mouse were obtained in a 200x magnification field. Only the intramuscular adipose tissue was analysed by selecting manually the area of interest in the images obtained with the aid of the image analysis software ImageJ 1.47v (National Institutes of Health, Bethesda, MD). For Foxp3 analysis, the total number of $Foxp3^+$ cells were counted in the images and divided by the total area analysed. Because it was difficult in the F4/80 staining to accurately count individual cells, the percentage of stained area was instead determined with ImageJ in the different images.

2.6. Isolation of Stromal Vascular Fraction

Samples from GAT, MAT, OAT and lymph node-free SAT from inguinal region, as well as MLN, were collected, placed in HBSS, supplemented with 4% BSA, 10mM HEPES Buffer Solution and 2mg/mL collagenase from *Clostridium histoliticum* type II (all from Sigma-Aldrich, St Louis, USA) and incubated in a water bath (37 ºC), for 50 minutes, under shaking each 10 minutes. Mesenteric lymph nodes were used as control and were incubated 30 minutes in the water bath. Then, digested samples were homogenized to single-cell suspensions, passed through 100 µm cell strainers (BD Biosciences Pharmingen, San Diego, CA) and centrifuged at 269 g, 10 minutes, 4 °C, for further flow cytometry analysis. The supernatant was discarded being the SVF-containing pellet resuspended in HBSS medium, supplemented with 1% BSA, 1% penicillin/streptomycin, 10mM HEPES Buffer and 0.1M β-mercaptoethanol, according to cell counting in the hemocytometer.

2.7. Cell sorting

For cell sorting of macrophages present in GAT, the procedure described above for isolation of SVF cells was used except the cells were recovered in PBS supplemented with 5 mM EDTA, 25 mM HEPES and 2% FBS instead of HBSS. Cells were then incubated with anti-mouse CD16/CD32 for blocking Fc receptors, followed

by incubation with APC eFluor 780 anti-mouse F4/80 (BM8). Cells were then sorted in FACS Aria sorter (BD) accordingly to expression of F4/80.

2.8. Cytospin preparation

Cytospins of the abovementioned SVF cells and F4/80^{+}-sorted cells were prepared. Briefly, SVF-derived cells (1×10^{5}) were centrifuged at 195 g for 5 minutes using Cytospin3 apparatus (Shandon). Then, cytospin sections were fixed in ice-cold methanol, air dried and stored at -20 °C, for further analysis.

2.9. Hemacolor Staining

SVF cytospin sections from each adipose tissue sample were stained for 2 minutes in a solution of Hemacolor II and, then 3 minutes in a solution of Hemacolor III. Deionized water was used to wash cytospin sections after Hemacolor staining solutions. At the end, cell sections were permanently mounted with Entellan ® (Merck).

2.10. Flow cytometry analysis

The evaluation of cell surface markers and the subsequent cellular lineage of the SVF-derived cells from different fat depots were performed using flow cytometric analysis (FACS). A number of 1×10^{6} cells *per* sample of adipose tissue, from both control and NCT-infected mice, were stained.

SVF-derived cells were incubated with Fixable Viability Dye (FVD) eFluor 450 (1:100, eBioscience) for exclusion of dying cells. Before surface staining cells were incubated with anti-mouse CD16/CD32 in PBS, 2% BSA, 2 mM EDTA for Fc receptor blocking. For macrophage analysis, SVF cells were surface stained with Alexa Fluor 488® anti-mouse CD206 (clone C068C2, 1:100, BioLegend), APC eFluor® 780 anti-mouse F4/80 (clone BM8, 1:100, eBioscience), Brilliant Violet 510™ anti-mouse CD3 (clone 17A2, 1:100, BioLegend), PE anti-mouse NK1.1 (clone PK136, 1:100, eBioscience), PerCP-Cyanine 5.5 CD19 (clone 1D3, 1:100, eBioscience).

For the analysis of both Foxp3 and Tbet expression, the surface staining was performed with FITC anti-mouse CD4 (clone RM4-5, 1:100, eBioscience), APC anti-mouse CD25 (clone PC61.5, 1:100, eBioscience), APC-eFluor® 780 anti-mouse NK1.1 (clone PK136, 1:100, eBioscience) and BV510 anti-mouse CD3 (clone 17A2, 1:25, BioLegend). Cells were then fixed and permeabilized (Foxp3 fixation/permeabilization buffer, eBioscience, San Diego, CA), washed, and pre-incubated with anti-mouse CD16/CD32 (clone 93, 1:100, eBioscience) before intracellular staining with PE anti-mouse/rat Foxp3 (clone FJK-16s, 1:50), PE-Cy7 anti-mouse Tbet (clone eBio4b10,

1:100) or respective isotype controls (all from eBioscience, San Diego, CA) monoclonal antibodies according to manufacturer's instructions.

For the analysis of natural killer cells and T lymphocytes, the surface staining was performed with FITC anti-mouse TCR γδ (clone eBioGL3, 1:75, eBioscience), APC anti-mouse NK1.1 (clone PK136, 1:100, eBioscience), APC-eFluor® 780 anti-mouse CD8 (clone 53-6.7, 1:100, eBioscience), eFluor® 450 anti-mouse TCRαβ (clone H57-597, 1:75, eBioscience) and Brilliant Violet 510™ anti-mouse CD4 (clone RM4-5, 1:50, BioLegend). Cells were then fixed with 2% formaldehyde (Sigma), washed and permeabilized with 0.5% saponin (Sigma) in FACS. Once again, cells were incubated with anti-mouse CD16/32 (clone 93, 1:100, eBioscience) before intracellular staining with PE anti-mouse IL-10 (clone JES5-16E3, 1:100, eBioscience), PerCP-Cy5.5 anti-mouse IFN-γ (clone XMG1.2, 1:100, eBioscience) and PE-Cy7 anti-mouse IL-4 (clone BVD6-24G2, 1:100, eBioscience) or respective isotype controls (all from eBioscience, San Diego, CA) monoclonal antibodies according to manufacturer's instructions. Data acquisition was performed on a FACSCanto™ II system (BD Biosciences, San Jose, CA) using the FACSDiva™ software (BD) and compensated and analysed in FlowJo version 9.7.5. (Tree Star, Inc., Ashland, OR). A Bioexponential transformation was applied to improve data visualization.

2.11. RNA isolation and quantitative Real-Time Polymerase Chain Reaction (RT-PCR) analysis

Total RNA was extracted from SVF-derived cells of C57BL/6 mice, seven days or two months post-infection, using TriReagent™ (Sigma-Aldrich) according to manufacturer's instructions. All RNA samples were recovered in 10 µL of nuclease-free water (Sigma-Aldrich) and quantified using Nanodrop ND-1000 apparatus (Thermo Scientific). Synthesis of cDNA was then performed from 0.3-11 µg of total RNA prepared as described above in a 10 µl final volume using Maxima® First Strand cDNA Synthesis kit for RT-qPCR (Fermentas, Thermo Scientific), according to manufacturer's instructions. The PCR program run was as follows (25ºC, 10 min.; 50ºC, 30 min.; 85ºC, 5 min) using TProfessional Basic Thermocycler (Biometra GmbH, Goettingen, Germany). Real Time PCR was then used for the quantification of tumor necrosis factor-alpha (*TNF-α*), interleukin-10 (*IL-10*), arginase-1 (*Arg-1*) and inducible nitric oxide synthetase type 2 (*iNOS2*) mRNA expression levels with the Kapa SYBR Fast qPCR Kit (Kapa Biosystems Inc, Wilmington, MA) in a Rotor Gene 6000 Corbett (Qiagen). As reference genes were use hypoxanthine phosphoribosyl-transferase I (*HPRT*), a widely use reference gene, and Non-POU-domain containing octamer

binding protein (*NoNo*), described as being the most suitable reference gene for normalization comparatively to other when working with the cell line 3T3-L1 [97]. For the quantification of mRNA expression levels, the reaction was performed in a final volume of 10 µL containing 0.2µM of each specific primer: *NoNo* forward: TGC TCC TGT GCC ACC TGG TAC TC, *NoNo* reverse:CCG GAG CTG GAC GGT TGA ATG C; *Hprt* forward: ACA TTG TGG CCC TCT GTG TG, *Hprt* reverse: TTA TGT CCC CCG TTG ACT GA, *Arg1* Forward: CTC CAAG CCA AAG TCC TTA GAG; *Arg1* Reverse AGG AGC TGT CAT TAG GGA CAT C; Nos2 Forward CCA AGC CCT CAC CTA CTT CC; *Nos2* Reverse CTC TGA GGG CTG ACA CAA GG; *IL-10* Forward GCT CTT ACT GAC TGG CAT GAG; *IL-10* Reverse CGC AGC TCT AGG AGC ATG TG, *IFN-γ* forward: TGG CAA AAG GAT GGT GAC ATG, *IFN-γ* reverse: GAC TCC TTT TCC GCT TCC TGA (all from Tib Molbiol, Berlin, Germany) and 1× Master Mix plus 1 µL of the newly-synthesized cDNA. The three-step cycling qRT-PCR program was performed as follows: PCR initial activation step at 95ºC, 5 minutes and amplification in 35 cycles (denaturation [95ºC, 10s]; annealing temperature [62ºC, 20s]). At the end of each annealing phase fluorescence was measured in "single" acquisition mode with the channel setting F2/F1. Quantitative evaluation of fluorescence signals from the PCR products was performed with the Rotor-Gene software (version 1.7.75) and was determined by plotting the fluorescence signals vs the cycle numbers at which the signals crossed the baseline. The baseline adjustment was performed in "minimize error" mode. The correlation coefficient among the standard reactions assured linearity. The specificity of the qRT-PCR products was further confirmed through the melting curve.

Analysis of real-time PCR data was made by the comparative CT method. Individual relative gene expression values were calculated using the following formula: $2^{-(\text{Ct gene of interest} - \text{Ct constitutive gene})}$ [98].

2.12. DNA extraction

DNA extraction was performed in all AT samples, as well as in brain and lungs, as described by Nishikawa *et al* [99]. Briefly, samples were digested overnight with 1% sodium dodecyl sulphate (SDS) solution containing 1mg/mL Proteinase K, in a water bath at 55 ºC. DNA was then isolated using the phenol (Sigma, St Louis, USA)-choroform (MercK, Darmstadt, Germany) method, followed by ethanol precipitation. DNA from *N. caninum* tachyzoites was similarly extracted and used as positive control. Isolated DNA was recovered in an adequate volume of DNA/RNAse-free water (Sigma-Aldrich) and quantified using Nanodrop ND1000 apparatus (Thermo Scientific).

2.13. PCR for the detection of NcT

N. caninum DNA was detected using primers and a TaqMan probe designed for the Nc5 gene of *N. caninum*. The Real Time PCR was performed using the Rotor-Gene Probe PCR kit (Qiagen) in a Rotor-Gene 6000 Corbett apparatus (Qiagen). DNA amplification was performed using 1μl of DNA corresponding to 500-2000 ng in a final volume of of 10μl. Master mix was prepared containing 0,2 μM of each primer (Forward primer, Neo S: 5'- GTTGCTCTGCTGACGTGTCG; Reverse primer Neo A 5'-GCTACCAACTCCCTCGGTT), 0.2 μM of Taqman® probe Neo TM (6FAM-CCCGTTCACACACTATAGTCACAAACAAAA-BBQ) (all designed by Tib Molbiol) and 1× Master Mix. The PCR program run was as follows: 1) PCR initial activation step at 95ºC, 3minutes 2) amplification in 60 cycles (including denaturation [95°C, 5s] and a combined annealing/extension [60°C, 20s]. At the end of each annealing phase fluorescence was measured in "single" acquisition mode with the channel setting F2/1. Samples containing DNA corresponding to 2×10^3 to 2×10^0 *N. caninum* tachyzoites were included as external standards, for creating a standard curve. Quantitative evaluation of fluorescence signals from the PCR products was performed with the Rotor-Gene software (version 1.7.75).

2.14. Cytokine serum measurements

Serum leptin and adiponectin levels in both *N.caninum*-inoculated and PBS-inoculated mice were quantified using commercially available ELISA kits (Merck Millipore, Billerica, MA) according to manufacturer's instructions.

2.15. Statistical analysis

Statistical significance of the results was performed using non-parametric Mann-Whitney test calculated with GraphPad Prism software. $p < 0.05$ was considered to be statistically significant.

3. Results

3.1. Detection of *N. caninum* tachyzoites in C57BL/6 mice infected by the intraperitoneal route

In order to determine if *N. caninum* can infect adipose tissue, C57BL/6 mice were challenged intraperitoneally with $1x10^7$ *N. caninum* tachyzoites. Paraffin-embedded GAT, MAT, OAT, SAT and IMAT samples collected from mice sacrificed seven days after infection were analysed by immunohistochemistry. Parasitic forms were detected in GAT and OAT (Fig.2A and 2B).

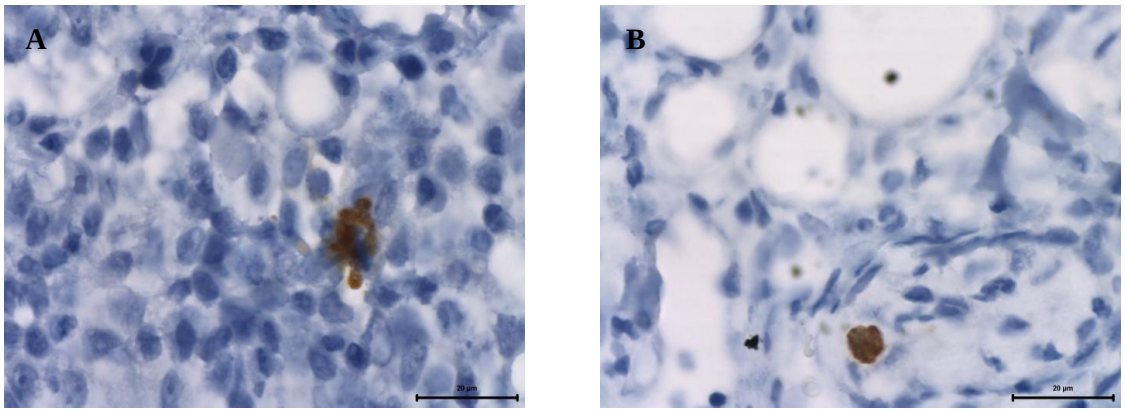

Fig.2 - Representative images of *N. caninum* immunohistochemistry staining in (A) omental adipose tissue and (B) gonadal adipose tissue of C57BL/6 mice infected with $1x10^7$ *N. caninum* tachyzoites and sacrificed seven days after i.p. challenge. Specific staining (brown) corresponds to *N. caninum* tachyzoites.

Seven days after challenge, parasitic forms were also detected in the lungs, a target organ in the acute phase of *N. caninum* infection and brain, a target organ during the chronic phase of infection [100] (Fig.3A and 3B).

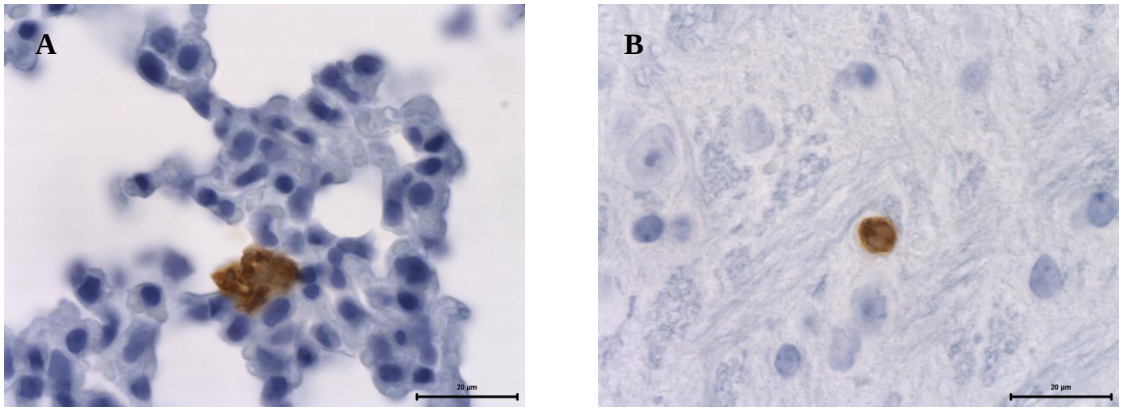

Fig.3 - Representative images of *N. caninum* immunohistochemistry staining in (A) lung and (B) brain of C57BL/6 mice infected with 1×10^7 *N. caninum* tachyzoites and sacrificed seven days after i.p. challenge. Specific staining (brown) corresponds to *N. caninum* tachyzoites.

To determine if *N. caninum* could be found in the SVF of adipose tissue, a hemacolor staining was performed in SAT, GAT, MAT and OAT seven days after infection. No parasitic forms were observed. However, parasitic DNA was detected by RT-PCR in all adipose tissue samples analysed. At this time point, parasitic DNA was also detected in the lungs and brain of infected mice (Fig.4).

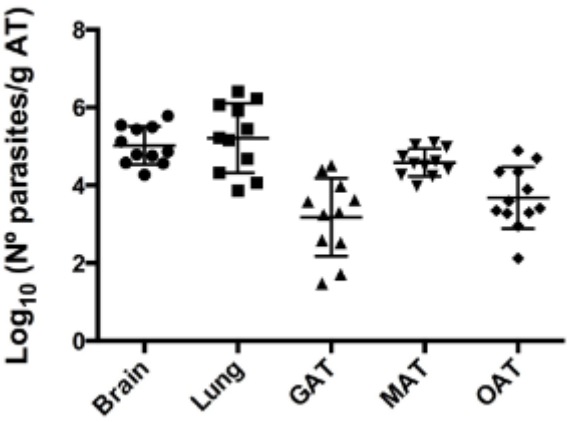

Fig.4 - Detection of parasitic DNA by RT-PCR in lung, brain, gonadal adipose tissue (GAT), mesenteric adipose tissue (MAT) and omental adipose tissue (OAT) samples of C57BL/6 mice seven days after i.p. inoculation with *N. caninum*.

Additionally, to verify if adipose tissue could be a place of parasitic persistence, the presence of *N. caninum* was assessed two months after infection in SAT, GAT, MAT and OAT. However, no parasitic DNA was detected in any of the analysed samples, as well as in the lungs of these mice. Nevertheless, parasitic DNA was detected in the brain of 6 out of 10 infected mice, indicating that a chronic infection was established.

3.2. Characterization of F4/80$^+$ cells in adipose tissue after *N. caninum* infection

As mentioned before, macrophages are key players in the immune response to foreign invaders of the body, such as infectious microorganisms. In fact, macrophage-depleted mice exhibited increased sensitivity to *N. caninum* infection [60]. So, this population was analysed in the collected adipose tissue seven days and two months after infection with *N. caninum,* by immunohistochemistry and flow cytometry.

The IMAT, SAT, GAT, MAT and OAT of control and infected mice were collected seven days after infection and analysed by immunohistochemistry, staining the F4/80 surface marker which is expressed by the majority of mature macrophages (Fig.5). Fig.5 is a representative example of F4/80 staining seven days after infection.

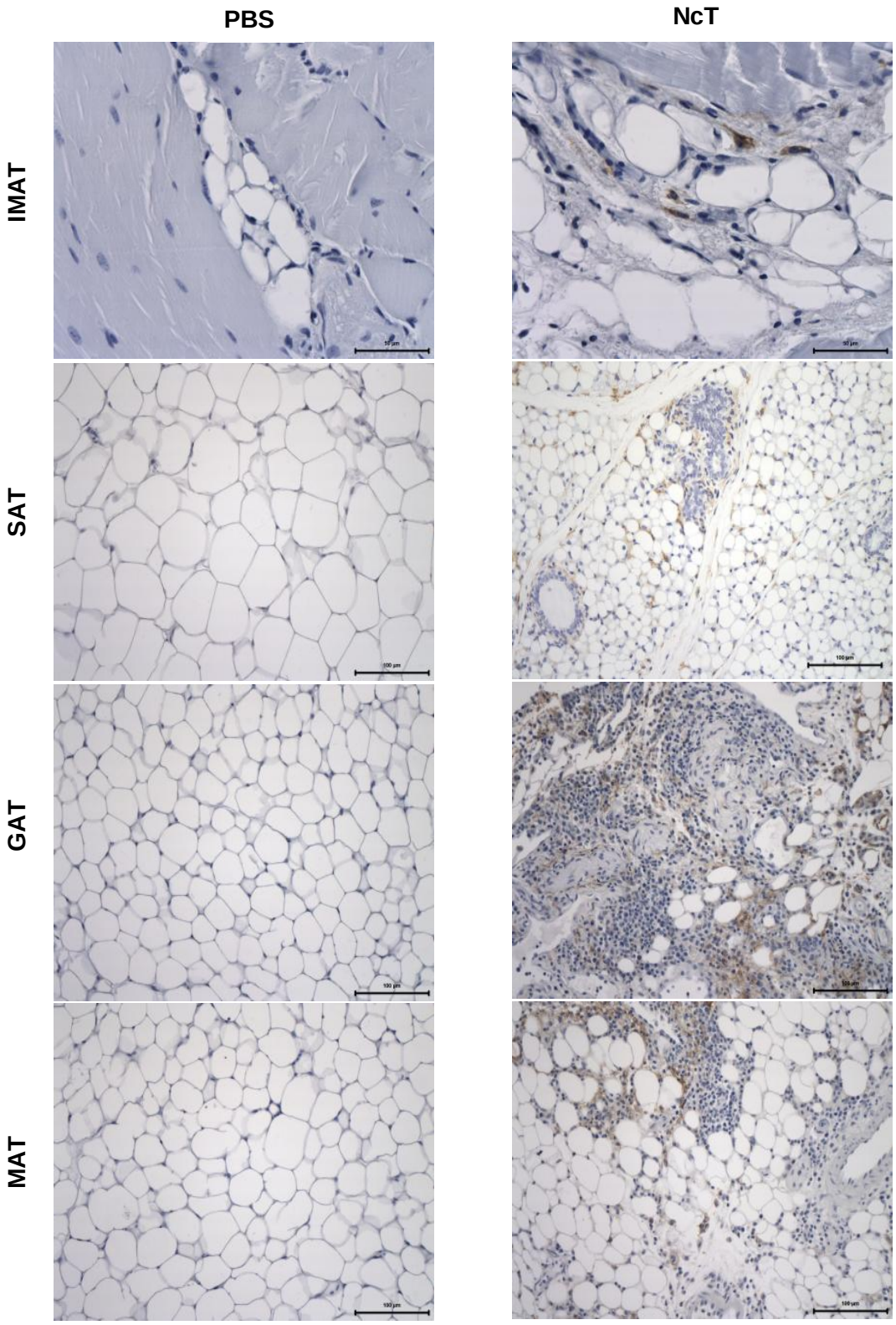

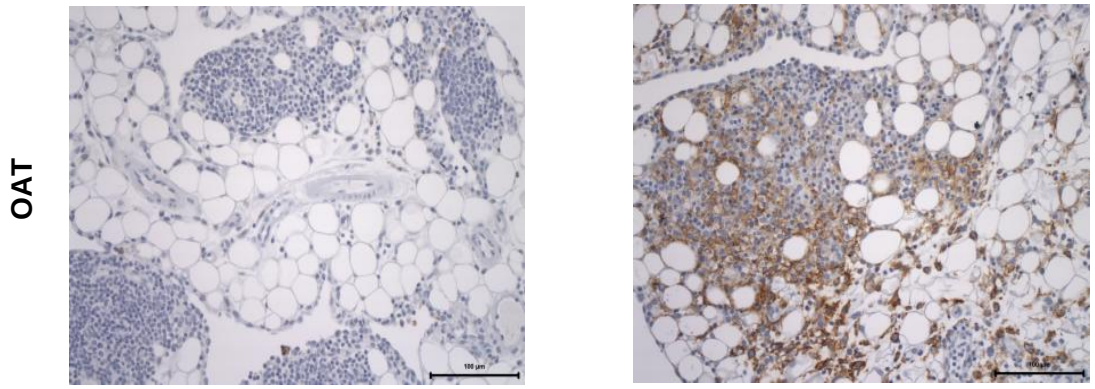

Fig.5 - Representative images of immunohistochemistry analysis of F4/80 staining. Intramuscular adipose tissue (IMAT), subcutaneous adipose tissue (SAT), gonadal adipose tissue (GAT), mesenteric adipose tissue (MAT) and omental adipose tissue (OAT) of C57BL/6 mice sacrificed seven days after i.p. challenge with *N. caninum* (NcT) or administration of PBS (PBS) were specific stained with a monoclonal antibody anti-F4/80. Brown color corresponds to F4/80^{+} cells.

The immunohistochemistry analysis shows a considerable increase in the expression of F4/80-stained area in IMAT, SAT, GAT, MAT and OAT of infected mice comparatively to non-infected mice (Fig.6).

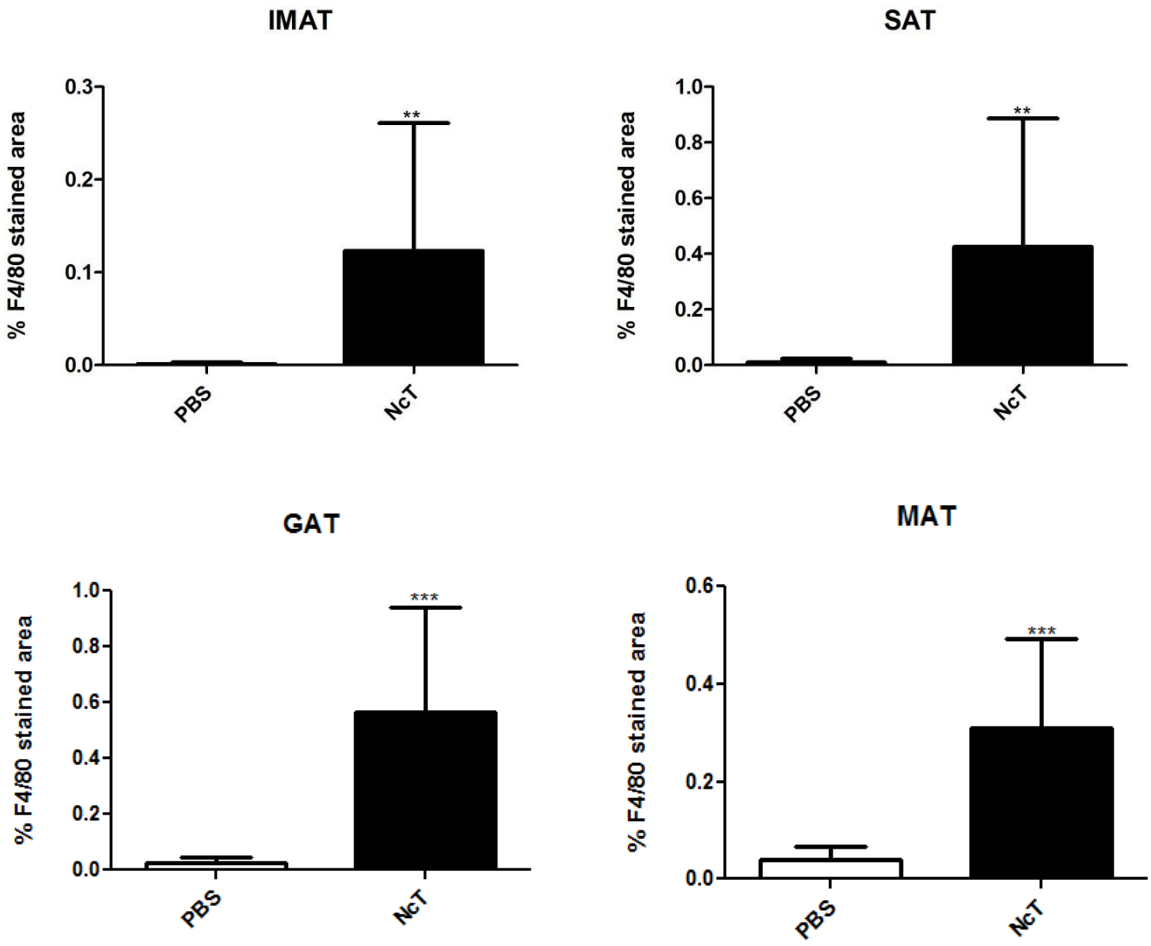

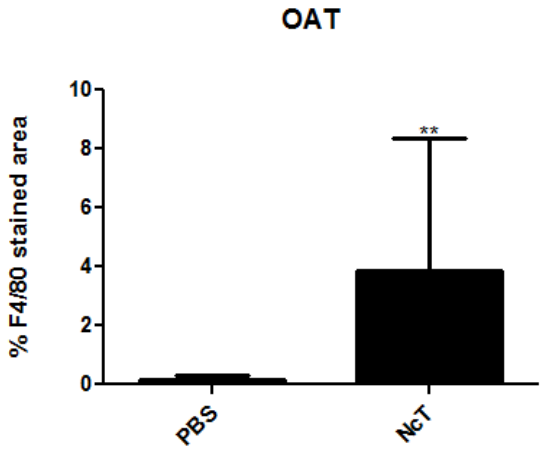

Fig.6 - Frequency of F4/80- stained area of analysed subcutaneous adipose tissue (SAT), mesenteric adipose tissue (MAT), omental adipose tissue (OAT), intramuscular adipose tissue (IMAT) and gonadal adipose tissue (GAT), seven days after challenge with *N. caninum* (NcT) or administration of PBS (PBS). Statistical significant differences between groups are indicated (Mann-Whitney U,**P*<0,05; ***P*<0,01; ****P*<0,005).

Additionally, two months after infection with *N. caninum* the same analysis was performed for F4/80. Fig.7 is a representative example of F4/80 staining two months after infection.

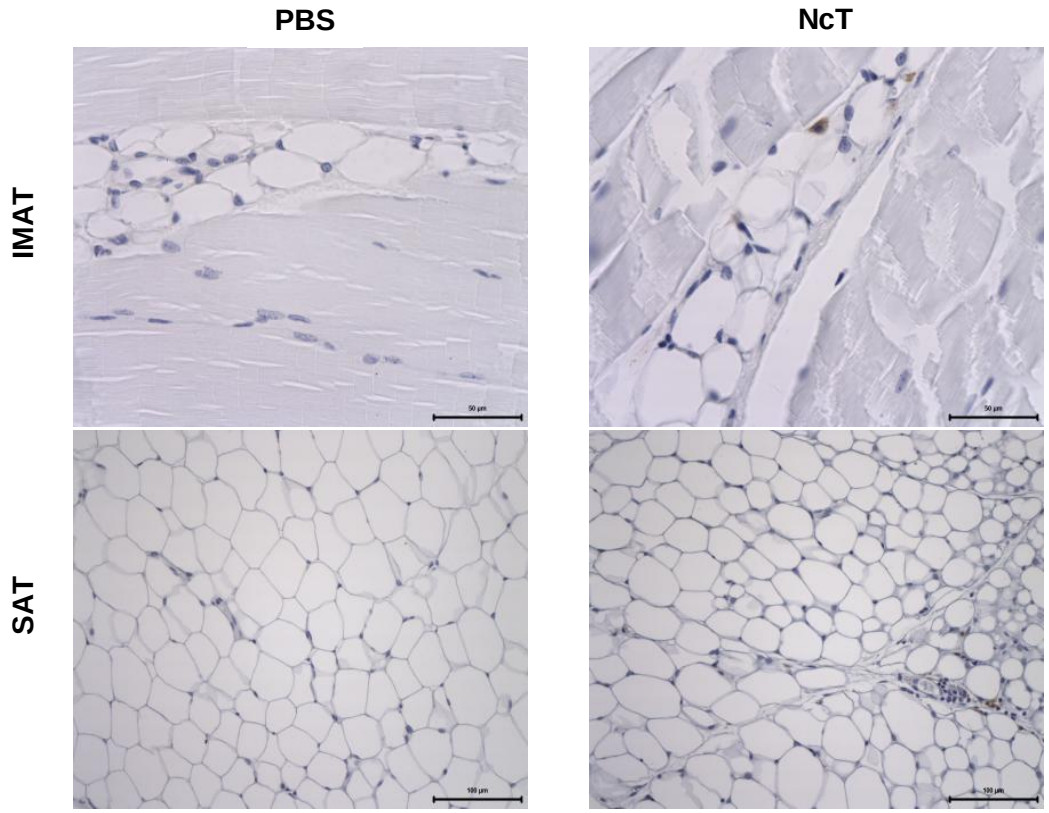

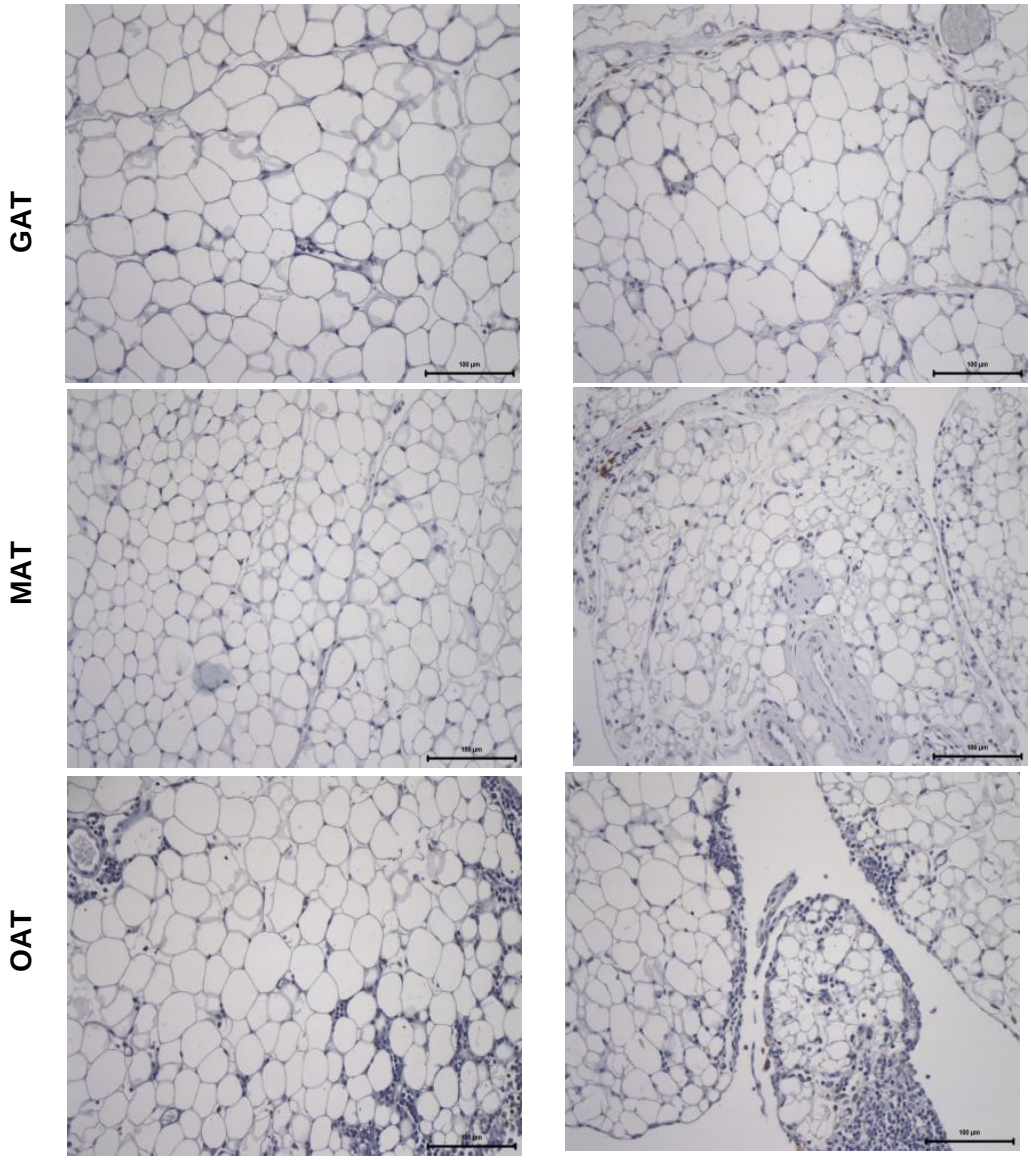

Fig.7 - Representative images of immunohistochemistry analysis of F4/80 staining. Intramuscular adipose tissue (IMAT), subcutaneous adipose tissue (SAT), gonadal adipose tissue (GAT), mesenteric adipose tissue (MAT) and omental adipose tissue (OAT) of C57BL/6 mice sacrificed two months after i.p. challenge with *N. caninum* (NcT) or administration of PBS (PBS) were specific stained with a monoclonal antibody anti-F4/80. Brown color corresponds to $F4/80^{+}$ cells.

The analysis of immunohistochemistry two months post-infection shows no differences in the F4/80-stained area between *N. caninum*-challenged mice and control group (Fig.8).

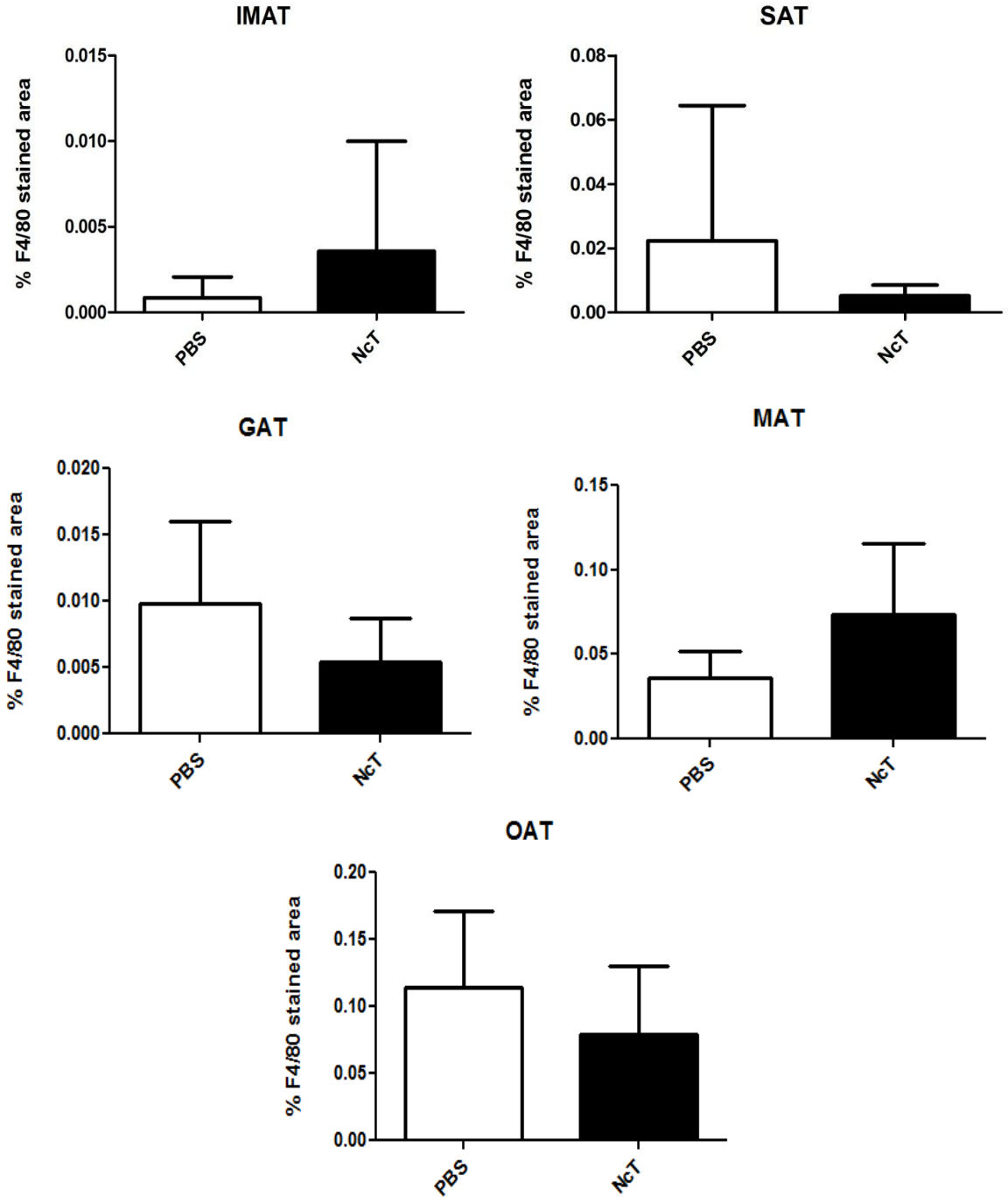

Fig.8 - Frequency of F4/80-stained area of analysed subcutaneous adipose tissue (SAT), mesenteric adipose tissue (MAT), omental adipose tissue (OAT), intramuscular adipose tissue (IMAT) and gonadal adipose tissue (GAT), two months after challenge with *N. caninum* (NcT) or administration of PBS (PBS). Bars represent the mean values of the respective group (± SD).

In spite of cell surface antigen F4/80 being commonly used as a marker for macrophages it was already described that other populations such as neutrophils and eosinophils can express this cell surface marker in lower amounts [101]. Accordingly, stromal vascular fraction isolated from GAT of infected mice shows cells expressing

F4/80 with morphology compatible with macrophages but also with eosinophils and neutrophils (Fig.9A and 9B).

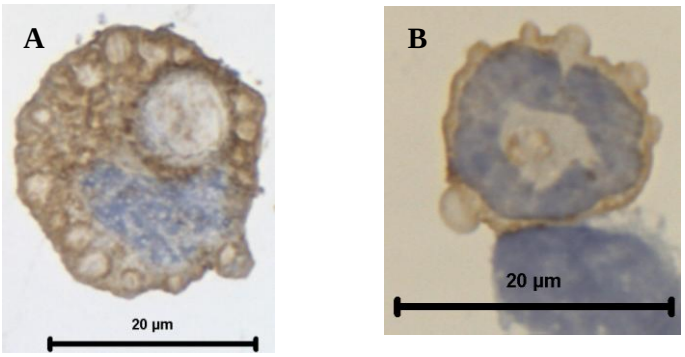

Fig.9 - Immunohistochemistry analysis of F4/80 in stromal vascular fraction cells isolated from gonadal adipose tissue of infected C57BL/6 mice, sacrificed seven days after the parasitic challenge. Cells were specific stained (brown coloration) with anti-mouse F4/80 antibody and counterstained with haematoxilyn. Cells with morphology compatible with macrophages **(A)** and polymorphonuclear cells **(B)** are observed.

Therefore, flow cytometry was used to better characterize the macrophage population. By flow cytometry analysis two distinct populations, which stain for F4/80, could be defined - F4/80^{high} autofluorescence high (AF) cells and F4/80^{int} cells (Fig.10A). To better understand which cells were detected in these two different gates, sorted cells from GAT of infected mice were analysed. Despite F4/80^{high} AF ^{high} cells exhibited macrophage morphology, sorted F4/80^{int} cells turned out to be mainly polymorphonuclear cells (Fig.10B and Fig.10C).

A

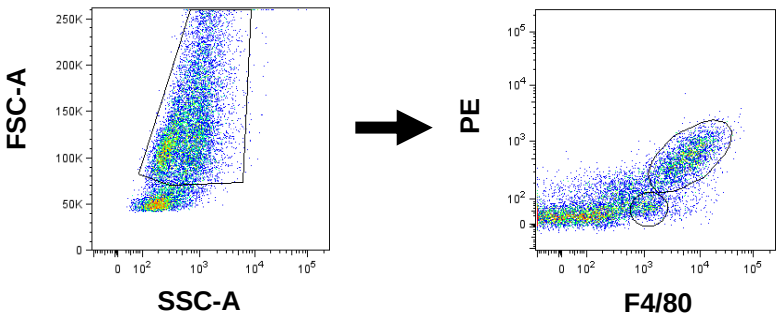

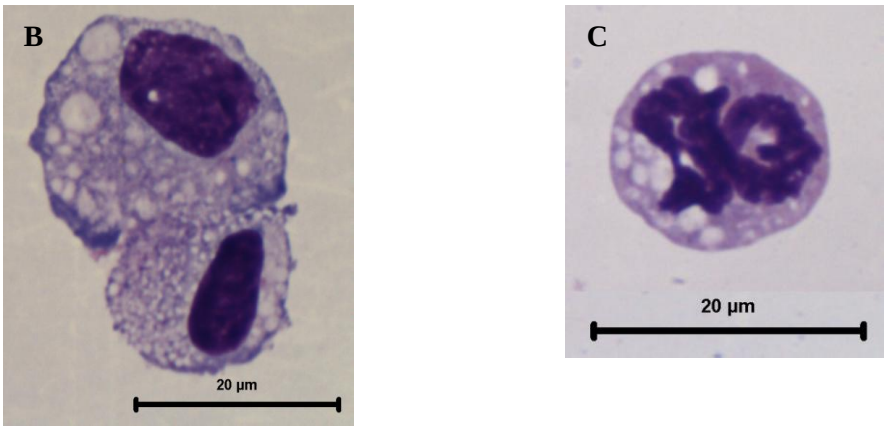

Fig.10 – (A) Representative dot plots of stromal vascular fraction cells from gonadal adipose tissue of mice seven days after i.p. administration of 1×10^7 *N. caninum* tachyzoites. Hemacolor staining of sorted F4/80^{high} AF ^{high} (B) and F4/80^{int} (C) stromal vascular fraction cells from gonadal adipose tissue of mice seven days after *N. caninum*.

In the following analysis, macrophages were therefore defined as F4/80^{high} cells. Previous work in our laboratory has shown, by using flow cytometry an increase number of M2-type macrophages, defined as CD206^{+}F4/80^{+}cells, in GAT, MAT and OAT and of CD206^{-}F4/80^{+}cells, M1 macrophages, in the GAT, MAT, OAT and SAT of seven day-infected mice (Teixeira *et al.* unpublished results) comparatively to control mice. Therefore, two months after challenge with *N. caninum* the number of M2 macrophages in adipose tissue was assessed with the marker CD206, and the gating strategy is shown in Fig.11.

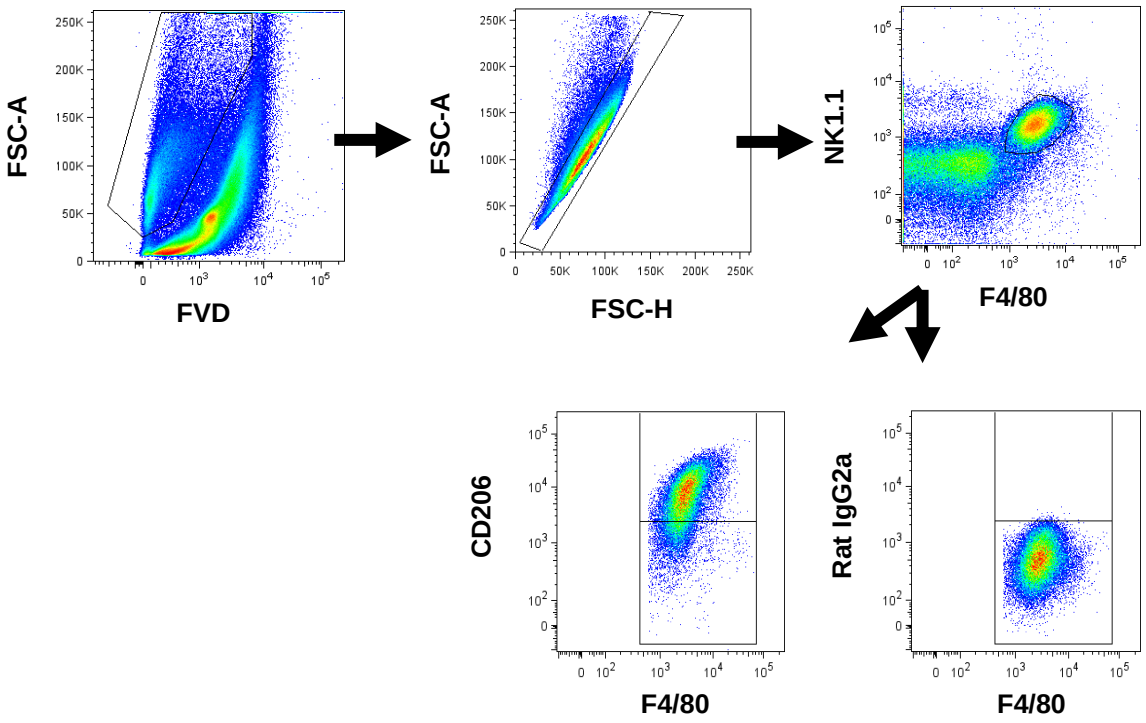

Fig.11 - Flow cytometry gating strategy used to define macrophages in the stromal vascular fraction of the different depots of adipose tissue analysed. Dead cells were excluded with Fixable Viability Dye (FVD) and singlets were then selected from FSC-A versus FSC-H dot plot. Macrophages were defined as F4/80^{high}. Representative dot plots of F4/80^{+}CD206^{+} SVF cells gated in F4/80^{high} are shown as well as respective isotype control.

No significant differences were observed in the number of macrophages in the different types of adipose tissue analysed between infected mice and control group (Fig.12). However, in MAT it is possible to observe a significant increase in the frequency of CD206^{-}F4/80^{+} cells, two months after challenge with *N. caninum* when compared with control group. Additionally, it is possible to observe a significant decrease in frequency in CD206^{+}F4/80^{+} cells in MAT at this time point in infected group comparatively with control group (Fig.12).

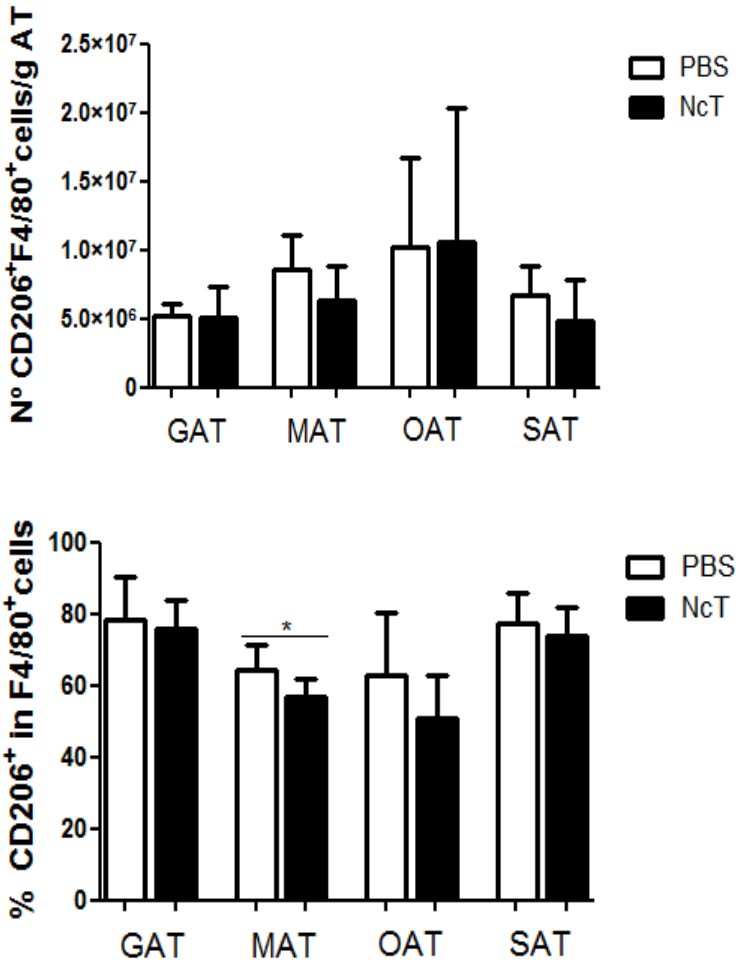

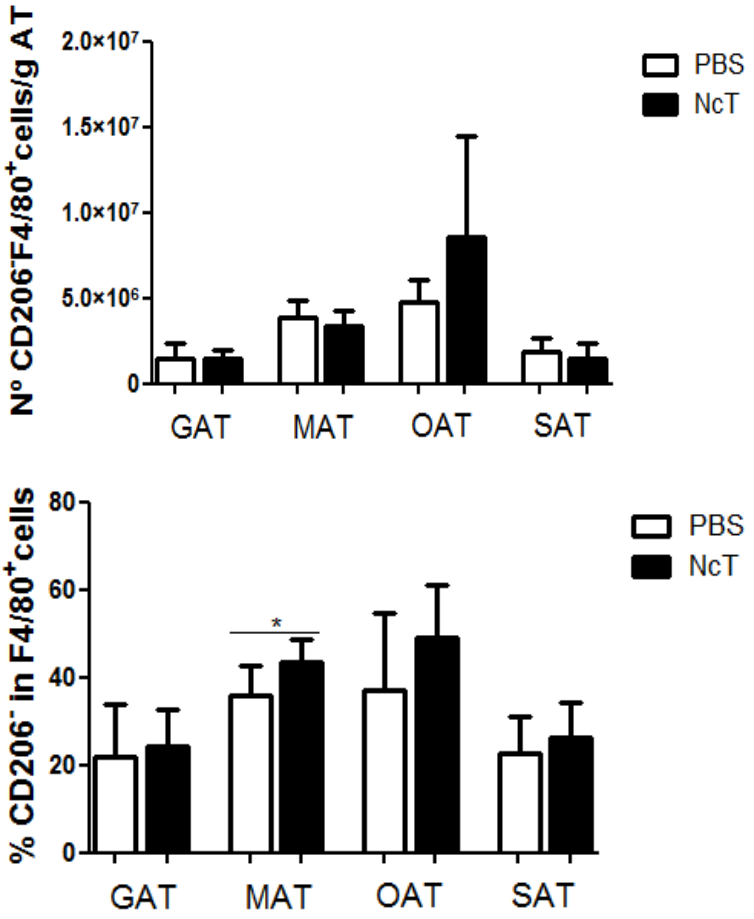

Fig.12 – Frequencies and numbers of F4/80$^+$ CD206$^+$ or F4/80$^+$ CD206$^-$ cells per gram of gonadal adipose tissue (GAT), mesenteric adipose tissue (MAT), omental adipose tissue (OAT) and subcutaneous adipose tissue (SAT) at two months after i.p. challenge with 1×10^7 *N. caninum* (NcT) or administration of PBS (PBS). Bars represent mean values of the respective group (± SD). Statistical significant differences between groups is indicated (Mann-Whitney U,**P*<0,05; ***P*<0,01; ****P*<0,005).

As mentioned above, seven days post-infection with *N. caninum* previous work has shown an increase in number of both M1 and M2 macrophages in adipose tissue of infected mice. Therefore, arginase 1 (*Arg-1*) and inducible nitric oxide synthase 2 (*Nos2*) mRNA levels were evaluated seven days and two months post-infection. *Arg-1* encoded enzyme is associated with M2-type macrophages whereas *Nos2* gene is associated with M1-type macrophages and its encoded enzyme controls the production of nitric oxide [102].

GAT was the tissue with higher frequency of macrophages in the SVF and for that reason was used to evaluate mRNA levels. Results for seven days post-infection are shown in Fig.13. It is possible to observe a significant increase in both *Nos2* and *Arg-1* mRNA expression levels between infected and non-infected mice.

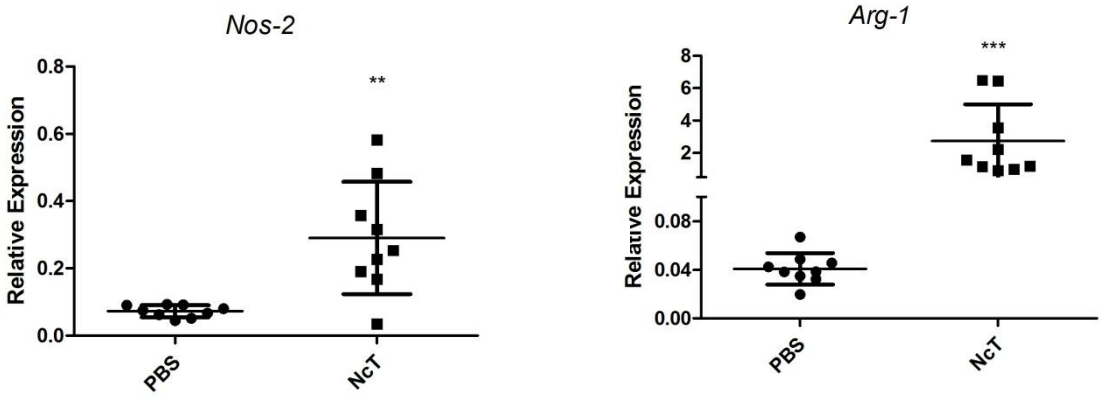

Fig.13 - Relative levels of inducible nitric oxide synthase (*Nos-2*) and arginase 1 (*Arg-1*) normalized to Non-POU-domain containing octamer binding protein mRNA, detected by Real Time PCR in the SFV of gonadal adipose tissue of mice seven days after i.p. administration of 1×10^7 *N. caninum* (NcT) tachyzoites or PBS (PBS). Each symbol represents an individual mouse. Horizontal lines represent the mean values of the respective group (± SD). Statistical significant differences between groups is indicated (Mann-Whitney U, *$P < 0.05$; ** $P \leq 0.01$; *** $P \leq 0.001$).

Contrastingly, two months post-infection with *N. caninum* there were no significant differences in both mRNA expression levels analyzed between control and infected mice (Fig.14).

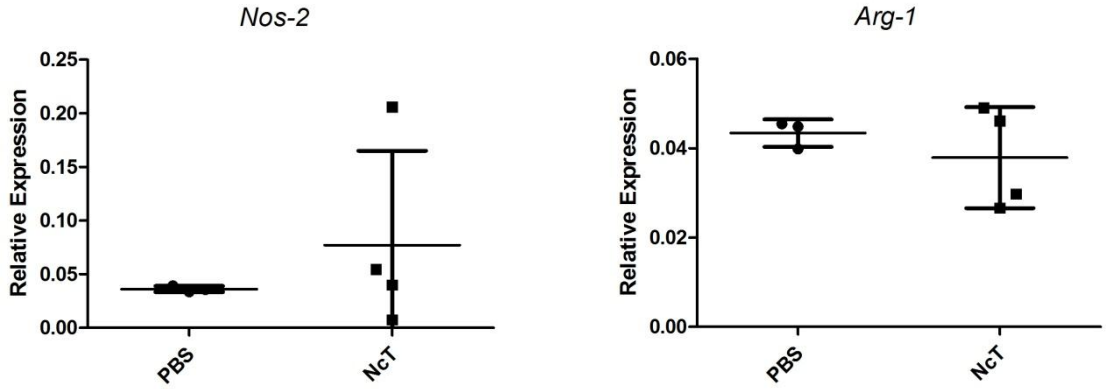

Fig.14 - Relative levels of inducible nitric oxide synthase (*Nos-2*) and arginase 1 (*Arg-1*) normalized to Non-POU-domain containing octamer binding protein mRNA, detected by Real Time PCR in the SFV of gonadal adipose tissue of mice two months after i.p. administration of 1×10^7 *N. caninum* (NcT) tachyzoites or PBS (PBS). Each symbol represents an individual mouse. Horizontal lines represent the mean values of the respective group (± SD).

3.3. Characterization of T helper 1 cells in adipose tissue after *N. caninum* infection

T-bet is a transcription factor regulating T helper 1 (Th1) cell lineage. T-bet-deficient $CD4^+$ T cells only produce small amounts of IFN-γ under Th1 cell-polarizing conditions and fail to mount effective Th1 cell responses during infections with

parasites [103]. Additionally, in the acute infection of *N. caninum*, BALB/c IFN-γ deficient mice were very susceptible to the *N. caninum* infection whereas significant levels of IFN-γ production were observed in resistant wild type mice [104]. Therefore, it was interesting to assess the behavior of this population under infection with this parasite. Th1 cells were defined as $CD4^{+}CD3^{+}NK1.1^{-}Foxp3^{-}T\text{-}bet^{+}$, according to the gating strategy shown in Fig.15.

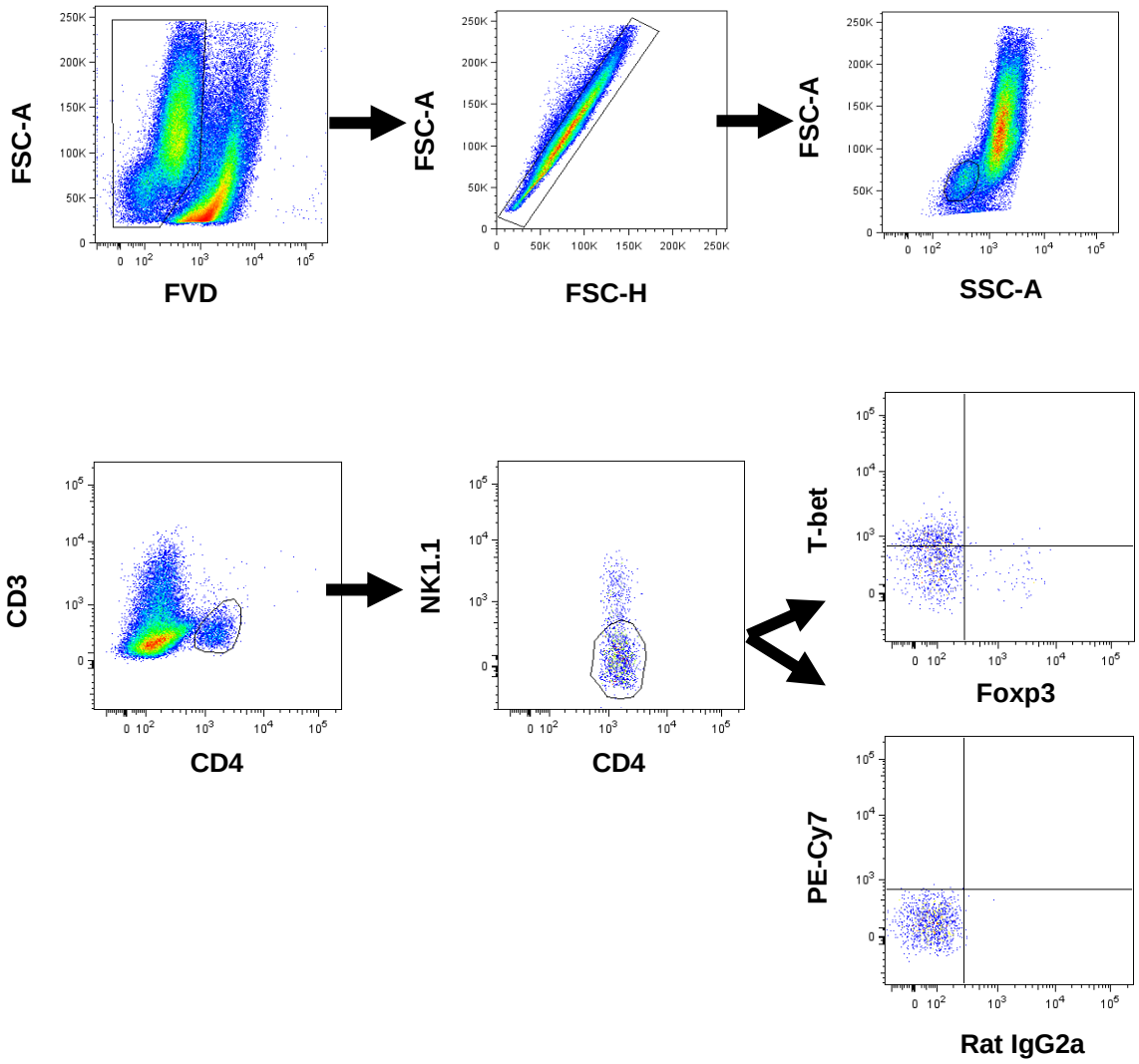

Fig.15 - Flow cytometry representative example of gate strategy used to define Th1 cells in stromal vascular fraction isolated from adipose tissue. Dead cells were excluded with Fixable Viability Dye (FVD) and singlets were then selected from FSC-A versus FSC-H dot plot. T helper cells were defined as $CD3^{+}$ $CD4^{+}$. NK cells were excluded and Th1 cells were defined as $T\text{-}bet^{+}$ $Foxp3^{-}$ cells. Respective isotype control is shown.

Two months after infection, it is possible to observe a significant increase in the frequency of Th1 cells in SAT and MAT in infected animals comparatively to the control group. Regarding to the number of Th1 cells in adipose tissue two months after

challenge, there were a significant increase in GAT, MAT and OAT of infected animals (Fig.16).

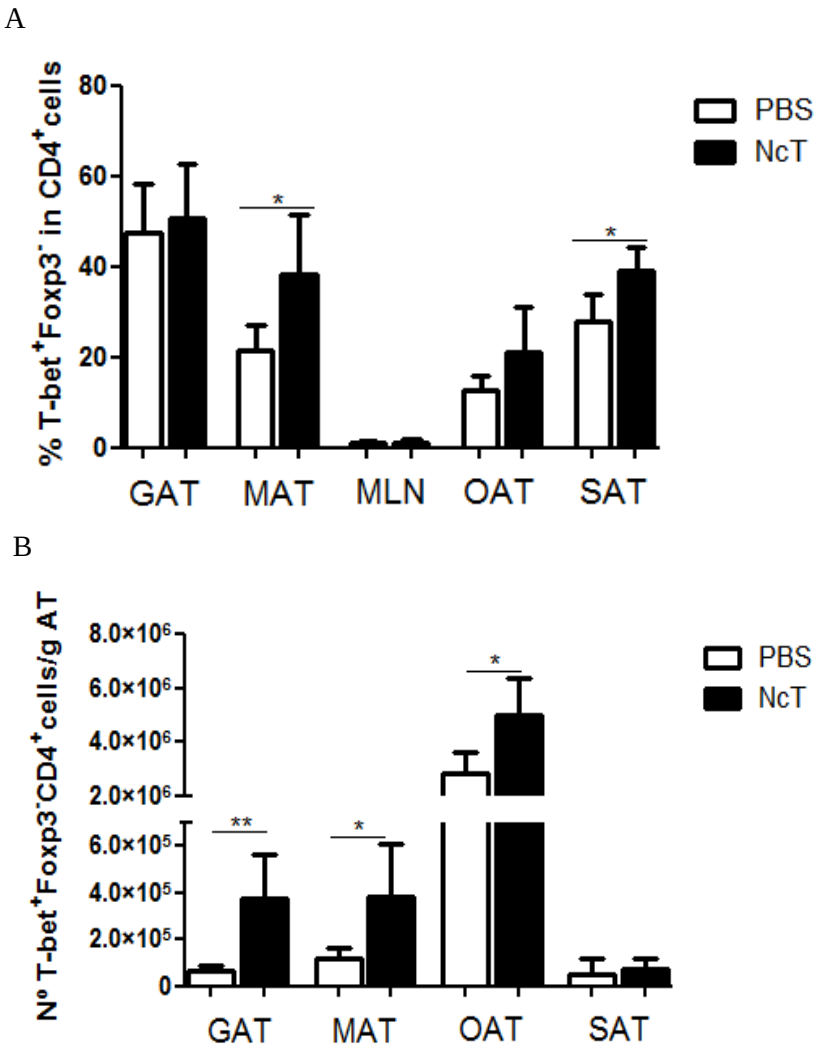

Fig.16 – Frequency (A) and number (B) of T-bet^{+}Foxp3^{-}CD4^{+} cells *per gram* of gonadal adipose tissue (GAT), mesenteric adipose tissue (MAT), omental adipose tissue (OAT) and subcutaneous adipose tissue (SAT), two months after i.p. challenge with 1×10^{7} *N. caninum* or PBS, as indicated. For mesenteric lymph nodes (MLN) only the frequency of cells was determined. Bars represent mean values of the respective group (± SD). Statistical significant differences between groups is indicated (Mann-Whitney U,**P*<0,05; ***P*<0,01; ****P*<0,005).

Th1 cells are host immunity effectors against intracellular protozoa and their key effector cytokine is IFN-γ. For that reason, expression of IFN-γ mRNA levels was evaluated in GAT of infected mice seven days after challenge with *N. caninum* (Fig.17). A significant increase in the expression of IFN-γ mRNA was detected in infected mice when compared with non-infected controls.

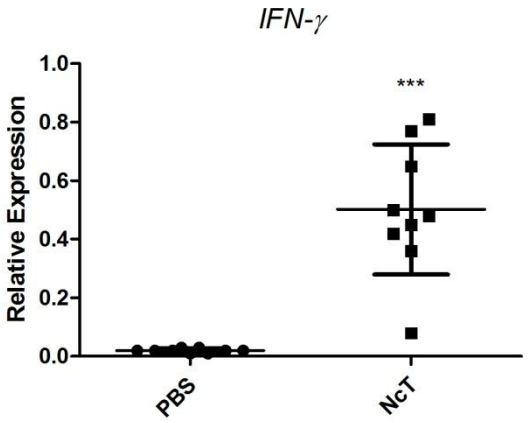

Fig.17 - Relative levels of *IFN-γ* mRNA, normalized to Non-POU-domain containing octamer binding protein mRNA, detected by Real Time PCR in the SFV of gonadal adipose tissue of mice seven days after i.p. administration of 1×10^7 *N. caninum* tachyzoites (NcT) or PBS (PBS). Horizontal lines represent the mean values of the respective group (± SD). Statistical significant differences between groups is indicated (Mann-Whitney U, *$P < 0.05$; ** $P \leq 0.01$; *** $P \leq 0.001$).

3.4. Characterization of regulatory T cells in adipose tissue after infection with *N. caninum*

Regulatory T cells are a subpopulation of T cells which modulate the immune system, with a very important role preventing excessive inflammation in infections caused by parasites [105]. It was previously reported that *N. caninum* infection induces an expansion of spleen $CD4^+CD25^+Foxp3^+$ T cells in mice [106]. So, this population was analysed in the collected adipose tissue seven days and two months after infection with *N. caninum,* by immunohistochemistry and flow cytometry.

By immunohistochemistry, seven days after infection IMAT, SAT, GAT, MAT and OAT of control and infected mice were collected and analysed using an anti-Foxp3 monoclonal antibody marker. Fig.18 is a representative example of Foxp3 staining seven days after challenge.

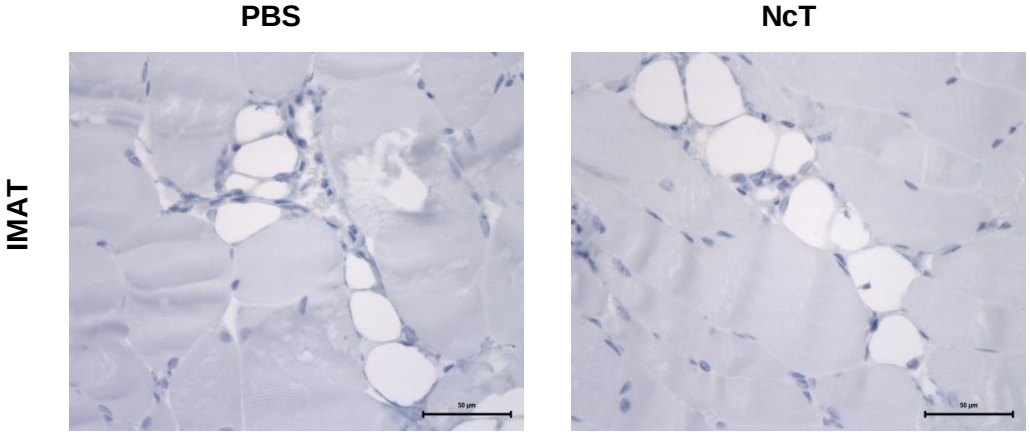

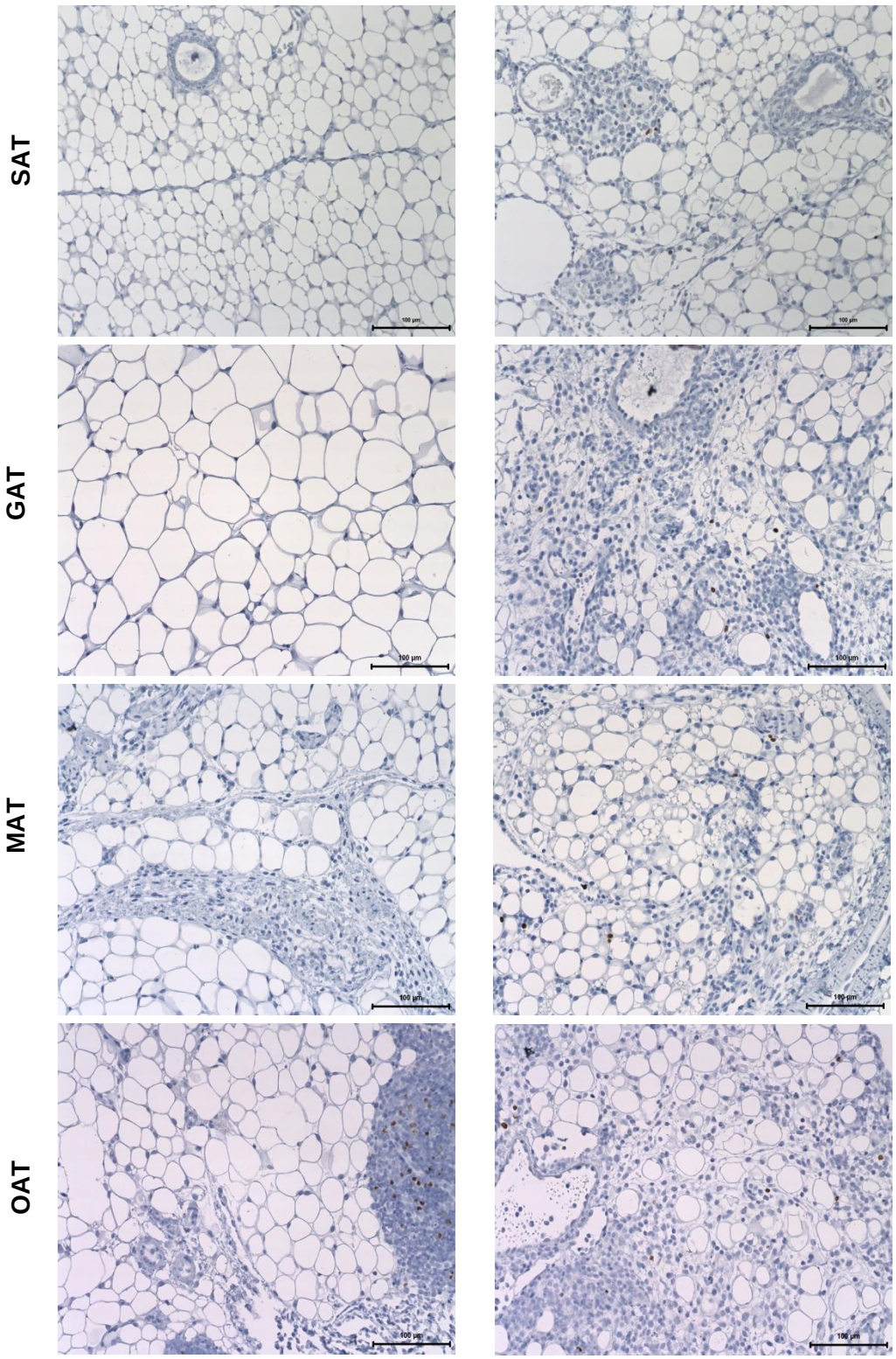

Fig.18 - Representative images of immunohistochemistry analysis of Foxp3 staining. Intramuscular adipose tissue (IMAT), subcutaneous adipose tissue (SAT), gonadal adipose tissue (GAT), mesenteric adipose tissue (MAT) and omental adipose tissue (OAT) of C57BL/6 mice sacrificed seven days after i.p. challenge with *N. caninum* (NcT) or administration of PBS (PBS) were specific stained with a monoclonal anti-mouse Foxp3. Brown color corresponds to $Foxp3^+$ cells.

Seven days after challenge, an increase number of Treg cells was observed in SAT, GAT, MAT and OAT. Foxp3^{+} cells number was found not to differ between controls and infected mice in IMAT, 7 days after challenge (Fig.19).

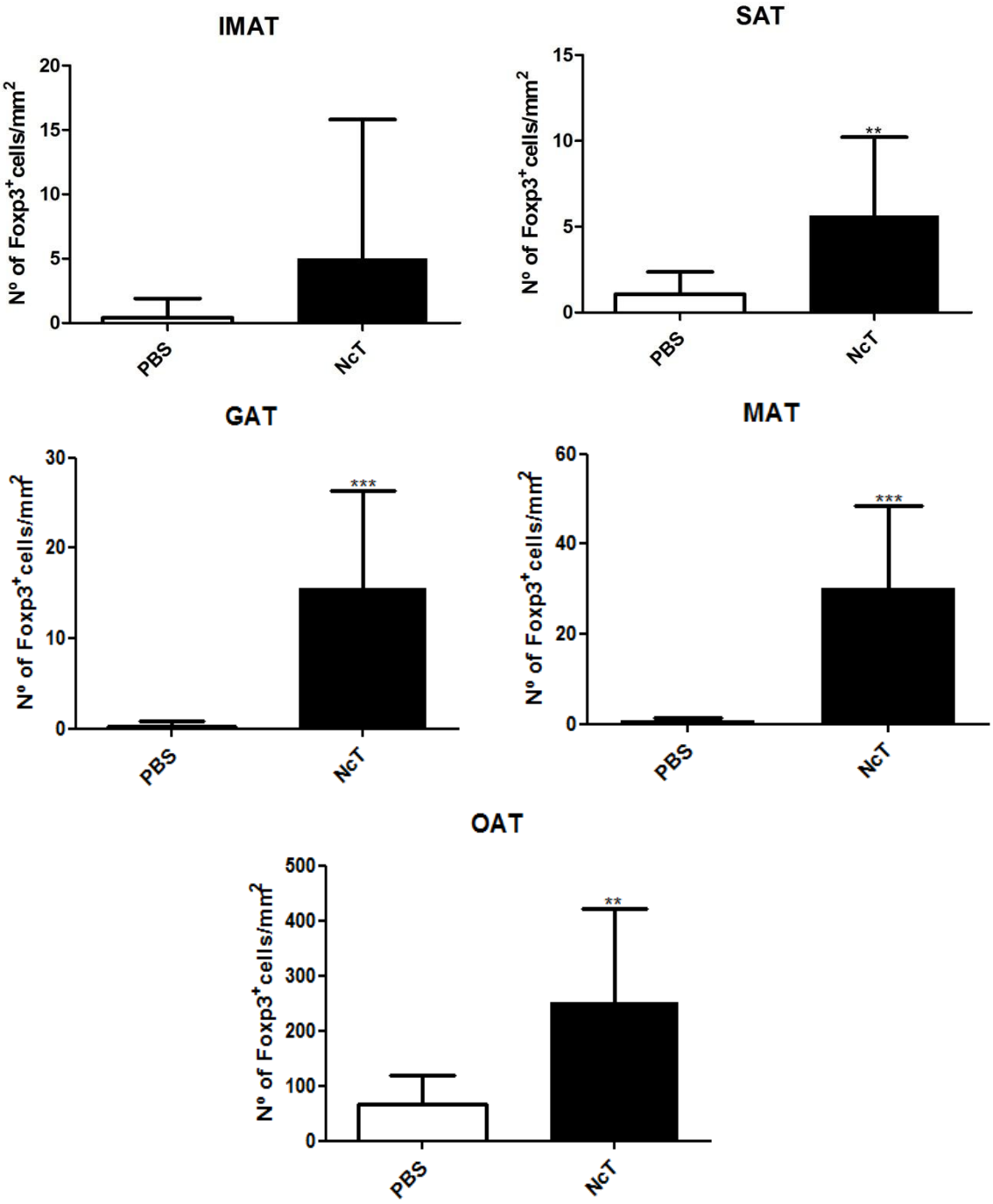

Fig.19 - Frequency of Foxp3^{+} stained area of analysed subcutaneous adipose tissue (SAT), mesenteric adipose tissue (MAT), intramuscular adipose tissue (IMAT), omental adipose tissue (OAT) and gonadal adipose tissue (GAT), seven days after challenge with *N. caninum* (NcT) or administration of PBS (PBS). Bars represent the mean values of the respective group (± SD). Statistical significant differences between groups is indicated (Mann-Whitney U,*P<0,05; **P<0,01; ***P<0,005).

On the other hand, two months after infection with *N. caninum* the same analysis was performed for Foxp3. Fig.20 is a representative example of Foxp3 staining two months after infection.

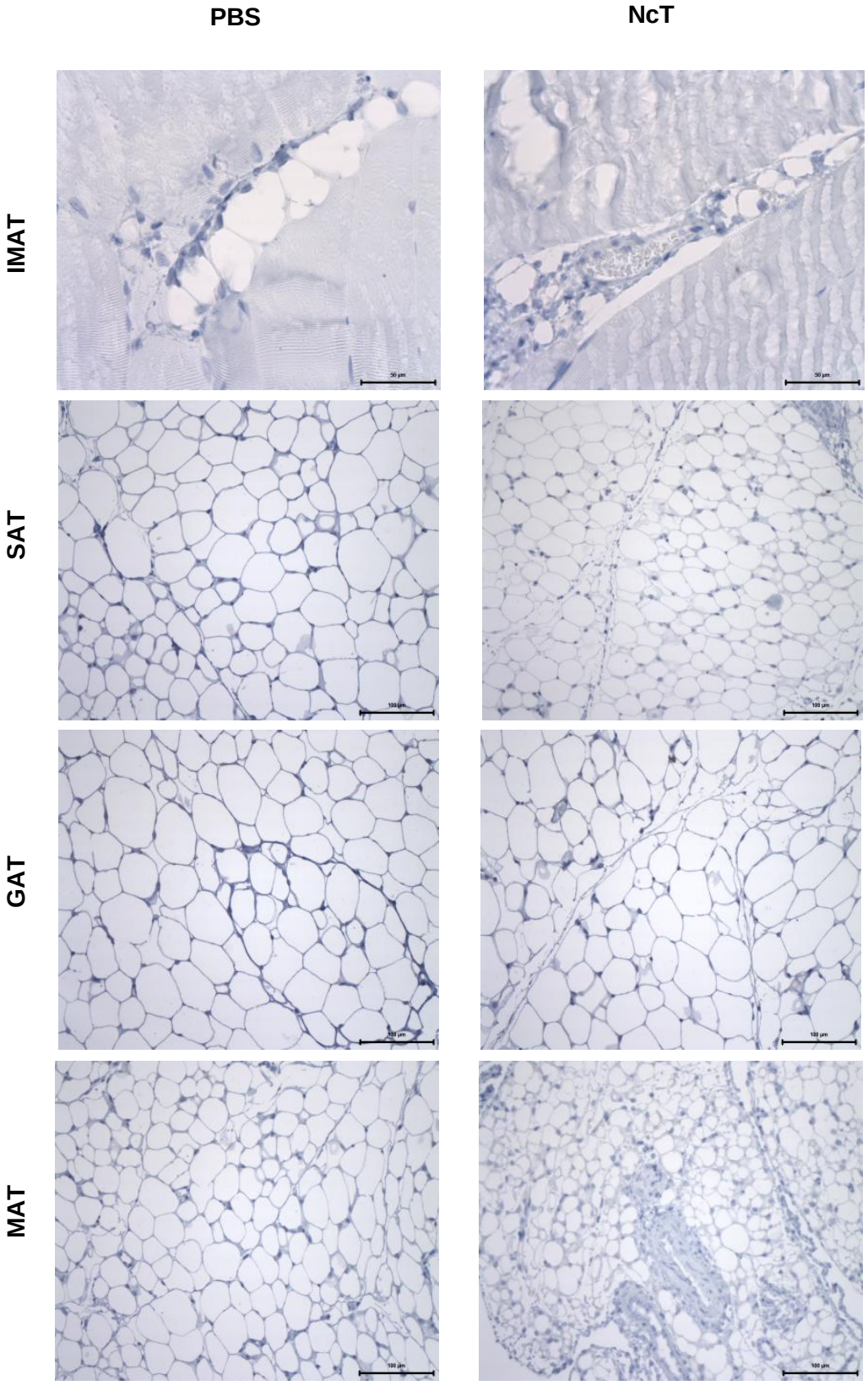

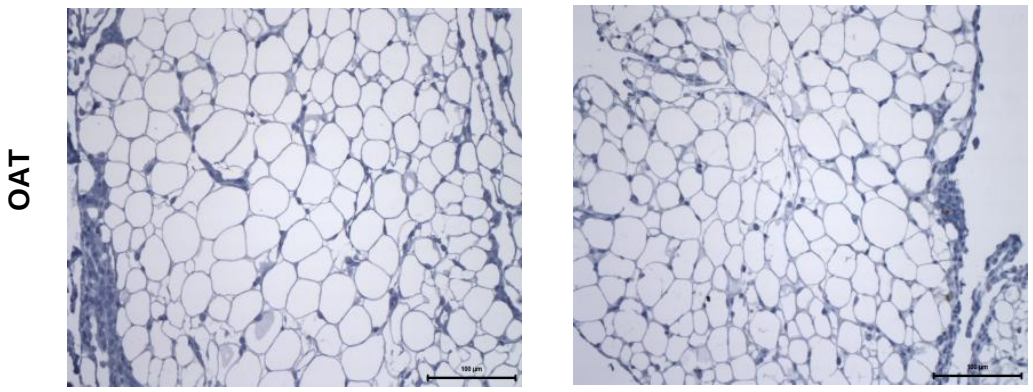

Fig.20 - Representative images of immunohistochemistry analysis of Foxp3 staining. Intramuscular adipose tissue (IMAT), subcutaneous adipose tissue (SAT), gonadal adipose tissue (GAT), mesenteric adipose tissue (MAT) and omental adipose tissue (OAT) of C57BL/6 mice sacrificed two months after i.p. challenge with *N. caninum* (NcT) or administration of PBS (PBS) were specific stained with a monoclonal anti-mouse Foxp3. Brown color corresponds to $Foxp3^+$ cells.

The immunohistochemistry analysis shows no significant differences in the Foxp3-stained area between *N. caninum*-challenged mice and control group (Fig.21).

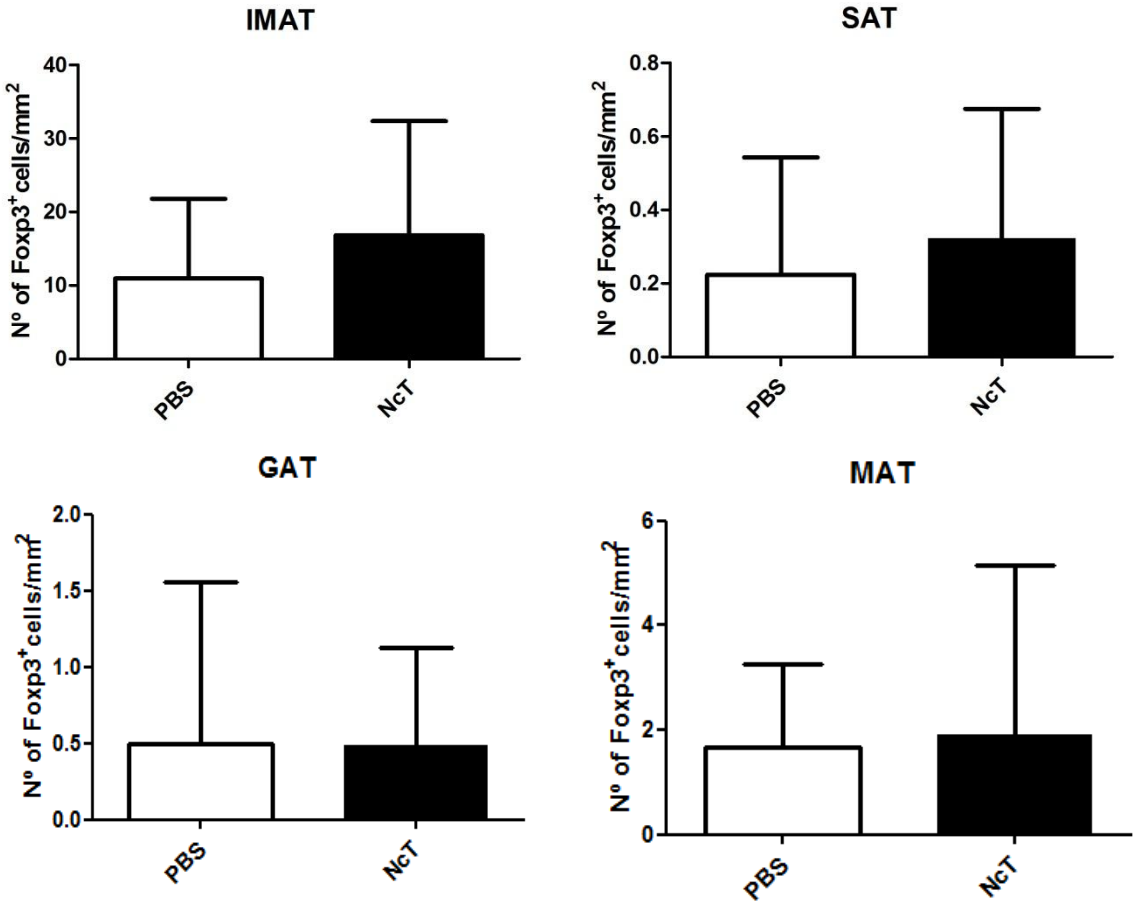

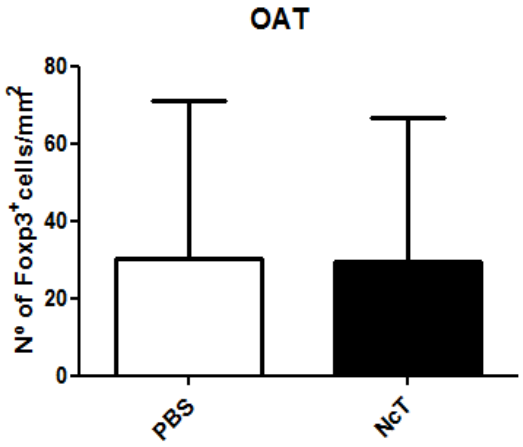

Fig.21 - Frequency of Foxp3$^+$ stained area of analysed subcutaneous adipose tissue (SAT), mesenteric adipose tissue (MAT), omental adipose tissue (OAT), intramuscular adipose tissue (IMAT) and gonadal adipose tissue (GAT), two months after challenge with *N. caninum* (NcT) or administration of PBS (PBS). Bars represent the mean values of the respective group (± SD).

Previous work on our laboratory showed an increase in number of Foxp3$^+$CD25$^+$CD4$^+$ T cells in GAT, OAT and SAT seven days post-infection by flow cytometry analysis (Teixeira *et al.* unpublished results). To further assess Treg cell population, we analyzed the number and frequency of Foxp3$^+$CD25$^+$CD4$^+$ T cells by flow cytometry, two months after i.p. challenge. The gating strategy is shown in Fig.22.

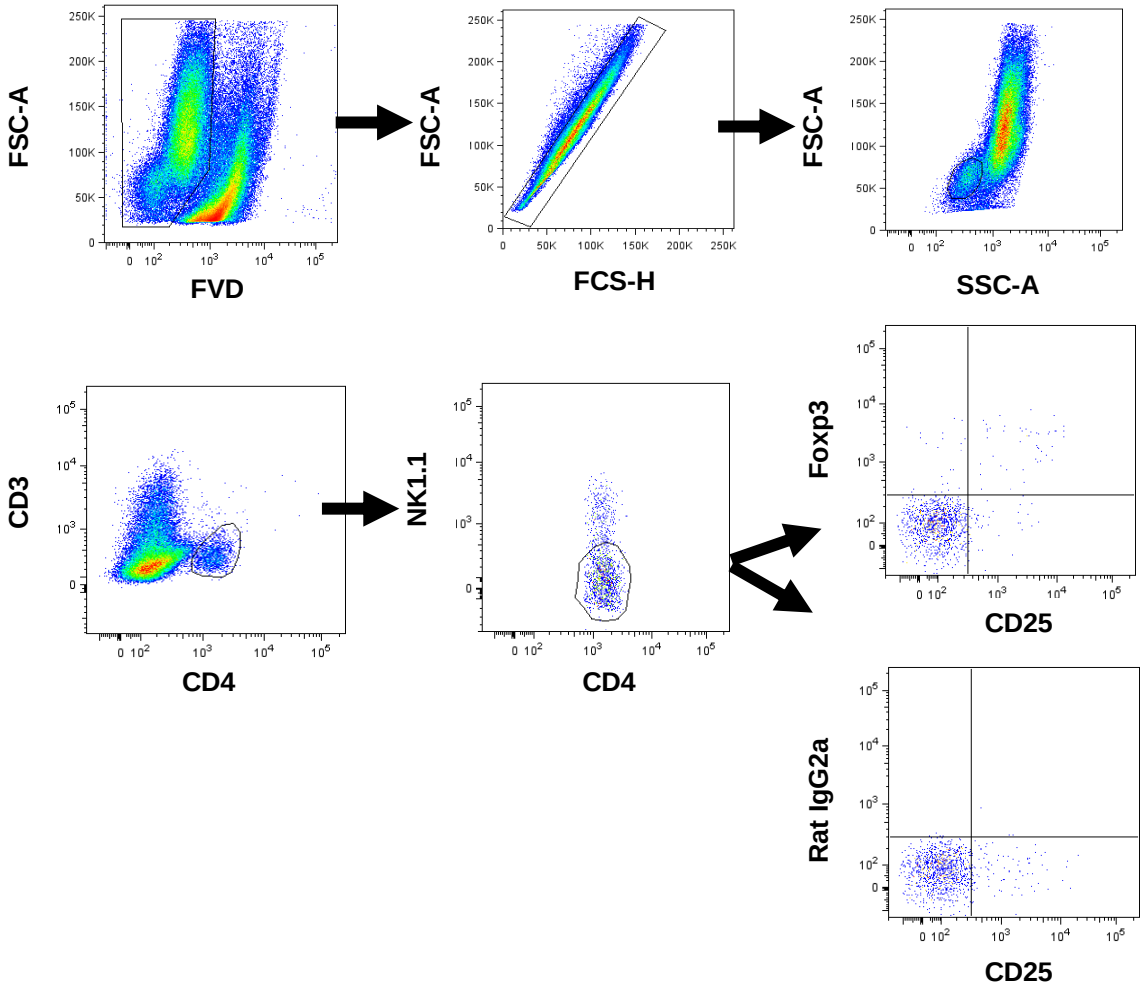

Fig.22 - Flow cytometry representative example of gate strategy used to define regulatory T cells in stromal vascular fraction isolated from adipose tissue. Dead cells were excluded with Fixable Viability Dye (FVD) and singlets were then selected from FSC-A versus FSC-H dot plot. T helper cells were defined as $CD3^+$ $CD4^+$. NK cells were excluded and regulatory T cells were defined as CD25 Foxp3 double positive cells. Respective isotype control is shown.

As shown in Fig.23A, an increase number of $Foxp3^+CD25^+CD4^+$ and $Foxp3^+CD25^-CD4^+$ T cells was observed in GAT two months post-infection as compared with non-infected mice, while in MAT, OAT and SAT no significant differences were found. Regarding to frequencies of $Foxp3^+CD25^+CD4^+$ T cells, it was observed a significant decrease in MAT and SAT whereas in GAT and OAT no significant differences were observed. Additionally, in $Foxp3^+CD25^-CD4^+$ it was observed a significant decrease in MAT of infected group compared to control two months after challenge with *N. caninum* (Fig.23B).

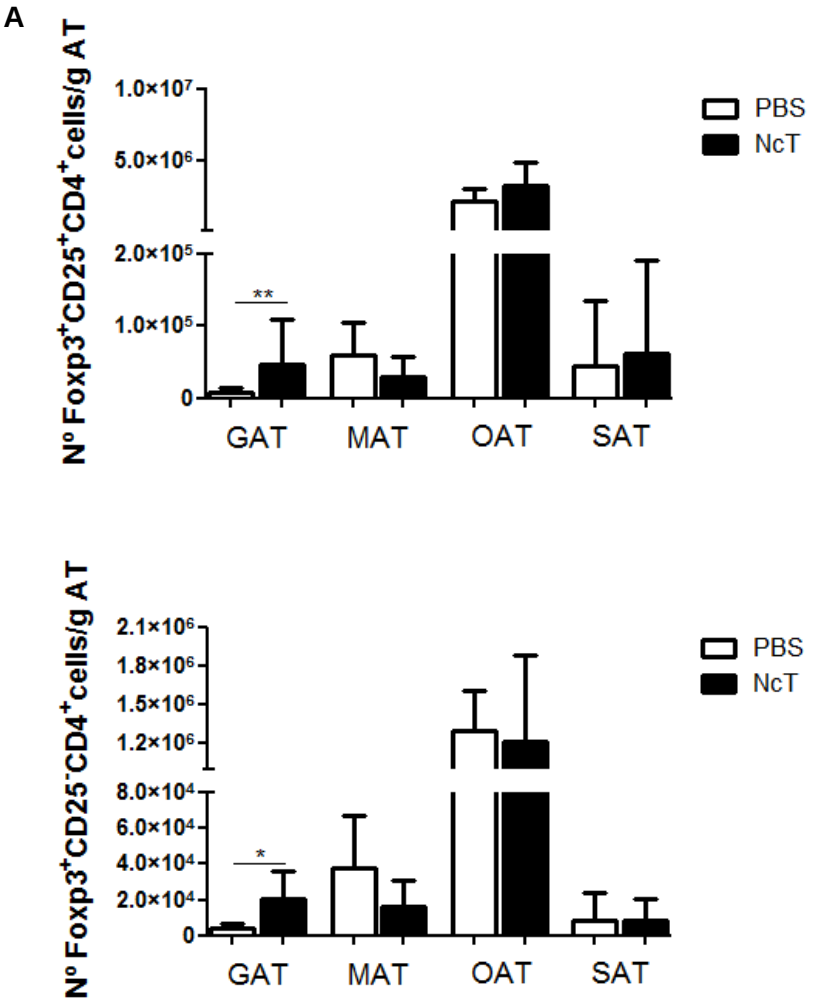

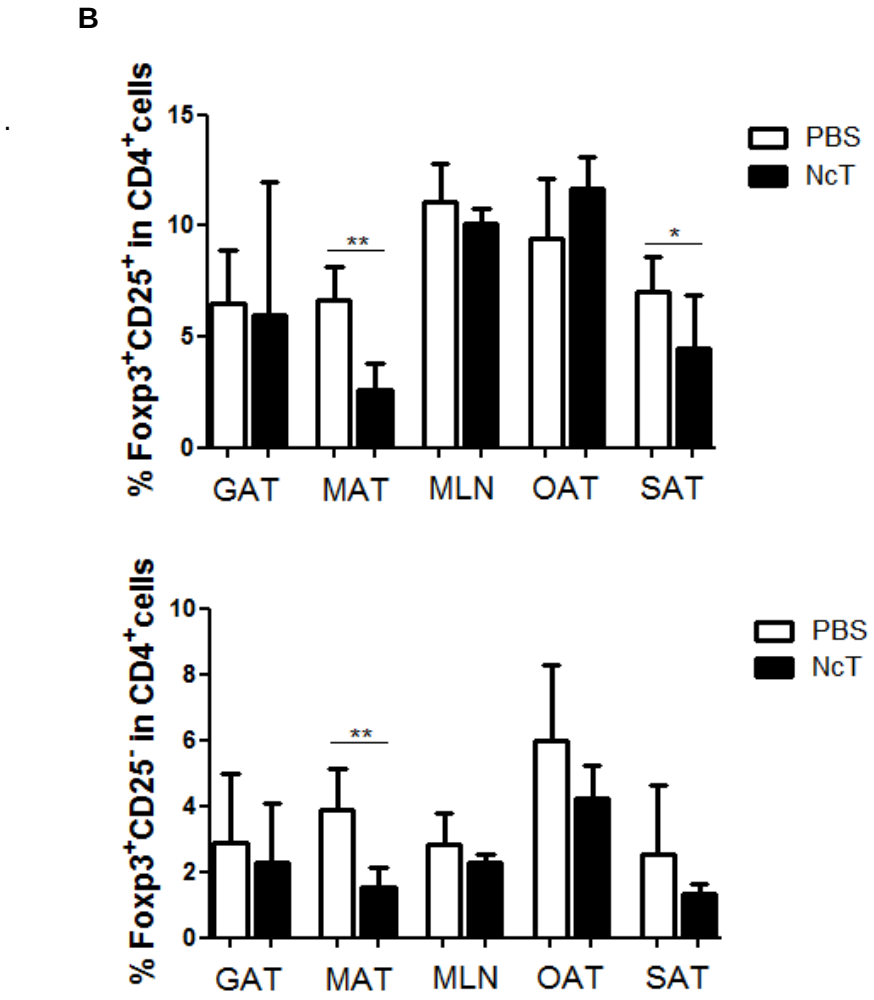

Fig.23 - Total number of cells (A) and percentages (B) of Foxp3$^+$CD25$^+$ cells, Foxp3$^+$CD25$^-$ cells on total CD4$^+$CD3$^+$NK$^-$cells in gonadal adipose tissue (GAT), mesenteric adipose tissue (MAT), omental adipose tissue (OAT) and subcutaneous adipose tissue (SAT) from C57BL/6 mice sacrificed two months after i.p. challenge with 1×10^7 *N. caninum* (NcT) or PBS (PBS). For mesenteric lymph nodes (MLN) only the frequency of cells was determined. Bars represent means plus one SD. Statistical significant differences between groups is indicated (Mann-Whitney U, *$P < 0.05$; ** $P \leq 0.01$; *** $P \leq 0.001$).

The number and frequency of effector T cells, defined as Foxp3$^-$CD25$^+$CD4$^+$, was also assessed. No significant differences in all types of adipose tissue samples analysed were found (Fig.24A). Concerning to the frequency of Foxp3$^-$CD25$^+$CD4$^+$ cells, a significant decrease was observed in MAT of infected mice comparatively with the control group, two months after challenge (Fig.24B).

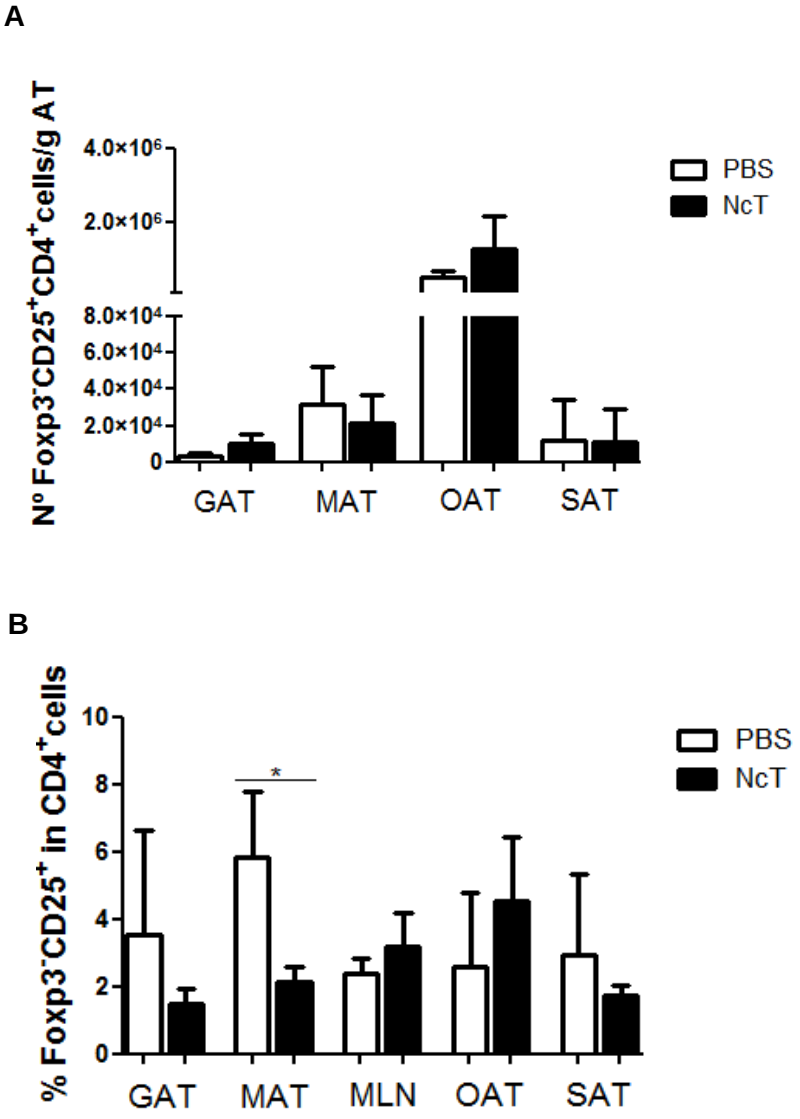

Fig.24 - Total number of cells (A) and frequencies (B) of $CD25^+$ $Foxp3^-$ cells on total $CD4^+CD3^+NK^-$cells in gonadal adipose tissue (GAT), mesenteric adipose tissue (MAT), omental adipose tissue (OAT) and subcutaneous adipose tissue (SAT) from C57BL/6 mice sacrificed two months after i.p. challenge with 1×10^7 *N. caninum* (NcT) or PBS (PBS). For mesenteric lymph nodes (MLN) only the frequency of cells was determined. Statistical significant differences between groups is indicated (Mann-Whitney U, $*P < 0.05$; ** $P \leq 0.01$; *** $P \leq 0.001$).

A population of Treg cells specialized in regulating Th1 cells, expressing the transcription factor T-bet, has been described during type 1 inflammation [103]. Therefore, since a marked presence of Th1 cells was observed in the adipose tissue of the infected mice, we also investigated the presence of these regulatory cells there (Fig.25). As shown in Fig.25A, the number of $T\text{-}bet^+Foxp3^+CD4^+$ cells was significant higher in GAT in infected animals comparatively with control group. Regarding to frequencies, there was a significant decrease in MAT in infected animals with *N. caninum* when compared with control group (Fig.25B).

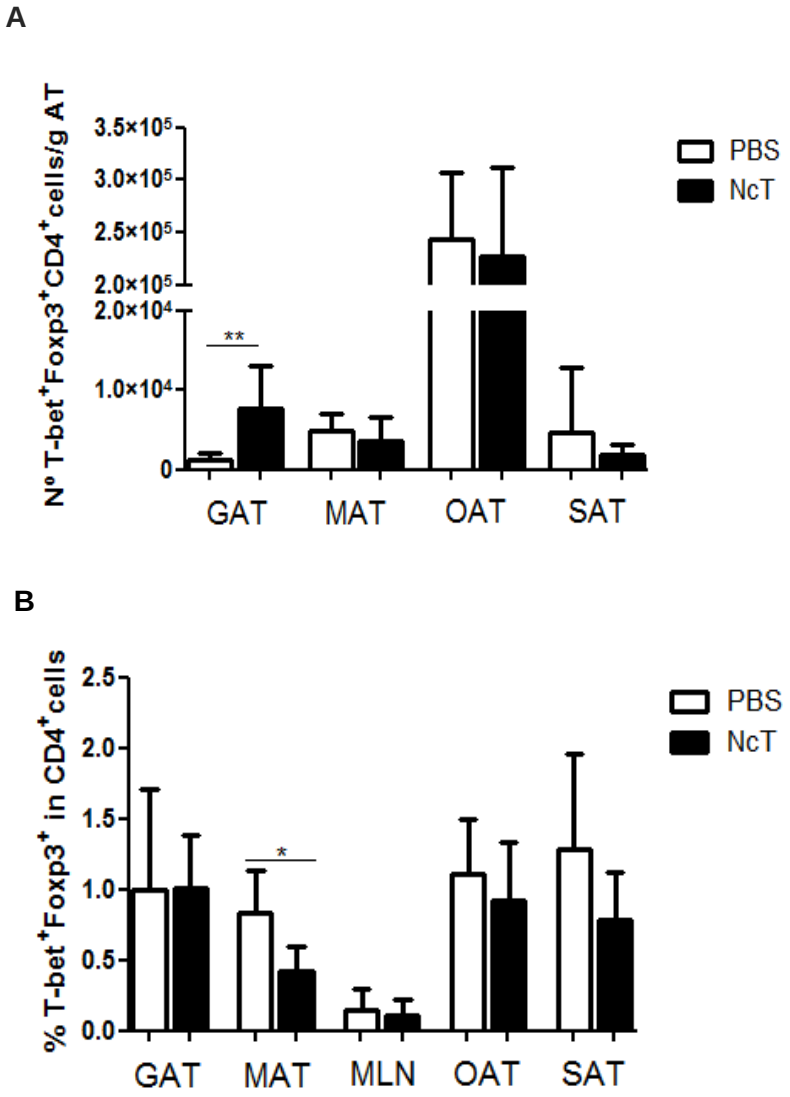

Fig.25 - Total number of cells (A) and frequencies (B) of T-bet^{+} Foxp3^{+}CD4^{+} cells in gonadal adipose tissue (GAT), mesenteric adipose tissue (MAT), omental adipose tissue (OAT) and subcutaneous adipose tissue (SAT) from C57BL/6 mice sacrificed two months after i.p. challenge with 1×10^{7} *N. caninum* (NcT) or PBS (PBS). For mesenteric lymph nodes (MLN) only the frequency of cells was determined. Statistical significant differences between groups is indicated (Mann-Whitney U, *$P < 0.05$; ** $P \leq 0.01$; *** $P \leq 0.001$).

The ratio of effector cells of the Th1 type over Treg cells was found to be higher in infected mice with *N. caninum* than in control group in SAT and MAT samples analysed at two months upon infection (Fig.26).

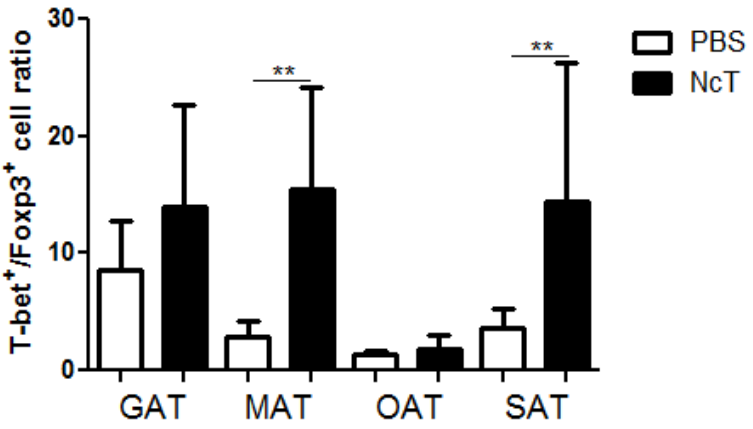

Fig.26 – The ratio of Th1 cells (T-bet$^+$Foxp3$^-$CD4$^+$) and total Treg cells (Foxp3$^+$T-bet$^-$CD4$^+$) of gonadal adipose tissue (GAT), mesenteric adipose tissue (MAT), omental adipose tissue (OAT) and subcutaneous adipose tissue (SAT) from C57BL/6 mice sacrificed two months after i.p. challenge with 1×10^7 *N. caninum* (NcT) or PBS (PBS). Statistical significant differences between groups is indicated (Mann-Whitney U, *$P < 0.05$; ** $P \leq 0.01$; *** $P \leq 0.001$).

Treg cells have been described as having high IL-10 transcript levels [107]. Therefore, IL-10 mRNA levels were determined in GAT of infected mice seven days and two months after challenge with *N. caninum*. It was observed a significant increase in IL-10 levels in infected mice when *NoNo* was used as reference gene, seven days after challenge (Fig.27A). Two months post-infection, there were no significant differences between infected and non-infected mice in IL-10 levels (Fig.27B).

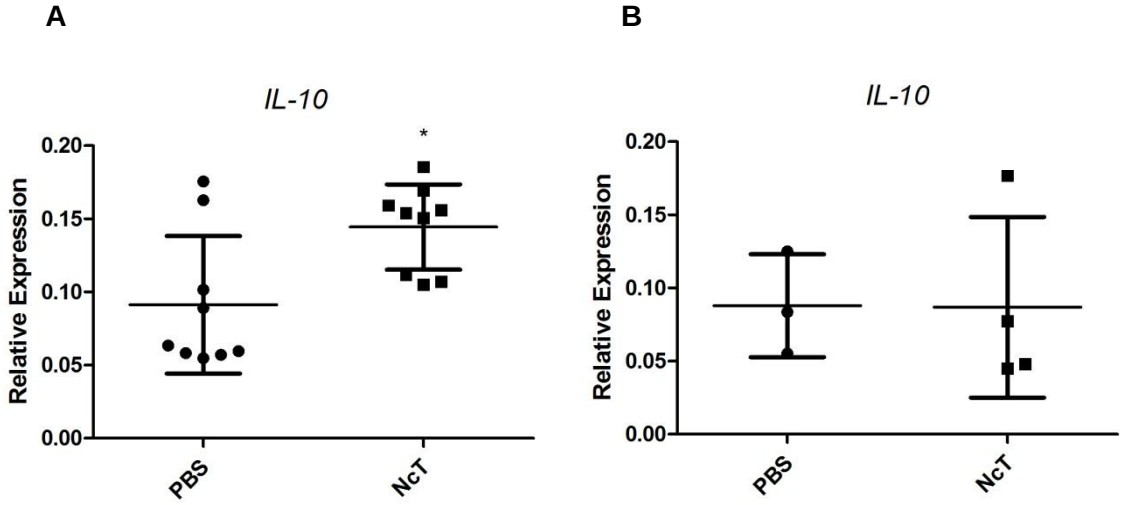

Fig.27 - Relative levels of *IL-10* mRNA, normalized to Non-POU-domain containing octamer binding protein mRNA, detected by Real Time PCR in the SFV of gonadal adipose tissue of mice seven days (A) and two months (B) after i.p. administration of 1×10^7 *N. caninum* tachyzoites (NcT) or PBS (PBS). Horizontal lines represent the mean values of the respective group (± SD). Statistical significant differences between groups is indicated (Mann-Whitney U, *$P < 0.05$; ** $P \leq 0.01$; *** $P \leq 0.001$).

3.5. Serum levels of adipokines

It was described that leptin could enhance the production of pro-inflammatory Th1-type cytokines and suppress the production of anti-inflammatory Th2 cytokines such as IL-4 in $CD4^+$ T cells [108]. On the other hand, adiponectin promotes the differentiation of anti-inflammatory M2 macrophages [108].

In order to understand if *N. caninum* infection could influence the production of adipokines, the serum levels of leptin, a pro-inflammatory adipokine [108] and adiponectin, an anti-inflammatory adipokine [108] were evaluated at different time points after challenge (Fig.28). As shown in Figure 28A, a significant increase of leptin serum levels was detected two months upon infection between infected and control group, while seven days after infection no significant differences were found. Nevertheless, in serum levels of adiponectin there were no significant differences observed at seven days and two months post-infection between infected mice and control group (Fig.28B).

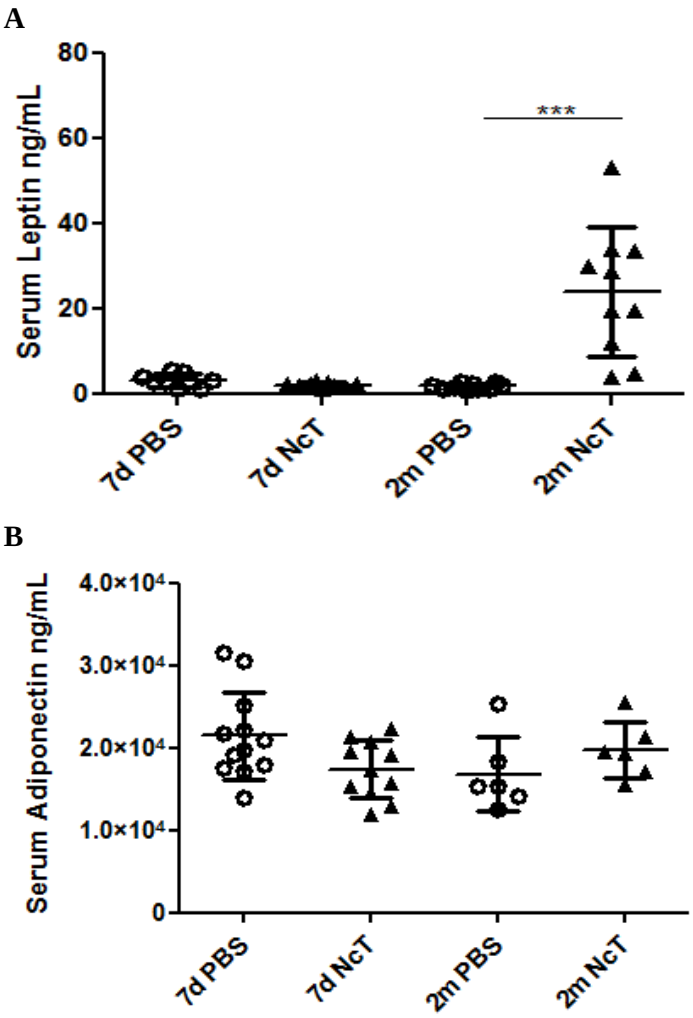

Fig.28 - Serum levels of (A) leptin and (B) adiponectin, of C57BL/6 mice seven days (7d) and two months (2m) after i.p. administration of 1×10^7 *N. caninum* tachyzoites (NcT) or PBS (PBS). Horizontal lines represent the mean values of the respective group (± SD). Statistical significant differences between groups is indicated (Mann-Whitney U, *$P < 0.05$; ** $P \leq 0.01$; *** $P \leq 0.001$; ****$P \leq 0.0001$).

4. Cytokine production by adipose tissue immune cell population

In this work it was possible to verify a significant increase in the expression of IFN-γ seven days after challenge with *N. caninum* in infected mice comparatively with the control group. Given that and due to the key role of this cytokine in protection against this parasite, its expression by different immune cell populations was assessed in adipose tissue.

On the other hand, IL-10 cytokine is a very important factor preventing excessive inflammation, namely, in parasitic infections [105]. For that reason, IL-10 expression was also assessed in order to determine the balance between these two cytokines with distinct and opposite roles in infection.

4.1. IFN-γ production by NK cells in adipose tissue after challenge with *N. caninum*

Recent data have shown a role for innate immune mechanisms involving Natural Killer cells that were able to lyse *N.* caninum-infected fibroblasts and produce IFN-γ in cattle [54]. This early induction of IFN-γ may be important in helping to control intracellular parasite multiplication and, in addition, may also create the appropriate cytokine environment for the induction of the adaptive immune response [54].

Knowing that NK cells mediate the so-called innate immunity, the frequency of these cells expressing IFN-γ was assessed twenty four hours after challenge with *N. caninum* in adipose tissue of C57BL/5 mice i.p. challenged with this parasite. The gating strategy is shown in Fig.29.

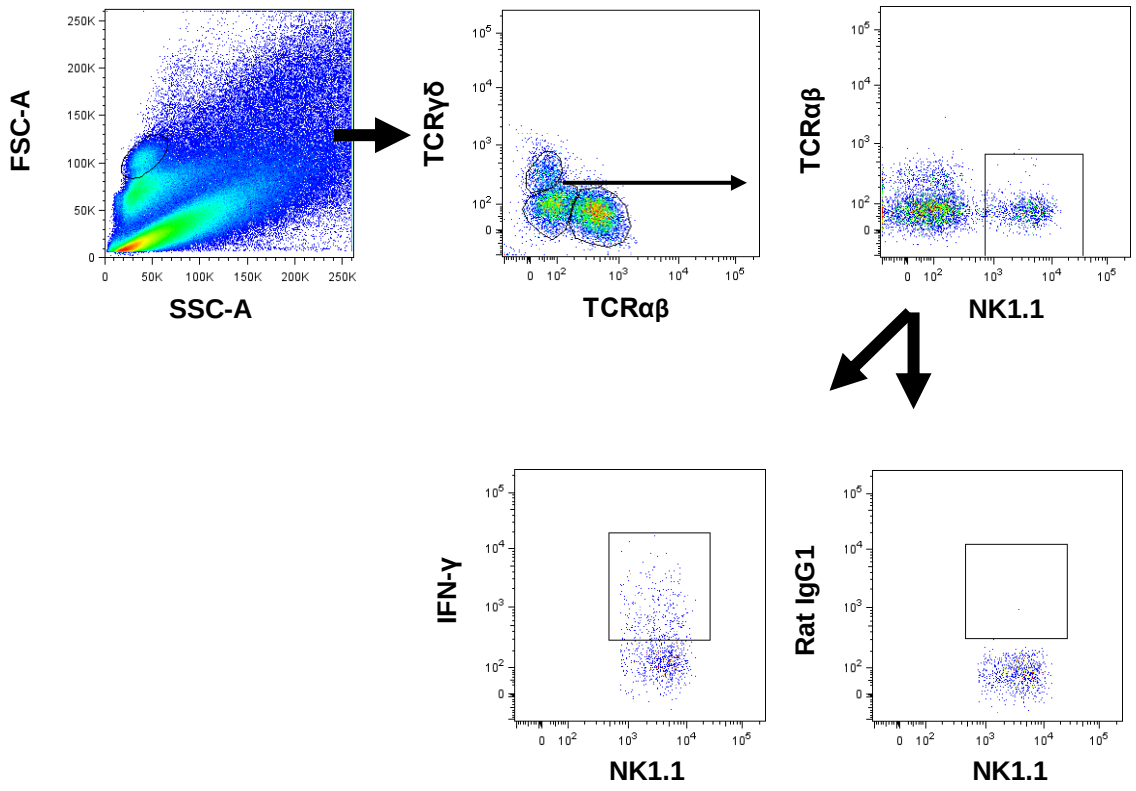

Fig. 29 - Flow cytometry representative example of gate strategy used to define NK cells in stromal vascular fraction isolated from adipose tissue. Inside leukocyte population, TCRγδ and TCRαβ population were excluded. NK1.1^{+} cells were selected and the production of IFN-γ was assessed. Respective isotype control is shown.

As Fig.30 shows, there was a significant increase the frequency of NK cells producing IFN-γ in SAT, GAT, MAT and OAT of infected animals comparatively with the control group.

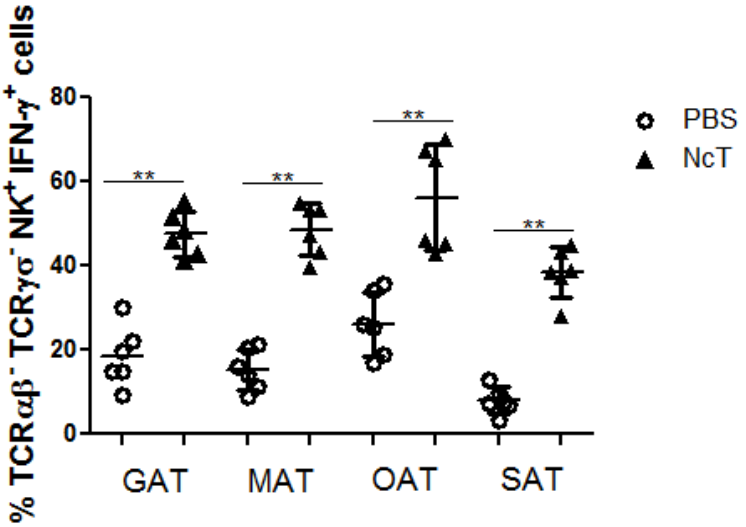

Fig.30 - Frequency of NK1.1^{+}IFN-γ^{+} cells in total NK1.1^{+} TCRγδ^{-} TCRαβ^{-} cells in gonadal adipose tissue (GAT), mesenteric adipose tissue (MAT), omental adipose tissue (OAT) and subcutaneous adipose tissue (SAT), detected in PBS (PBS) i.p.-treated or *N. caninum* (NcT) i.p.-infected mice, twenty-four hours after challenge. Each symbol represents an individual mouse. Horizontal lines represent the mean values of the respective group (± SD). Statistical significant differences between groups is indicated (Mann-Whitney U, *$P < 0.05$; ** $P \leq 0.01$; *** $P \leq 0.001$; ****$P \leq 0.0001$).

In order to understand if this population continues to produce IFN-γ longer in time, twenty-one days post-infection with *N. caninum* the frequency of IFN-γ-expressing NK cells was assessed (Fig.31). As shown, the frequency of NK cells producing IFN-γ is still significantly higher by that time in SAT, MAT, GAT and OAT from infected animals comparatively with the control group.

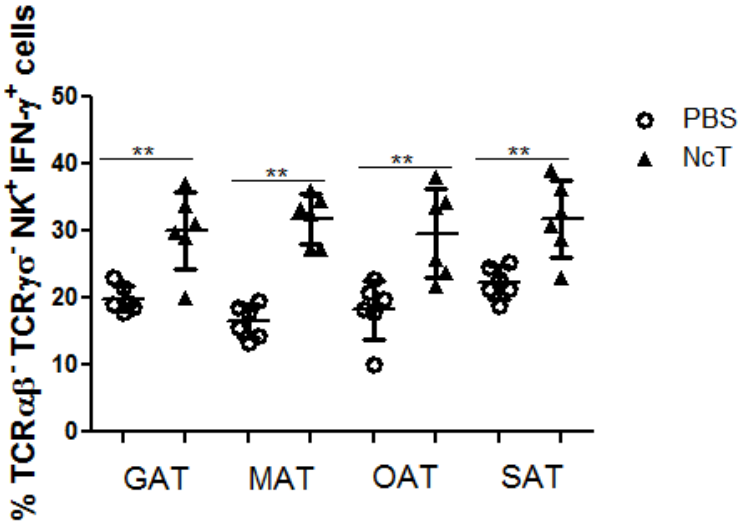

Fig.31 - Frequency of NK1.1^{+}IFN-γ^{+} cells in total NK1.1^{+} TCRγδ^{-} TCRαβ^{-} cells in gonadal adipose tissue (GAT), mesenteric adipose tissue (MAT), omental adipose tissue (OAT) and subcutaneous adipose tissue (SAT), detected in PBS (PBS) i.p.-treated or *N. caninum* (NcT) i.p.-infected mice, twenty-one days after challenge. Each symbol represents an individual mouse. Horizontal lines represent the mean values of the respective group (± SD). Statistical significant differences between groups is indicated (Mann-Whitney U, *$P < 0.05$; ** $P \leq 0.01$; *** $P \leq 0.001$; ****$P \leq 0.0001$).

4.2. IFN-γ and IL-10 production by TCRαβ^{+}CD4^{+} cells in adipose tissue after challenge with *N. caninum*

Immunological studies in a cattle model indicate that CD4^{+} T cells and the cytokines IFN-γ and IL-12 are key mediators in a protective immune response against *N. caninum* [63]. Additionally, BALB/c mice treated with a cell depleted monoclonal antibody specific for CD4 showed an increase in morbidity and mortality after *N. caninum* infection [61]. To evaluate the role in host defense against *N. caninum* of TCRαβ^{+}CD4^{+} cells, the production of IFN-γ and IL-10 by this population was assessed

in adipose tissue of i.p. infected mice by flow cytometry twenty four hours and twenty one days post-infection. The gating strategy is shown in Fig.32.

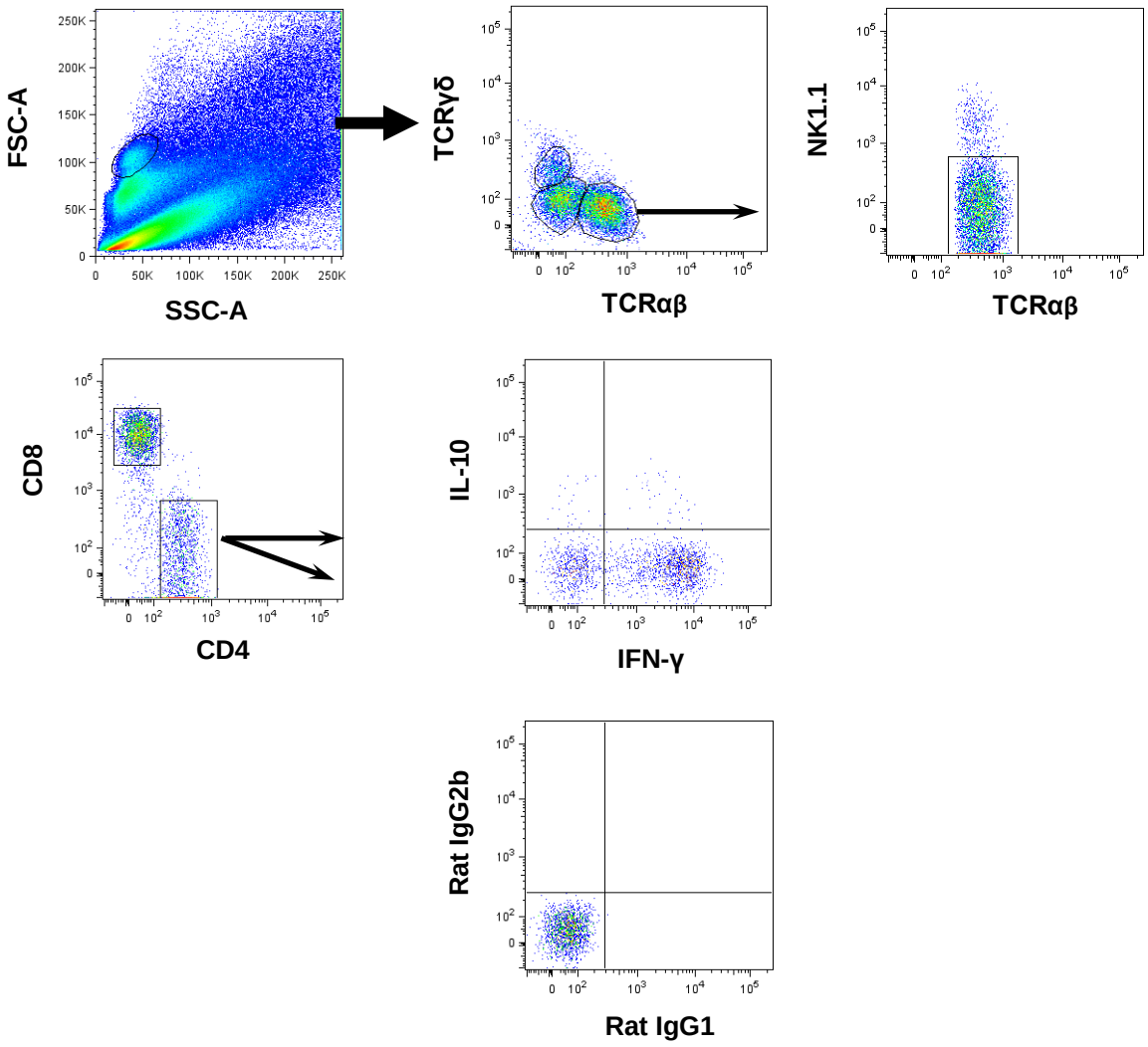

Fig.32 - Flow cytometry representative example of gate strategy used to define TCRαβ$^+$CD4$^+$ cells in stromal vascular fraction isolated from adipose tissue. Inside leukocyte population, TCRαβ population was selected and NK1.1$^+$ cells excluded. Cells expressing CD4 were then selected and the expression of IL-10 and IFN-γ assessed. Respective isotype control is shown.

As shown in Fig.33, the frequency of TCRαβ$^+$CD4$^+$IFN-γ$^+$IL-10$^-$ cells was found significantly increased in SAT from infected mice when compared to the control group, where in GAT, MAT and OAT there was no significant difference in the frequency of these cell populations, twenty-four hours after challenge (Fig.33A). The frequency of TCRαβ$^+$CD4$^+$IFN- γ$^-$IL-10$^+$ and TCRαβ$^+$CD4$^+$IFN-γ$^+$IL-10$^+$ cells was significantly increased in MAT from infected mice whereas no difference in the frequency of these cell populations in SAT, GAT and OAT of control and NcT challenged mice was observed, at this time point (Fig.33B and Fig.33C).

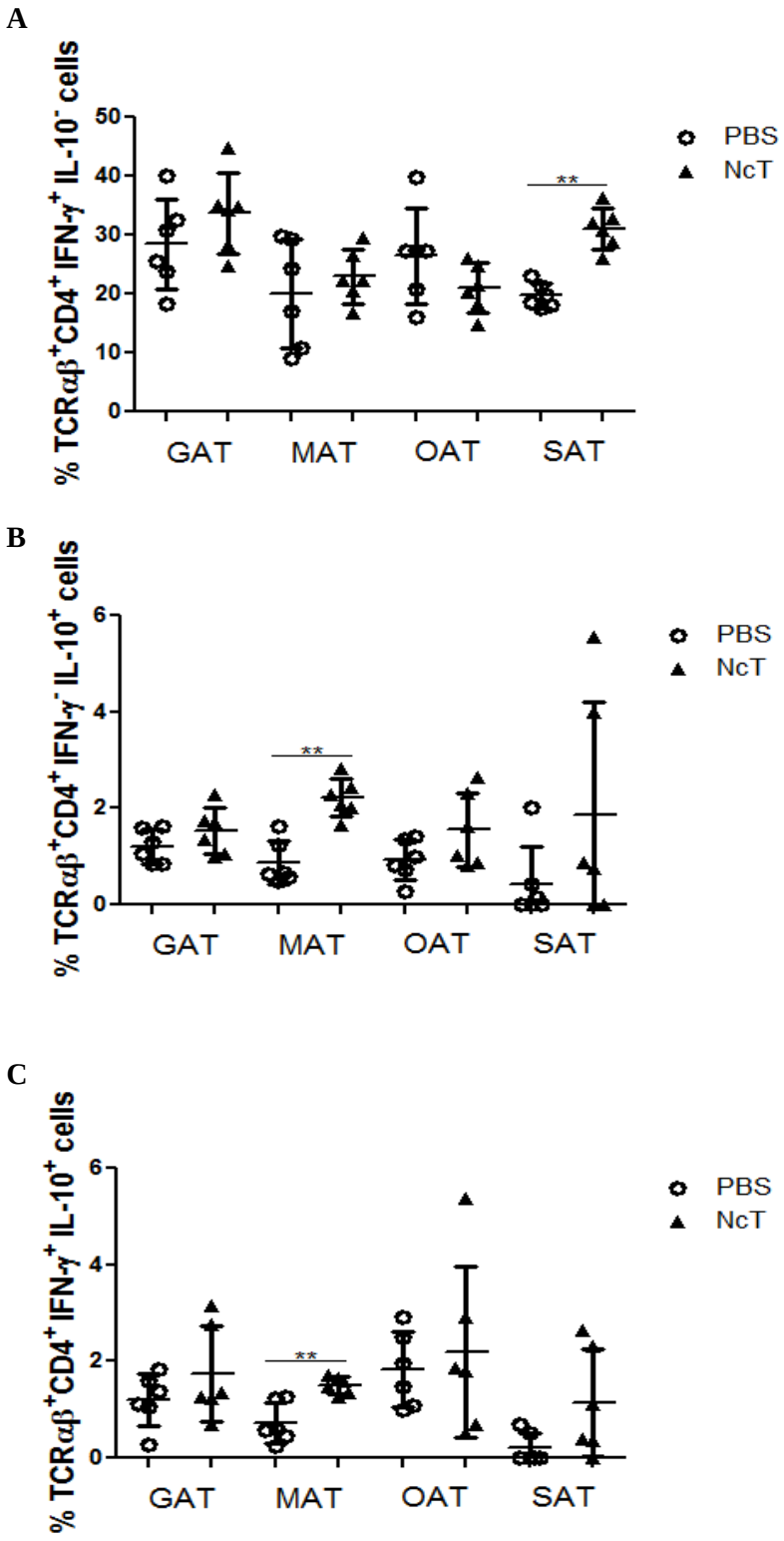

Fig.33 - Frequency of (A) TCRαβ$^+$CD4$^+$IFN-γ$^+$IL-10$^-$, (B) TCRαβ$^+$CD4$^+$IFN-γ$^-$IL-10$^+$ and (C) TCRαβ$^+$CD4$^+$IFN-γ$^+$IL-10$^+$ T cells in total TCRαβ$^+$NK1.1$^-$ cells from gonadal adipose tissue (GAT), mesenteric adipose tissue (MAT), omental adipose tissue (OAT) and subcutaneous adipose tissue (SAT), twenty-four hours after i.p. challenge with PBS (PBS) or 1×10^7 *N. caninum* tachyzoites (NcT). Each symbol represents an individual mouse. Horizontal lines represent the mean values of the respective group (± SD). Statistical significant differences between groups is indicated (Mann-Whitney U, *$P < 0.05$; ** $P \leq 0.01$; *** $P \leq 0.001$).

By twenty one days after challenge, as shown in Fig.34A, the frequency of TCRαβ^{+}CD4^{+}IFN-γ^{+}IL-10^{-} cells was found significantly increased in SAT, GAT, MAT and OAT from infected mice with *N. caninum* when compared to the control group. There were no significant differences in the frequency of TCRαβ^{+}CD4^{+}IFN- γ^{-}IL-10^{+} cells in all adipose tissue depots analyzed from infected mice comparatively to control group (Fig.34B). The frequency of TCRαβ^{+}CD4^{+}IFN-γ^{+}IL-10^{+} cells was significantly increased in GAT and MAT from infected mice (Fig.34C).

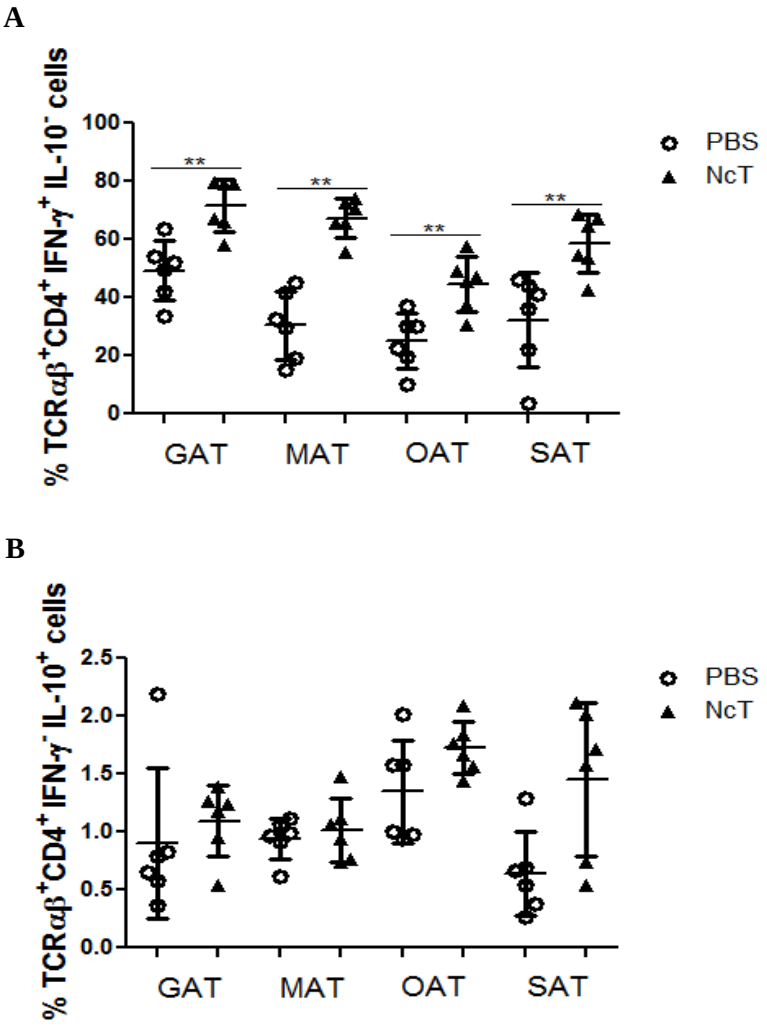

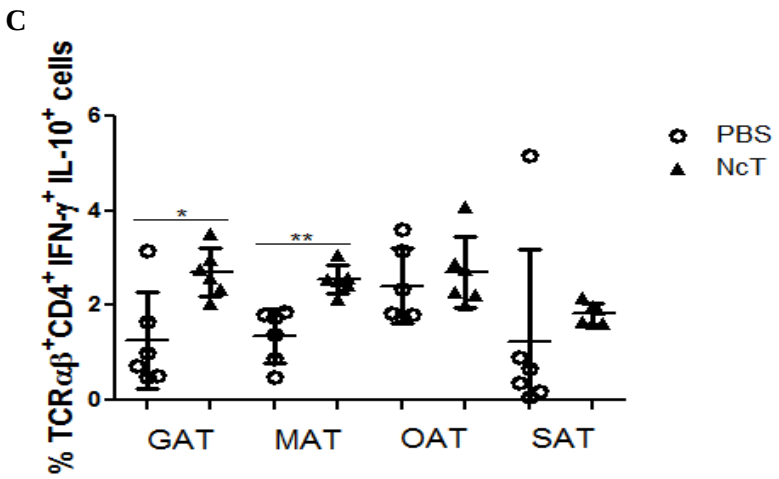

Fig.34 - Frequency of (A) TCRαβ$^+$CD4$^+$IFN-γ$^+$IL-10$^-$, (B) TCRαβ$^+$CD4$^+$IFN-γ$^-$IL-10$^+$ and (C) TCRαβ$^+$CD4$^+$IFN-γ$^+$IL-10$^+$ T cells in total TCRαβ$^+$NK1.1$^-$ cells from gonadal adipose tissue (GAT), mesenteric adipose tissue (MAT), omental adipose tissue (OAT) and subcutaneous adipose tissue (SAT), twenty-one days after i.p. challenge with PBS (PBS) or 1×10^7 *N. caninum* tachyzoites (NcT). Each symbol represents an individual mouse. Horizontal lines represent the mean values of the respective group (± SD). Statistical significant differences between groups is indicated (Mann-Whitney U, *$P < 0.05$; ** $P \leq 0.01$; *** $P \leq 0.001$).

4.3. IFN-γ and IL-10 production by TCRαβ$^+$CD8$^+$ cells in adipose tissue after challenge with *N. caninum*

The production of IFN-γ by CD8$^+$ T cells, which was also detected in calves experimentally infected with *N. caninum*, is an important mechanism in their host protective role against parasite infections [110]. In a murine model of i.g.-established neosporosis, CD8$^+$ T cells are also early major producers of the protective cytokine IFN-γ [110]. To evaluate the role of TCRαβ$^+$CD8$^+$ in adipose tissue cells after infection with *N. caninum*, the production of IFN-γ by this population was assessed in adipose tissue of i.p. infected mice by flow cytometry twenty four hours and twenty one days post-infection. The gating strategy was shown in Fig.35.

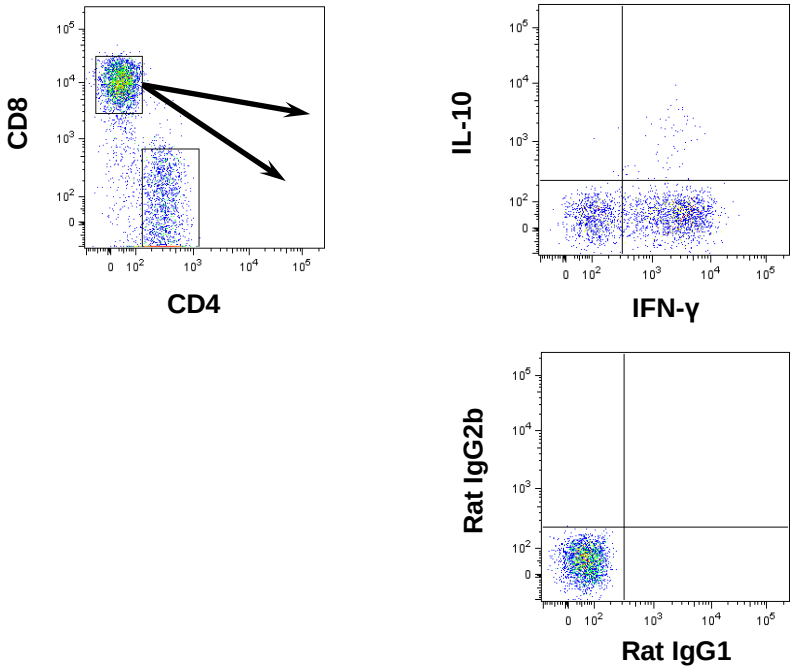

Fig.35 - Flow cytometry representative example of gate strategy used to define TCRαβ$^+$CD8$^+$ cells in stromal vascular fraction isolated from adipose tissue. Inside leukocyte population, TCRαβ population was selected and NK1.1$^+$ cells were excluded. Cells expressing CD8 were then selected and the expression of IL-10 and IFN-γ assessed. Respective isotype control is shown.

It can be observed that no significant differences were found in the frequency of TCRαβ$^+$CD8$^+$IFN-γ$^+$IL-10$^-$, TCRαβ$^+$CD4$^+$IFN-γ$^-$IL-10$^+$ and TCRαβ$^+$CD4$^+$IFN-γ$^+$IL-10$^+$ in the SAT, GAT, MAT and OAT from infected mice comparatively to controls, twenty-four hours after challenge (Fig.36A, Fig.36B and Fig.36C).

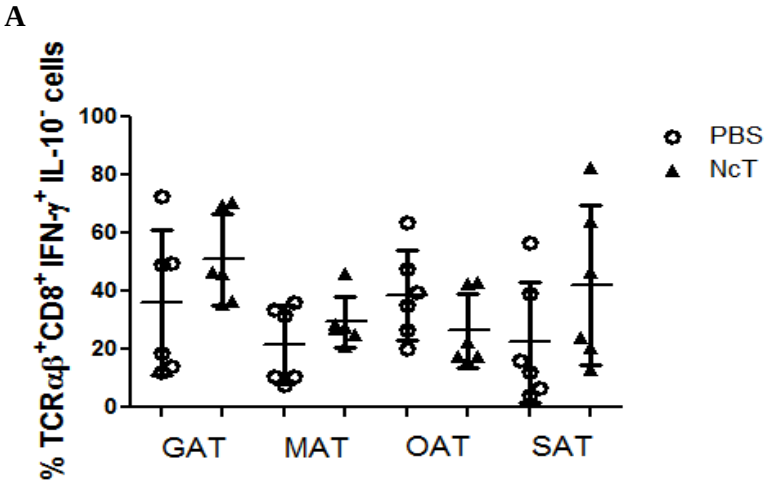

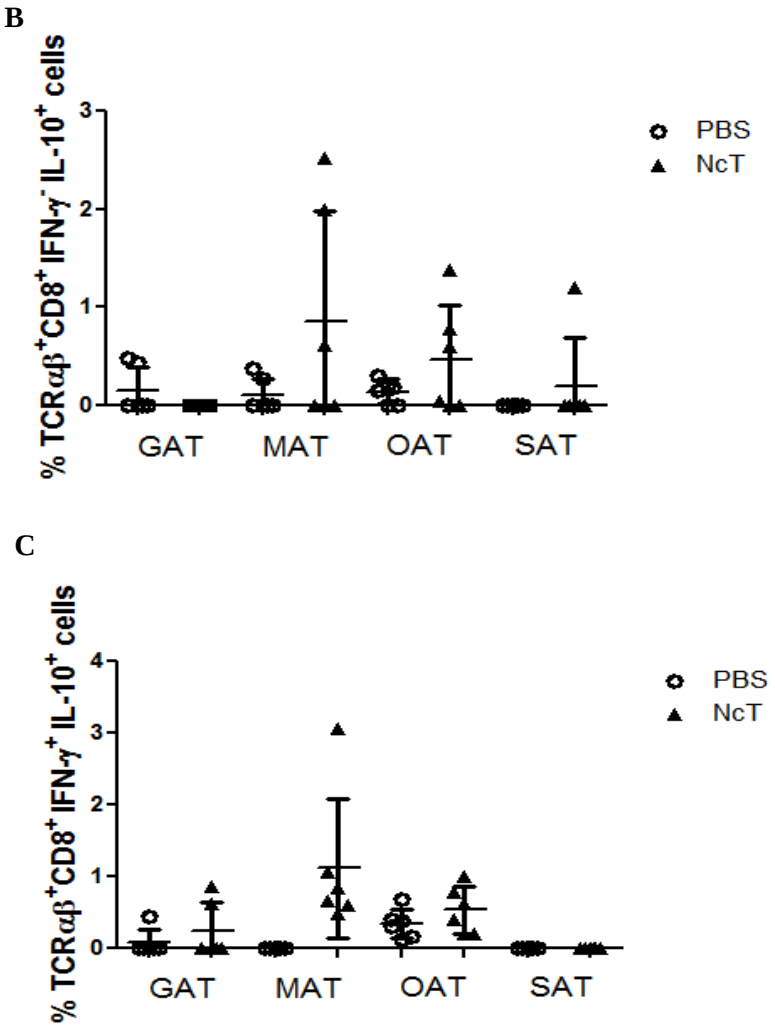

Fig.36 - Frequency of (A) TCRαβ$^+$CD8$^+$IFN-γ$^+$IL-10$^-$, (B) TCRαβ$^+$CD8$^+$IFN-γ$^-$IL-10$^+$ and (C) TCRαβ$^+$CD8$^+$IFN-γ$^+$IL-10$^+$ T cells in total TCRαβ$^+$NK1.1$^-$ cells from gonadal adipose tissue (GAT), mesenteric adipose tissue (MAT), omental adipose tissue (OAT) and subcutaneous adipose tissue (SAT), twenty-four hours after i.p. challenge with PBS (PBS) or 1×10^7 *N. caninum* tachyzoites (NcT). Each symbol represents an individual mouse. Horizontal lines represent the mean values of the respective group (± SD). Statistical significant differences between groups is indicated (Mann-Whitney U, *$P < 0.05$; ** $P \leq 0.01$; *** $P \leq 0.001$).

By twenty-one days after challenge with *N. caninum*, the frequency of TCRαβ$^+$CD4$^+$IFN-γ$^+$IL-10$^-$ cells was found significantly increased in SAT, MAT and OAT from infected mice when compared to the control group (Fig.37A). No significant differences in the frequency of TCRαβ$^+$CD4$^+$IFN- γ$^-$IL-10$^+$ cells were found in all adipose tissue depots analyzed from infected mice, comparatively to control group (Fig.37B). The frequency of TCRαβ$^+$CD4$^+$IFN-γ$^+$IL-10$^+$ cells was significantly increased in SAT, MAT and OAT from infected mice whereas no difference in the frequency of these cell populations in GAT of control and *N. caninum* challenged mice was observed twenty one days post-infection (Fig.37C).

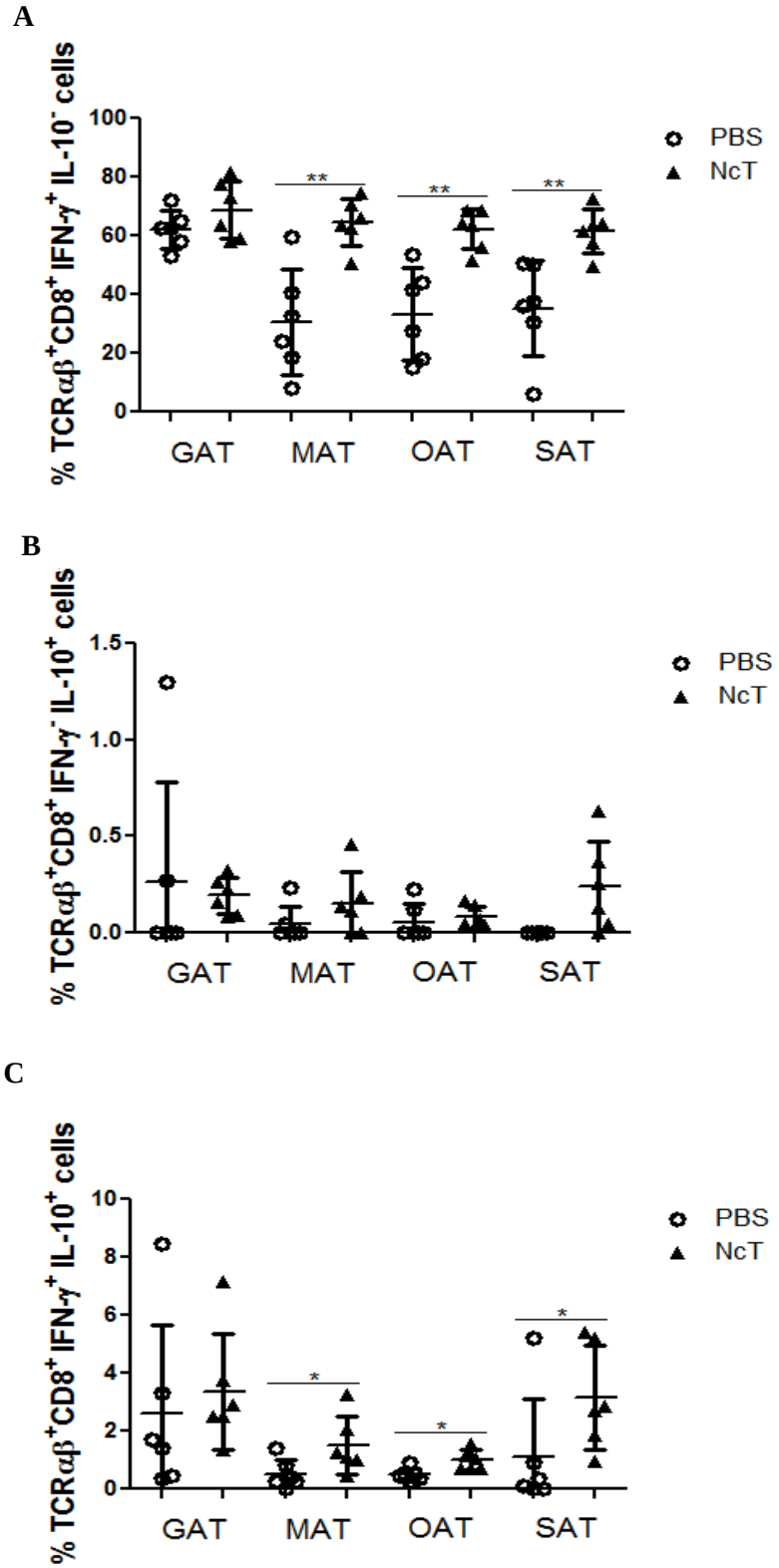

Fig.37 - Frequency of (A) TCRαβ$^+$CD8$^+$IFN-γ$^+$IL-10$^-$, (B) TCRαβ$^+$CD8$^+$IFN-γ$^-$IL-10$^+$ and (C) TCRαβ$^+$CD8$^+$IFN-γ$^+$IL-10$^+$ T cells in total TCRαβ$^+$NK1.1$^-$ cells from gonadal adipose tissue (GAT), mesenteric adipose tissue (MAT), omental adipose tissue (OAT) and subcutaneous adipose tissue (SAT), twenty-one days after i.p. challenge with PBS (PBS) or 1×10^7 *N. caninum* tachyzoites (NcT). Each symbol represents an individual mouse. Horizontal lines represent the mean values of the respective group (± SD). Statistical significant differences between groups is indicated (Mann-Whitney U, *$P < 0.05$; ** $P \leq 0.01$; *** $P \leq 0.001$).

4.4. IFN-γ production by TCRγδ⁺ cells in adipose tissue of mice infected with *N. caninum*

It was described that the reaction of γδ T cells to bacterial antigens and their ability to secrete IFN-γ is spontaneous and independent from the major histocompatibility complex. This is a very unique feature among lymphocytes, and this subpopulation is often described as a ‘‘bridge’’ between innate and acquired immunity [111]. It was also described that γδ T cells which appeared in the peritoneal cavity at an early stage of *Listeria monocytogenes* infection produce IFN-γ and participate in protection against the infection [112]. Fig.38 shows the gating strategy used to define this population.

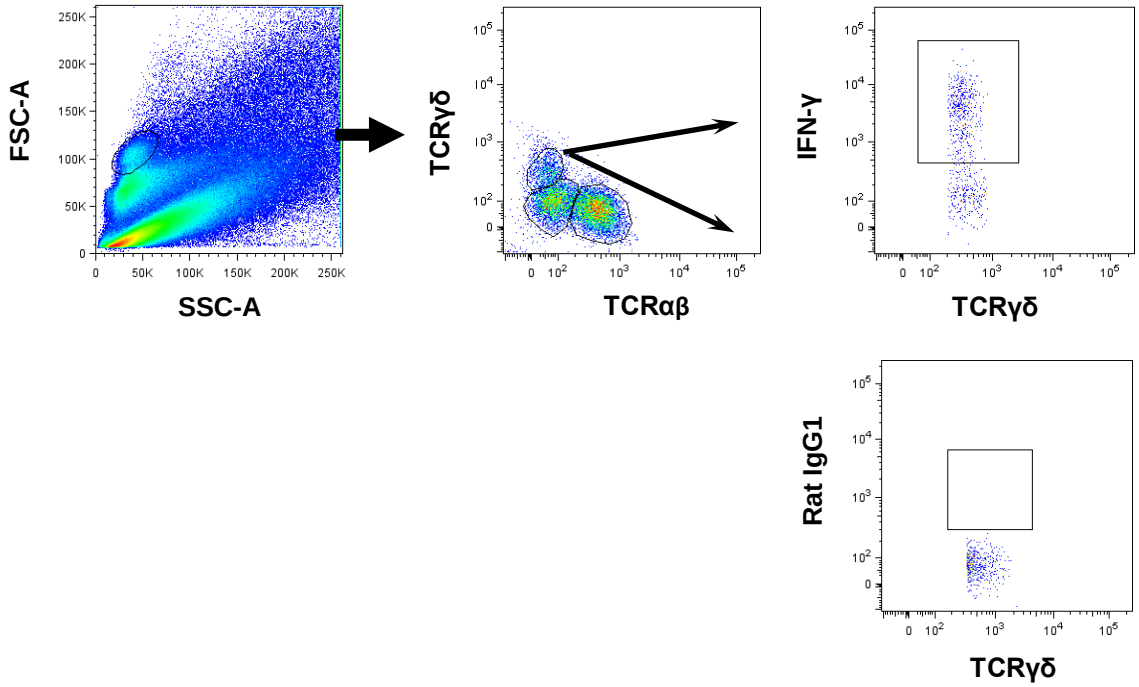

Fig.38 - Flow cytometry representative example of gate strategy used to define TCRγδ⁺IFN-γ⁺ cells in stromal vascular fraction isolated from adipose tissue. Inside leukocyte population, TCRγδ population were selected and the expression of IFN-γ evaluated. Respective isotype control is shown.

The frequency of TCRγδ⁺IFN-γ⁺ cells was assessed twenty-four hours after challenge with *N. caninum* in order to understand the role of this population in an early stage of infection. On Fig.39A, it is possible to observe that there were no significant differences in SAT, GAT, MAT and OAT of infected mice comparatively with the control group. However, twenty-one days after challenge with *N. caninum*, it is possible to

observe a significant increase in the frequency of TCRγδ^{+}IFN-γ^{+} in all adipose tissue depots analyzed in infected mice when compared with the control group (Fig.39B).

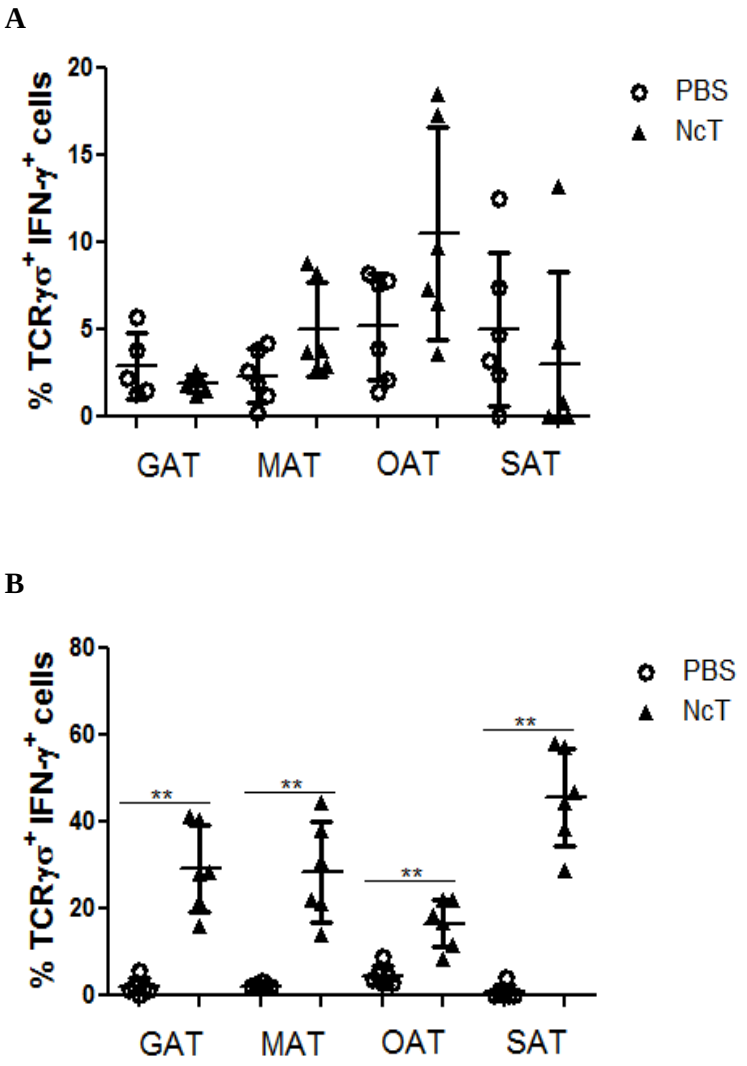

Fig.39 - Frequency of TCRγδ^{+}IFN-γ^{+} T cells in total TCRγδ^{+} in gonadal adipose tissue (GAT), mesenteric adipose tissue (MAT), omental adipose tissue (OAT) and subcutaneous adipose tissue (SAT), detected in PBS (PBS) i.p.-treated or *N. caninum* (NcT) i.p.-infected mice with 1×107 tachyzoites, (A) twenty four hours or (B) twenty one days after challenge. Each symbol represents an individual mouse. Horizontal lines represent the mean values of the respective group (± SD).Statistical significant differences between groups is indicated (Mann-Whitney U, *$P < 0.05$; ** $P \leq 0.01$; *** $P \leq 0.001$; ****$P \leq 0.0001$).

5. Discussion

Previous work on our laboratory has shown that in *N. caninum* infected mice, parasites could be detected as early as 6 hours upon the infectious challenge in SVF cells displaying macrophage morphology (Teixeira *et al.* unpublished results). This work demonstrates that parasitic forms could persist in adipose tissue at least seven days after challenge with *N. caninum*. Because adipose tissue has been demonstrated to be targeted and/or be a reservoir for several intracellular pathogens like *T. cruzi* or *C. burnetti* [113], it was hypothesized that adipose tissue could also be a reservoir for *N. caninum.* However no parasitic forms or parasitic DNA were detected two months after challenge indicating that adipose tissue may not be a reservoir for this parasite. Parasitic DNA was also detected in lungs and brain of infected mice, which is in agreement with a previous study in which parasite distribution kinetics was analyzed in *N. caninum* i.p.-challenged BALB/c mice [100]. These results demonstrate that *N. caninum* i.p. infection in mice can readily lead to adipose tissue parasitic colonization. Moreover, they also show that the immune response is effective in eradicating local infection, preventing *N. caninum* persistence in adipose tissue of infected hosts.

Further characterization of adipose tissue has shown a marked increase in F4/80-stained area earlier in infection with *N. caninum* in all adipose tissue depots analyzed. This shows that parasite dissemination throughout the body occurred after the i.p. inoculation. The increased F4/80-stained area observed may reflect an increase in the number of macrophages as well as an increase of that marker at their surface. This result was in line with others that demonstrate in *T. cruzi* infection a significant increase of macrophages in adipose tissue at early stages of infection [114]. Macrophages have a crucial role in the protective immune response against *N. caninum*, by increasing the production of NO and activating specific T lymphocytes [61, 63]. Nevertheless, polymorphonuclear cells, which could also express cell surface antigen F4/80, were also present in this tissue and could also be contributing for the increased F4/80 staining. Therefore to better characterize this cell population, flow cytometry was used. Previous work on laboratory showed elevated numbers of macrophages found in the adipose tissue earlier in infection at different anatomical locations (Teixeira *et al*. unpublished results). On the other hand, two months after challenge the numbers of macrophages in the different types of adipose tissue of infected mice were found to revert to control values.

As a consequence of the increase in the number of macrophages the levels of *Arg1* and *Nos2* mRNA were assessed in order to understand which macrophage response is elicited in adipose tissue upon *N. caninum* infection. It was already described that macrophage *Arg-1* is involved in preventing NO production because arginase can compete with NO synthase for their common substrate, arginine [102]. Indeed, the absence of *Arg-1* was associated with increased macrophage NO production and was linked to enhanced control of *T. gondii* infection [102]. The increase in both *Arg1* and *Nos2* mRNA levels detected seven days after challenge, suggest that a mixed M1/M2 type macrophage response was elicited by the parasite in the adipose tissue. The increased expression of *Nos2* mRNA could indicate that macrophages were producing NO in order to control the parasitic infection. The increased expression of *Arg1* mRNA could be important for the limitation of inflammatory response in order to prevent the tissue damage due to an exacerbated response [62]. Two months after infection, no differences were observed in both *Arg1* and *Nos2* mRNA levels in adipose tissue of infected mice which was in accordance with the flow cytometry analysis. As two months after the parasitic challenge, *N. caninum* was not detected in adipose tissue, in addition to the results of immunohistochemistry seven days after challenge and the increase in the *Nos2* mRNA levels seems to indicate that macrophages responding to *N. caninum* infection contribute to eradicate the infection locally in the adipose tissue.

Besides the observed increased number of macrophages in the adipose tissue at early stages of infection, an increase in $CD4^+$ T cells expressing the transcription factor T-bet was observed in some adipose tissue depots, two months after challenge with the parasite. Despite no increase was observed in the frequency of T-bet^+ cells in the MLN, interestingly the frequency of T-bet^+ cells increased in MAT and SAT was still detected two months after challenge. It was documented that murine macrophages showed greater activation and IFN-γ production during *N. caninum* infection [60]. Seven days after challenge, an increased expression of IFN-γ was observed in GAT of infected mice.

The increased F4/80 stained area detected seven days after challenge associated with increased IFN-γ mRNA expression, may indicate that adipose tissue macrophages infected *in vivo* with *N. caninum* are inducing IFN-γ production by adipose tissue T cells. The increased numbers of $CD4^+$ T cells expressing the transcription factor T-bet observed seven days after challenge with *N. caninum* (Teixeira *et al.* unpublished results), and observed two months in some depots in adipose tissue, associated with the fact that two months after infection parasitic DNA was no longer detected there, suggest that a protective immune response is elicited in the adipose tissue upon *N. caninum* infection.

In addition to the increase in T-bet$^+$ cells, increased numbers of adipose tissue Treg cells were observed in the different adipose tissue depots analysed. Previous work on our laboratory showed an increase in number of Foxp3$^+$CD25$^+$ cells in GAT, MAT, OAT and SAT seven days post-infection by flow cytometry analysis (Teixeira *et al.* unpublished results). This specific population is known to control the excessive inflammation in adipose tissue [107], and to control exacerbated immune response in parasitic infections [105]. Therefore the observed increase in Treg cell number, maintained in the GAT at least two months after the parasitic challenge, was indicative of a recruitment of this cell population to adipose tissue of infected mice. This could be important to control the local immune response in that tissue. Upon the observation of increased numbers of Foxp3$^+$ cells, *IL-10* mRNA levels in GAT of infected mice were determined as this cytokine could be produced by these cells. A slight increase of *IL-10* mRNA levels was observed in infected mice comparatively to control group, seven days after challenge. This result supports the premise that Tregs were important to tone down the immune response in the adipose tissue.

Additionally, it was possible to observe in GAT increased numbers of Fop3$^+$T-bet$^+$ cells that have been described to control Th1 type cells [103]. The ratio of effector cells of the Th1 type over Treg cells was calculated. An increased ratio was observed two months after infection in MAT and SAT suggesting that the inflammatory response in these tissues is maintained longer in time. This is further suggested by the lower frequency of CD206$^+$ macrophages observed at that time point.

Knowing that an alteration in the immune cell composition occurs within the adipose tissue upon *N. caninum* infection, its influence in the production of adipokines was investigated. Interestingly, a significant increase of leptin serum levels was observed two months upon infection suggesting a long-term effect of the parasitic challenge in the adipose tissue. This adipokine is mostly produced by adipose tissue and a correlation between body weight and leptin serum concentration was observed with high levels of leptin observed in heavier mice [108]. In this work, leptin levels were found to be higher without weight gain. Additionally, the elevated serum leptin observed in the infected mice may contribute to the low levels of Treg and increased numbers of Th1 cells observed in the adipose tissue independently of the presence of parasites. Infection by another protozoan parasite, *T. cruzi* has also been shown to affect serum leptin levels which were found below normal levels by 1 month of infection without affecting body weight [93].

Recent data have shown the important role of natural killer cells that were able to lyse *N. caninum*-infected fibroblasts and produce IFN-γ in cattle [54]. It is possible to

observe that early in infection with this parasite the frequency of NK cells producers of IFN-γ markedly increased in GAT, MAT, OAT and SAT. Consequently, this result suggests that NK cells may be an important source of that pro-inflammatory cytokine in the adipose tissue. However, twenty-one days after challenge the frequency of NK cells producers of IFN-γ is still slightly higher in infected mice comparatively with the control group in all adipose tissue depots analyzed. This result suggests that at this time point, the production of IFN-γ is still needed in order to control the infection.

Infection with *N. caninum* tends to provoke a cell-mediated immune response, involving $CD4^+$ T cells and IFN-γ production to help control the multiplication of the parasite. Macrophages activate specific T lymphocytes by presenting pathogen-derived antigens in association with major histocompatibility complex molecules. MHC class II knockout mice displayed sensitivity to *T. gondii* infection consistent with the absence of $CD4^+$ effector cells [62]. Twenty-one days after challenge with the parasite, the frequency of $CD4^+IFN\text{-}\gamma^+$ cells was significantly higher in infected animals comparatively with the control group in all adipose tissue depots analyzed. So, the observed result could be explained by the increase in number of macrophages earlier in infection. This result is in accordance with others demonstrating that T lymphocyte IFN-γ-secretion occurred after the interaction between T cells and macrophages [63]. Interestingly, a significant increased in the expression of $CD4^+IFN\text{-}\gamma^+$ cells were found in SAT twenty-four hours after challenge. This result is in accordance with other studies which indicates that in *Pneumocystis carinii* infection, $CD4^+$ cells are early producers of IFN-γ and play a critical role in resistance to infection [115]. $CD4^+$ T cells were found to produce IL-10 in the adipose tissue upon *N. caninum* infection. The majority of these $CD4^+$ T cells probably correspond to Treg cells, which were seen to increase in number at this place in several infections [107]. However, there were no significant differences in the frequency of $CD4^+IL\text{-}10^+$ cells between control and infected groups, twenty-one days after challenge.

There are several reports describing $CD4^+$ T cell clones simultaneously producing IFN-γ and IL-10. These $CD4^+$ T cells have been found during chronic infections, such as *Leishmania* and *T. gondii*. These cells are now considered able to prevent collateral immune damage, as well as being used by pathogens to prevent their elimination [109]. IL-10 stimulation allows the pathogen to evade IFN-γ dependent mechanisms of host resistance. In addition, overproduction of IFN-γ increased the sensitivity of the hosts to the pathogen [61]. The frequency of $CD4^+IFN\text{-}\gamma^+IL\text{-}10^+$ cells was significantly increased in GAT and MAT of infected mice, twenty one days upon infection. These results supports the crucial role $CD4^+$cells play in the IFN-γ mediated host immune responses to *N. caninum* infection.

$CD8^+$ T cells function is necessary for protection against *N. caninum*. As compared with $CD4^+$ T cells this cell population was described as early IFN-γ-producers upon *N. caninum* infection [110]. At an early stage of infection, IFN-γ production by this cell population were not very significant, while at twenty days after challenge the production of IFN-γ were increased in some adipose tissue depots. This result is in accordance with others that shown that $CD8^+$ T cells were producers of IFN-γ in murine toxoplasmosis and were involved in resistance to acute primary infection [116]. Also this population appears to be an important producer of IFN-γ during infection with *N. caninum,* indicating a possible protective role.

It was documented that γδ T cells were early producers of IFN-γ in response to bacterial antigens, without needing presentation by histocompatibility complex molecules. In cattle, studies have demonstrated an early accumulation of γδ T cells at sites of *Mycobacterium bovis* infection [117]. Despite the frequency of expression of IFN-γ by γδ T cells were not significantly different at early stages of infection, twenty one days after challenge a significant increase in this cytokine expression were observed in all adipose tissue depots analyzed. This result is in accordance with others, which showed that these cells played a host-protective role against *T. gondii* and *Listeria monocytoges* as IFN-γ-producers in early immune responses [112].

Overall, this work shows that a challenge with *N. caninum* contributes to a long-term inflammatory state in the adipose tissue even when parasites were no longer detected therein, providing convincing evidence that infection can have important long-term consequences in the adipose tissue physiology. Additionally, the increased macrophage numbers was accompanied by the increased presence of $CD4^+$ and $CD8^+$ T cells and Treg cells. $CD4^+$ T cells appeared to be differentiated towards the Th1 phenotype given the higher number of IFN-γ-producing cells. Moreover, $CD8^+$ T cells, $γδ^+$ T cells and NK cells were found to produce this pro-inflammatory cytokine, indicating a possible protective role of all these cellular subsets early after *N. caninum* infection.

Finally, due to the negative economical impact of *N. caninum* in both dairy and beef industries, a better understanding of *N. caninum* interaction with the host is required. So, more studies are needed in order to assess the importance of each population analyzed in the adipose tissue and their contribution to a protective or susceptible host immune response.

6. References

1. Botelho, A.S., et al., *Neospora caninum: high susceptibility to the parasite in C57BL/10ScCr mice.* Exp Parasitol, 2007. **115**(1): p. 68-75.
2. Dubey, J.P., G. Schares, and L.M. Ortega-Mora, *Epidemiology and control of neosporosis and Neospora caninum.* Clin Microbiol Rev, 2007. **20**(2): p. 323-67.
3. King, J.S., et al., *Implications of wild dog ecology on the sylvatic and domestic life cycle of Neospora caninum in Australia.* Vet J, 2011. **188**(1): p. 24-33.
4. Anderson, M., et al., *Neosporosis in dairy cattle.* Jpn J Vet Res, 2012. **60 Suppl**: p. S51-4.
5. Anderson, M.L., A.G. Andrianarivo, and P.A. Conrad, *Neosporosis in cattle.* Anim Reprod Sci, 2000. **60-61**: p. 417-31.
6. Dubey, J.P., *Review of Neospora caninum and neosporosis in animals.* Korean J Parasitol, 2003. **41**(1): p. 1-16.
7. McCann, C.M., et al., *Lack of serologic evidence of Neospora caninum in humans, England.* Emerg Infect Dis, 2008. **14**(6): p. 978-80.
8. McAllister, M.M., et al., *Dogs are definitive hosts of Neospora caninum.* Int J Parasitol, 1998. **28**(9): p. 1473-8.
9. Dubey, J.P., et al., *Redescription of Neospora caninum and its differentiation from related coccidia.* Int J Parasitol, 2002. **32**(8): p. 929-46.
10. Lindsay, D.S., J.P. Dubey, and R.B. Duncan, *Confirmation that the dog is a definitive host for Neospora caninum.* Vet Parasitol, 1999. **82**(4): p. 327-33.
11. Gondim, L.F., et al., *Transmission of Neospora caninum between wild and domestic animals.* J Parasitol, 2004. **90**(6): p. 1361-5.
12. Dubey, J.P. and D.S. Lindsay, *A review of Neospora caninum and neosporosis.* Vet Parasitol, 1996. **67**(1-2): p. 1-59.
13. Shivaprasad, H.L., R. Ely, and J.P. Dubey, *A Neospora-like protozoon found in an aborted bovine placenta.* Vet Parasitol, 1989. **34**(1-2): p. 145-8.
14. De Marez, T., et al., *Oral infection of calves with Neospora caninum oocysts from dogs: humoral and cellular immune responses.* Int J Parasitol, 1999. **29**(10): p. 1647-57.
15. Dijkstra, T., et al., *Dogs shed Neospora caninum oocysts after ingestion of naturally infected bovine placenta but not after ingestion of colostrum spiked with Neospora caninum tachyzoites.* Int J Parasitol, 2001. **31**(8): p. 747-52.

16. Barr, B.C., et al., *Experimental reproduction of bovine fetal Neospora infection and death with a bovine Neospora isolate.* J Vet Diagn Invest, 1994. **6**(2): p. 207-15.
17. Dubey, J.P., et al., *Induced transplacental transmission of Neospora caninum in cattle.* J Am Vet Med Assoc, 1992. **201**(5): p. 709-13.
18. Barr, B.C., et al., *Congenital Neospora infection in calves born from cows that had previously aborted Neospora-infected fetuses: four cases (1990-1992).* J Am Vet Med Assoc, 1993. **202**(1): p. 113-7.
19. Innes, E.A., et al., *Protection against vertical transmission in bovine neosporosis.* Int J Parasitol, 2001. **31**(13): p. 1523-34.
20. Dubey, J.P., et al., *Neosporosis-associated abortion in a dairy goat.* J Am Vet Med Assoc, 1996. **208**(2): p. 263-5.
21. Dubey, J.P. and D.S. Lindsay, *Neospora caninum induced abortion in sheep.* J Vet Diagn Invest, 1990. **2**(3): p. 230-3.
22. Dubey, J.P. and M.L. Porterfield, *Neospora caninum (Apicomplexa) in an aborted equine fetus.* J Parasitol, 1990. **76**(5): p. 732-4.
23. Woods, L.W., et al., *Systemic neosporosis in a California black-tailed deer (Odocoileus hemionus columbianus).* J Vet Diagn Invest, 1994. **6**(4): p. 508-10.
24. Buxton, D., et al., *Examination of red foxes (Vulpes vulpes) from Belgium for antibody to Neospora caninum and Toxoplasma gondii.* Vet Rec, 1997. **141**(12): p. 308-9.
25. Simpson, V.R., et al., *Foxes and neosporosis.* Vet Rec, 1997. **141**(19): p. 503.
26. Barber, J.S., et al., *Prevalence of antibodies to Neospora caninum in different canid populations.* J Parasitol, 1997. **83**(6): p. 1056-8.
27. Lindsay, D.S., et al., *Prevalence of agglutinating antibodies to Neospora caninum in raccoons, Procyon lotor.* J Parasitol, 2001. **87**(5): p. 1197-8.
28. Lindsay, D.S., et al., *Prevalence of Neospora caninum and Toxoplasma gondii antibodies in coyotes (Canis latrans) and experimental infections of coyotes with Neospora caninum.* J Parasitol, 1996. **82**(4): p. 657-9.
29. Gondim, L.F., et al., *Coyotes (Canis latrans) are definitive hosts of Neospora caninum.* Int J Parasitol, 2004. **34**(2): p. 159-61.
30. Bjerkas, I., M.C. Jenkins, and J.P. Dubey, *Identification and characterization of Neospora caninum tachyzoite antigens useful for diagnosis of neosporosis.* Clin Diagn Lab Immunol, 1994. **1**(2): p. 214-21.
31. Dubey, J.P., A. Koestner, and R.C. Piper, *Repeated transplacental transmission of Neospora caninum in dogs.* J Am Vet Med Assoc, 1990. **197**(7): p. 857-60.

32. Cole, R.A., et al., *Vertical transmission of Neospora caninum in dogs.* J Parasitol, 1995. **81**(2): p. 208-11.
33. Barber, J.S. and A.J. Trees, *Naturally occurring vertical transmission of Neospora caninum in dogs.* Int J Parasitol, 1998. **28**(1): p. 57-64.
34. Gondim, L.F., et al., *Transplacental transmission and abortion in cows administered Neospora caninum oocysts.* J Parasitol, 2004. **90**(6): p. 1394-400.
35. Basso, W., et al., *Prevalence of Neospora caninum infection in dogs from beef-cattle farms, dairy farms, and from urban areas of Argentina.* J Parasitol, 2001. **87**(4): p. 906-7.
36. Trees, A.J., H.C. Davison, and A. Otter, *Bovine abortion, Neospora caninum and dogs.* Vet Rec, 1998. **143**(12): p. 343.
37. Davison, H.C., et al., *Experimental studies on the transmission of Neospora caninum between cattle.* Res Vet Sci, 2001. **70**(2): p. 163-8.
38. Williams, D.J., et al., *Endogenous and exogenous transplacental transmission of Neospora caninum - how the route of transmission impacts on epidemiology and control of disease.* Parasitology, 2009. **136**(14): p. 1895-900.
39. Romero, J.J. and K. Frankena, *The effect of the dam-calf relationship on serostatus to Neospora caninum on 20 Costa Rican dairy farms.* Vet Parasitol, 2003. **114**(3): p. 159-71.
40. Dubey, J.P. and G. Schares, *Diagnosis of bovine neosporosis.* Vet Parasitol, 2006. **140**(1-2): p. 1-34.
41. Hay, W.H., et al., *Diagnosis and treatment of Neospora caninum infection in a dog.* J Am Vet Med Assoc, 1990. **197**(1): p. 87-9.
42. Anderson, M.L., B.C. Barr, and P.A. Conrad, *Protozoal causes of reproductive failure in domestic ruminants.* Vet Clin North Am Food Anim Pract, 1994. **10**(3): p. 439-61.
43. De Meerschman, F., et al., *Clinical, pathological and diagnostic aspects of congenital neosporosis in a series of naturally infected calves.* Vet Rec, 2005. **157**(4): p. 115-8.
44. Bjorkman, C., et al., *An IgG avidity ELISA to discriminate between recent and chronic Neospora caninum infection.* J Vet Diagn Invest, 1999. **11**(1): p. 41-4.
45. Haddad, J.P., I.R. Dohoo, and J.A. VanLeewen, *A review of Neospora caninum in dairy and beef cattle--a Canadian perspective.* Can Vet J, 2005. **46**(3): p. 230-43.
46. Reichel, M.P., et al., *What is the global economic impact of Neospora caninum in cattle - the billion dollar question.* Int J Parasitol, 2013. **43**(2): p. 133-42.

47. Monney, T. and A. Hemphill, *Vaccines against neosporosis: what can we learn from the past studies?* Exp Parasitol, 2014. **140**: p. 52-70.
48. Lindsay, D.S., et al., *Mouse model for central nervous system Neospora caninum infections.* J Parasitol, 1995. **81**(2): p. 313-5.
49. Long, M.T., T.V. Baszler, and B.A. Mathison, *Comparison of intracerebral parasite load, lesion development, and systemic cytokines in mouse strains infected with Neospora caninum.* J Parasitol, 1998. **84**(2): p. 316-20.
50. Liddell, S., M.C. Jenkins, and J.P. Dubey, *Vertical transmission of Neospora caninum in BALB/c mice determined by polymerase chain reaction detection.* J Parasitol, 1999. **85**(3): p. 550-5.
51. Kano, R., et al., *Relationship between type 1/type 2 immune responses and occurrence of vertical transmission in BALB/c mice infected with Neospora caninum.* Vet Parasitol, 2005. **129**(1-2): p. 159-64.
52. Ritter, D.M., et al., *Immune factors influencing the course of infection with Neospora caninum in the murine host.* J Parasitol, 2002. **88**(2): p. 271-80.
53. Bartley, P.M., et al., *Long-term passage of tachyzoites in tissue culture can attenuate virulence of Neospora caninum in vivo.* Parasitology, 2006. **133**(Pt 4): p. 421-32.
54. Klevar, S., et al., *Natural killer cells act as early responders in an experimental infection with Neospora caninum in calves.* Int J Parasitol, 2007. **37**(3-4): p. 329-39.
55. Innes, E.A., *The host-parasite relationship in pregnant cattle infected with Neospora caninum.* Parasitology, 2007. **134**(Pt 13): p. 1903-10.
56. Maley, S.W., et al., *Characterization of the immune response in the placenta of cattle experimentally infected with Neospora caninum in early gestation.* J Comp Pathol, 2006. **135**(2-3): p. 130-41.
57. Almeria, S., et al., *Specific anti-Neospora caninum IgG1 and IgG2 antibody responses during gestation in naturally infected cattle and their relationship with gamma interferon production.* Vet Immunol Immunopathol, 2009. **130**(1-2): p. 35-42.
58. Bartley, P.M., et al., *Maternal and foetal immune responses of cattle following an experimental challenge with Neospora caninum at day 70 of gestation.* Vet Res, 2012. **43**: p. 38.
59. Hemphill, A., N. Vonlaufen, and A. Naguleswaran, *Cellular and immunological basis of the host-parasite relationship during infection with Neospora caninum.* Parasitology, 2006. **133**(Pt 3): p. 261-78.

60. Abe, C., et al., *Macrophage Depletion Prior to Neospora caninum Infection Results in Severe Neosporosis in Mice.* Clin Vaccine Immunol, 2014. **21**(8): p. 1185-8.
61. Nishikawa, Y., et al., *In the absence of endogenous gamma interferon, mice acutely infected with Neospora caninum succumb to a lethal immune response characterized by inactivation of peritoneal macrophages.* Clin Diagn Lab Immunol, 2001. **8**(4): p. 811-6.
62. Tanaka, T., et al., *Growth-inhibitory effects of interferon-gamma on Neospora caninum in murine macrophages by a nitric oxide mechanism.* Parasitol Res, 2000. **86**(9): p. 768-71.
63. Dion, S., et al., *Functional activation of T cells by dendritic cells and macrophages exposed to the intracellular parasite Neospora caninum.* Int J Parasitol, 2011. **41**(6): p. 685-95.
64. Liu, C.H., et al., *Cutting edge: dendritic cells are essential for in vivo IL-12 production and development of resistance against Toxoplasma gondii infection in mice.* J Immunol, 2006. **177**(1): p. 31-5.
65. Teixeira, L., et al., *Plasmacytoid and conventional dendritic cells are early producers of IL-12 in Neospora caninum-infected mice.* Immunol Cell Biol, 2010. **88**(1): p. 79-86.
66. Innes, E.A., et al., *The host-parasite relationship in bovine neosporosis.* Vet Immunol Immunopathol, 2005. **108**(1-2): p. 29-36.
67. Tanaka, T., et al., *The role of CD4(+) or CD8(+) T cells in the protective immune response of BALB/c mice to Neospora caninum infection.* Vet Parasitol, 2000. **90**(3): p. 183-91.
68. Teixeira, L., et al., *Characterization of the B-cell immune response elicited in BALB/c mice challenged with Neospora caninum tachyzoites.* Immunology, 2005. **116**(1): p. 38-52.
69. Regidor-Cerrillo, J., et al., *Neospora caninum infection during early pregnancy in cattle: how the isolate influences infection dynamics, clinical outcome and peripheral and local immune responses.* Vet Res, 2014. **45**: p. 10.
70. Monney, T., et al., *RecNcMIC3-1-R is a microneme- and rhoptry-based chimeric antigen that protects against acute neosporosis and limits cerebral parasite load in the mouse model for Neospora caninum infection.* Vaccine, 2011. **29**(40): p. 6967-75.
71. Carruthers, V. and J.C. Boothroyd, *Pulling together: an integrated model of Toxoplasma cell invasion.* Curr Opin Microbiol, 2007. **10**(1): p. 83-9.

72. Innes, E.A., et al., *Developing vaccines to control protozoan parasites in ruminants: dead or alive?* Vet Parasitol, 2011. **180**(1-2): p. 155-63.
73. Romero, J.J., E. Perez, and K. Frankena, *Effect of a killed whole Neospora caninum tachyzoite vaccine on the crude abortion rate of Costa Rican dairy cows under field conditions.* Vet Parasitol, 2004. **123**(3-4): p. 149-59.
74. Weston, J.F., C. Heuer, and N.B. Williamson, *Efficacy of a Neospora caninum killed tachyzoite vaccine in preventing abortion and vertical transmission in dairy cattle.* Prev Vet Med, 2012. **103**(2-3): p. 136-44.
75. Weber, F.H., et al., *On the efficacy and safety of vaccination with live tachyzoites of Neospora caninum for prevention of neospora-associated fetal loss in cattle.* Clin Vaccine Immunol, 2013. **20**(1): p. 99-105.
76. Saely, C.H., K. Geiger, and H. Drexel, *Brown versus white adipose tissue: a mini-review.* Gerontology, 2012. **58**(1): p. 15-23.
77. Usui, C., et al., *Visceral fat is a strong predictor of insulin resistance regardless of cardiorespiratory fitness in non-diabetic people.* J Nutr Sci Vitaminol (Tokyo), 2010. **56**(2): p. 109-16.
78. Platell, C., et al., *The omentum.* World J Gastroenterol, 2000. **6**(2): p. 169-176.
79. Kaminski, D.A. and T.D. Randall, *Adaptive immunity and adipose tissue biology.* Trends Immunol, 2010. **31**(10): p. 384-90.
80. Kershaw, E.E. and J.S. Flier, *Adipose tissue as an endocrine organ.* J Clin Endocrinol Metab, 2004. **89**(6): p. 2548-56.
81. Fain, J.N., et al., *Comparison of the release of adipokines by adipose tissue, adipose tissue matrix, and adipocytes from visceral and subcutaneous abdominal adipose tissues of obese humans.* Endocrinology, 2004. **145**(5): p. 2273-82.
82. Galli, S.J., N. Borregaard, and T.A. Wynn, *Phenotypic and functional plasticity of cells of innate immunity: macrophages, mast cells and neutrophils.* Nat Immunol, 2011. **12**(11): p. 1035-44.
83. Elgazar-Carmon, V., et al., *Neutrophils transiently infiltrate intra-abdominal fat early in the course of high-fat feeding.* J Lipid Res, 2008. **49**(9): p. 1894-903.
84. Schaffler, A. and J. Scholmerich, *Innate immunity and adipose tissue biology.* Trends Immunol, 2010. **31**(6): p. 228-35.
85. Mathis, D., *Immunological goings-on in visceral adipose tissue.* Cell Metab, 2013. **17**(6): p. 851-9.
86. Schipper, H.S., et al., *Adipose tissue-resident immune cells: key players in immunometabolism.* Trends Endocrinol Metab, 2012. **23**(8): p. 407-15.

87. Boehm, T., *Design principles of adaptive immune systems.* Nat Rev Immunol, 2011. **11**(5): p. 307-17.
88. Luckheeram, R.V., et al., *CD4(+)T cells: differentiation and functions.* Clin Dev Immunol, 2012. **2012**: p. 925135.
89. Winer, S., et al., *Obesity predisposes to Th17 bias.* Eur J Immunol, 2009. **39**(9): p. 2629-35.
90. Maloy, K.J., et al., *CD4+CD25+ T(R) cells suppress innate immune pathology through cytokine-dependent mechanisms.* J Exp Med, 2003. **197**(1): p. 111-9.
91. Wozniak, S.E., et al., *Adipose tissue: the new endocrine organ? A review article.* Dig Dis Sci, 2009. **54**(9): p. 1847-56.
92. Nagajyothi, F., et al., *Response of adipose tissue to early infection with Trypanosoma cruzi (Brazil strain).* J Infect Dis, 2012. **205**(5): p. 830-40.
93. Combs, T.P., et al., *The adipocyte as an important target cell for Trypanosoma cruzi infection.* J Biol Chem, 2005. **280**(25): p. 24085-94.
94. Lutwick, L.I., *Brill-Zinsser disease.* Lancet, 2001. **357**(9263): p. 1198-200.
95. Bechah, Y., et al., *Adipose tissue serves as a reservoir for recrudescent Rickettsia prowazekii infection in a mouse model.* PLoS One, 2010. **5**(1): p. e8547.
96. Gray, K.S., C.M. Collins, and S.H. Speck, *Characterization of omental immune aggregates during establishment of a latent gammaherpesvirus infection.* PLoS One, 2012. **7**(8): p. e43196.
97. Arsenijevic, T., et al., *Murine 3T3-L1 adipocyte cell differentiation model: validated reference genes for qPCR gene expression analysis.* PLoS One, 2012. **7**(5): p. e37517.
98. Schmittgen, T.D. and K.J. Livak, *Analyzing real-time PCR data by the comparative C(T) method.* Nat Protoc, 2008. **3**(6): p. 1101-8.
99. Nishikawa, Y., et al., *Protective efficacy of vaccination by recombinant vaccinia virus against Neospora caninum infection.* Vaccine, 2001. **19**(11-12): p. 1381-90.
100. Collantes-Fernandez, E., et al., *Temporal distribution and parasite load kinetics in blood and tissues during Neospora caninum infection in mice.* Infect Immun, 2006. **74**(4): p. 2491-4.
101. Mitchell, A.J., et al., *Technical advance: autofluorescence as a tool for myeloid cell analysis.* J Leukoc Biol, 2010. **88**(3): p. 597-603.
102. El Kasmi, K.C., et al., *Toll-like receptor-induced arginase 1 in macrophages thwarts effective immunity against intracellular pathogens.* Nat Immunol, 2008. **9**(12): p. 1399-406.

103. Lazarevic, V., L.H. Glimcher, and G.M. Lord, *T-bet: a bridge between innate and adaptive immunity.* Nat Rev Immunol, 2013. **13**(11): p. 777-89.
104. Nishikawa, Y., et al., *A role for balance of interferon-gamma and interleukin-4 production in protective immunity against Neospora caninum infection.* Vet Parasitol, 2003. **116**(3): p. 175-84.
105. Belkaid, Y. and K. Tarbell, *Regulatory T cells in the control of host-microorganism interactions (*).* Annu Rev Immunol, 2009. **27**: p. 551-89.
106. Teixeira, L., et al., *Analysis of the immune response to Neospora caninum in a model of intragastric infection in mice.* Parasite Immunol, 2007. **29**(1): p. 23-36.
107. Feuerer, M., et al., *Lean, but not obese, fat is enriched for a unique population of regulatory T cells that affect metabolic parameters.* Nat Med, 2009. **15**(8): p. 930-9.
108. Kwon, H. and J.E. Pessin, *Adipokines mediate inflammation and insulin resistance.* Front Endocrinol (Lausanne), 2013. **4**: p. 71.
109. Flores-Garcia, Y., et al., *IL-10-IFN-gamma double producers CD4+ T cells are induced by immunization with an amastigote stage specific derived recombinant protein of Trypanosoma cruzi.* Int J Biol Sci, 2011. **7**(8): p. 1093-100.
110. Correia, A., et al., *Mucosal and systemic T cell response in mice intragastrically infected with Neospora caninum tachyzoites.* Vet Res, 2013. **44**: p. 69.
111. Serwatowska-Bargiel, A., et al., *T-cell subpopulations alphabeta and gammadelta in cord blood of very preterm infants: the influence of intrauterine infection.* Arch Immunol Ther Exp (Warsz), 2013. **61**(6): p. 495-501.
112. Kadena, T., et al., *TCR alpha beta+ CD4- CD8- T cells differentiate extrathymically in an lck-independent manner and participate in early response against Listeria monocytogenes infection through interferon-gamma production.* Immunology, 1997. **91**(4): p. 511-9.
113. Bechah, Y., et al., *Persistence of Coxiella burnetii, the agent of Q fever, in murine adipose tissue.* PLoS One, 2014. **9**(5): p. e97503.
114. Tanowitz, H.B., et al., *Adipose tissue, diabetes and Chagas disease.* Adv Parasitol, 2011. **76**: p. 235-50.
115. Theus, S.A., et al., *Cytokine responses to the native and recombinant forms of the major surface glycoprotein of Pneumocystis carinii.* Clin Exp Immunol, 1997. **109**(2): p. 255-60.
116. Shirahata, T., et al., *CD8+ T lymphocytes are the major cell population involved in the early gamma interferon response and resistance to acute primary Toxoplasma gondii infection in mice.* Microbiol Immunol, 1994. **38**(10): p. 789-96.

117. McGill, J.L., et al., *The role of gamma delta T cells in immunity to Mycobacterium bovis infection in cattle.* Vet Immunol Immunopathol, 2014. **159**(3-4): p. 133-43.